Aqueous Photochemistry of Syringic Acid as a Model for the Environmental Photochemical Behaviour of Humic Substances

by

Erin Kathryn Dallin
B.Sc., University of Victoria, 2005

A Thesis Submitted in Partial Fulfillment of the
Requirements for the Degree of

MASTER OF SCIENCE

in the Department of Chemistry

Aqueous Photochemistry of Syringic Acid as a Model for the Environmental Photochemical Behaviour of Humic Substances

by

Erin Kathryn Dallin
B.Sc., University of Victoria, 2005

Supervisory Committee

Dr. P. Wan, (Department of Chemistry)
Co-Supervisor

Dr. E. Krogh, (Department of Chemistry, Malaspina University-College)
Co-Supervisor

Dr. A.G. Briggs, (Department of Chemistry)
Departmental Member

Dr. L. Rosenberg, (Department of Chemistry)
Departmental Member

Dr. C. Hamilton, (Axys Analytical Services Ltd.; Sidney, BC)
External Examiner

Supervisory Committee

Dr. P. Wan, (Department of Chemistry)
Co-Supervisor

Dr. E. Krogh, (Department of Chemistry, Malaspina University-College)
Co-Supervisor

Dr. A.G. Briggs, (Department of Chemistry)
Departmental Member

Dr. L. Rosenberg, (Department of Chemistry)
Departmental Member

Dr. C. Hamilton, (Axys Analytical Services Ltd.; Sidney, BC)
External Examiner

Abstract

The aqueous photochemistry of 4-hydroxy-3,5-dimethoxybenzoic acid (syringic acid) has been studied as a model humic substance in order to better understand the reactions that compounds of this type undergo in the natural environment. Syringic acid was chosen since it has been identified as a component of humic substances in the environment and bears many of chemical moieties found in structures of this type. In addition, there has been speculation that humic substances are responsible for some of the production of halomethanes that are released into the environment. Photolysis of these compounds in marine and estuarine waters may be responsible for the release of halomethanes which are known stratospheric ozone depleters. Photochemical product studies of syringic acid and related compounds along with UV-Vis spectrometry, laser

flash photolysis and membrane introduction mass spectrometry were carried out in aqueous solutions to study its photochemical transformations.

Syringic acid was found to form methanol at a 0.01 quantum yield upon its photolysis in basic solution. Other major photoproducts included 3-methoxygallic acid and 3,5-dimethoxybenzoic acid. Chloromethane was identified as a minor photoproduct in chloride enriched solution by following its production via membrane introduction mass spectrometry. The proposed mechanism for the formation of these photoproducts involves an initial photoprotonation of the benzene ring, resulting in a carbocation that can facilitate the nucleophilic attack by water or chloride, to produce methanol or chloromethane, respectively. The formation of 3,5-dimethoxybenzoic acid is via a novel pathway that involves the loss of the hydroxy group from the aromatic ring after the photoprotonation.

Table of Contents

Chapter 3

Experimental

List of Tables

List of Figures

List of Abbreviations

DOM	Dissolved Organic Matter
DMSO	Dimethylsulfoxide
EDG	Electron Donating Group
ESI-MS	Electrospray Ionization Mass Spectrometry
EWG	Electron Withdrawing Group
GC	Gas Chromatography
HOMO	Highest Occupied Molecular Orbital
LFP	Laser Flash Photolysis
LUMO	Lowest Unoccupied Molecular Orbital
MIMS	Membrane Introduction Mass Spectrometry
MS	Mass Spectrometry / Mass Spectrometer
NMR	Nuclear Magnetic Resonance
PCB	Polychlorinated Biphenyl
PDMS	Polydimethylsiloxane
Φ	Quantum Yield
SVOC	Semi-Volatile Organic Compound
TLC	Thin Layer Chromatography
UV-Vis	Ultraviolet-Visible
VOC	Volatile Organic Compound
YAG	Yttrium Aluminum Garnet

Acknowledgements

I would like to thank Dr. Peter Wan for his assistance, guidance and support in the experiments conducted at UVic and Dr. Erik Krogh, Dr. Chris Gill and Skye Creba for their help and guidance with the MIMS work at Malaspina Univeristy-College. The research groups at both UVic and Malaspina were also instrumental in helping me to finish my project. Their kindness, humour and friendship are most appreciated. And finally, I would like to thank my husband David and the rest of my family for their love and support.

Chapter 1

Introduction

1.1 Overview of Environmental Photochemistry

While ground state chemistry is concerned mainly with bond cleavages where the input of energy (if needed) is heat, photochemistry involves the absorption of electromagnetic energy in the form of photons to induce chemical changes. The absorption of a photon by a molecular species provides the necessary energy to promote an electron from a bonding or non-bonding orbital into an antibonding orbital (example; $\pi \rightarrow \pi*$ or $n \rightarrow \pi*$), giving rise to an electronically excited state from which reaction can occur.[1]

Environmental photochemistry is a sub-discipline of photochemistry that focuses on the phototransformation of materials at the Earth's surface (or in the atmosphere) where the incident solar radiation is predominantly in the range of 290 - 600 nm. This type of photochemistry can either be described as direct or indirect, where direct photolysis involves a chromophore absorbing a photon to reach the excited state while indirect photolysis refers to the creation of an excited state via energy transfer.[1] Both direct and indirect photolysis can induce chemical transformations which are considered either deleterious or beneficial to the environment according to the human perspective.

An example that is considered detrimental is polychlorinated biphenyls (PCBs), which are anthropogenic molecules that bioaccumulate and are known to act as carcinogens. When photolysed in aqueous media, model PCBs dechlorinate with

substitution of the chlorine by an OH group (from water; photosolvolysis), yielding chlorohydroxybiphenyls as major (or exclusive) products.[2-5] Machala *et al.*[6] have shown that the toxicity of these chlorohydroxybiphenyls is responsible for some tumour development in biological organisms. In contrast, there are many kinds of natural photochemical reactions where the end product has no adverse effect on the environment. In fact, many of these reactions are essential to the functioning of natural systems. A prime example is photosynthesis which is essential to life.

One important area of environmental photochemistry involves the photo-transformation of humic substances. This topic is briefly outlined in this introduction, with emphasis on the photoreactivity of specific functional groups relevant to the body of work presented in the following chapters.

1.2 Humic Substances and Chloromethane Formation

Dissolved organic matter (DOM) is a class of natural organic materials containing molecules derived from detritus or organisms in the environment. Humic substances are the largest component of DOM[7, 8], and include a large assemblage of complex chemical structures characterized by the presence of polyphenols, carboxyls, methoxyls, quinones, carbohydrate and peptide functionalities. [9-12] The structural features of humic substances are known to depend on the nature of various terrestrial and aquatic inputs as well as a variety of conditions and natural processing. An example of a structural representation of a humic substance meant to convey the elements, structures and functionalities consistent with the observed composition and properties is shown by structure **1**.[13]

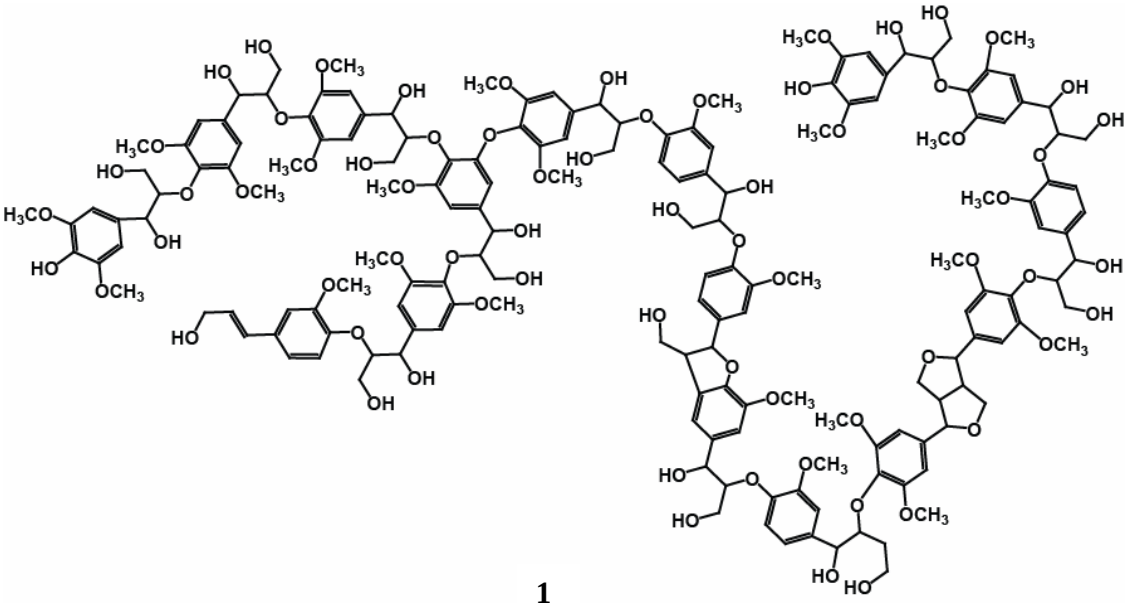

1

Humic substances are ubiquitous and play very important roles in the functioning of natural systems by interacting with inorganic or organic species in aquatic environments. In this manner, they are known to influence the distribution and transport of various chemicals, some of which are considered to be pollutants by human standards.[9] Furthermore, Rook has demonstrated that chlorine-treated natural waters containing humic substances can produce chloroform and other disinfection by-products.[14]

In addition, humic substances can strongly absorb or attenuate sunlight, thereby photoinducing the transformation of non-absorbing organic species or reacting via direct photolysis.[7, 10] An example is found in the work done by Forest *et al.*,[7] where they studied catechin (**2**) and hydroxybenzhydrols as models for the environmental photochemistry of tannins and lignins (humic substance models). They found that **2** underwent a reversible photoisomerization to epicatechin (**3**), representing a

photochemical reaction that enables **2** to act as a natural sunscreen without producing by-products (Equation 1.1).

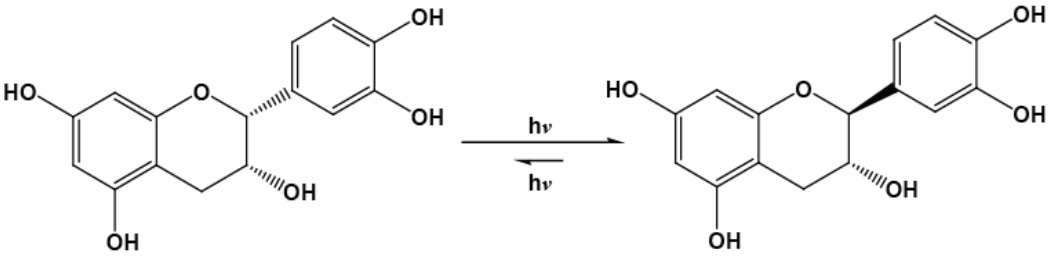

(1. 1)

3 **2**

Through their ability to absorb sunlight, humic substances are also known to act as sensitizers or precursors for the production of hydroxyl radicals[10], singlet oxygen ($^1O_2$) [15-17], solvated electrons ($e^-_{(aq)}$)[18-21], $O_2^{\bullet -}$ [22, 23], $CO_2^{\bullet -}$[24-28] and hydrogen peroxide[10]. Laser flash photolysis (LFP) studies have shown that humic substances from soils and natural waters produce $e^-_{(aq)}$ upon absorption of near UV radiation.[21, 29, 30] In addition, polyhydroxy aromatic compounds[31, 32] and carboxylic acids[33] are also known to photoproduce $e^-_{(aq)}$. The importance of the $e^-_{(aq)}$ is that they are highly reactive and strongly reducing species[34] that react with a variety of inorganic or organic electron acceptors such as O_2 and H^+ or molecules that contain electronegative atoms. These reactions can lead to the formation of other reactive species (such as hydrogen peroxide or hydroxyl radicals) (Scheme 1. 1).[35]

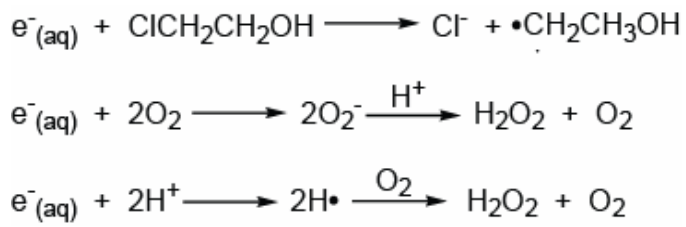

Scheme 1. 1

Besides the formation of the reactive species discussed above, humic substances are also known to release methanol into the environment.[36] Methanol is the second most abundant organic gas in the atmosphere after methane, with emissions equaling roughly 6% of the identified terrestrial biogenic organic carbon found in the mid to upper troposphere.[36] The predominant sources of this chemical in the atmosphere are from plant growth and decay, and biomass burning, while atmospheric oxidation of CH_4, vehicles and industrial activities play a much smaller role.[37] The lifetime of methanol in the surface boundary layer (i.e. the region of the troposphere up to the region where weather patterns exist) is approximately 3 to 6 days where the lifetime due to reaction with gaseous hydroxyl radicals (HO) alone is roughly 19 days.[36] Methanol is a significant atmospheric source of formaldehyde through its reaction with HO, where hydrogen radicals and ozone are also formed to a smaller extent. Photochemically, methanol can also be a source of formic acid.[38, 39]

Humic substances are also active in photochemical reactions where halomethanes (CH_3I, CH_3Br and CH_3Cl) are formed in seawater.[40] These reactions are presumed to involve the aromatic methoxy groups on DOM lignin precursors where halo-radicals and methyl radicals from humic substances may be responsible for the production of

halomethane.[41] Studies of humic substances in lake waters[42] and in coastal seawater[41] show that there are detectable fluxes of methyl and acetyl radicals. Other mechanisms of formation of these halomethanes from humic substances are presently unknown although there is growing interest in the topic.[43]

The global significance of humic substances in the formation of halomethanes is that these volatile compounds are capable of resulting in the net transfer of halogens from surface marine waters into the lower and upper atmosphere.[40] With a tropospheric lifetime of roughly 1.5 years, CH_3Cl is long lived enough to migrate into the stratosphere, whereupon it is exposed to high energy photons capable of homolytically cleaving the carbon-halogen bond. The chlorine radicals thus formed participate in a catalytic cycle resulting in net ozone loss (Scheme 1. 2).[44, 45]

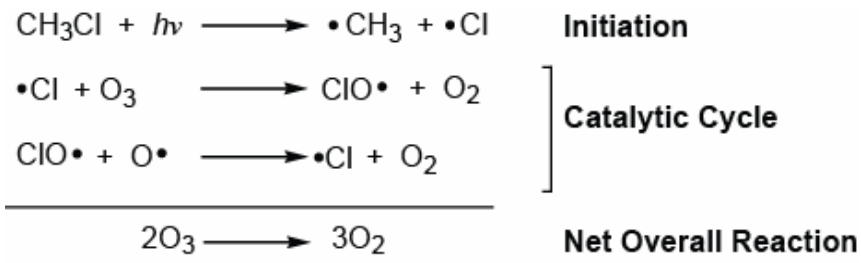

Scheme 1. 2

Among CH_3I, CH_3Br and CH_3Cl, the latter is the most abundant halomethane in the atmosphere due to its higher volatility and low chemical reactivity (compared to CH_3I and CH_3Br). When compared to other chlorine containing compounds, CH_3Cl is responsible for approximately 16% of the chlorine-catalysed ozone destruction in the stratosphere.[46, 47]

Despite their significant health and deleterious environmental effects, all three of the above mentioned halomethanes are used in industry. CH_3Br and CH_3I are both used as soil and space fumigants to control fungi, nematodes and weeds.[48-51] Additionally, both chemicals are used in various chemical manufacturing processes, such as methylating agents.[49, 50, 52] CH_3Cl is used in the production of methylated silicones and in the production of agricultural chemicals, methyl cellulose, quaternary amines and butyl rubber, and was at one time used as a refrigerant until it was replaced with Freon.[49, 53]

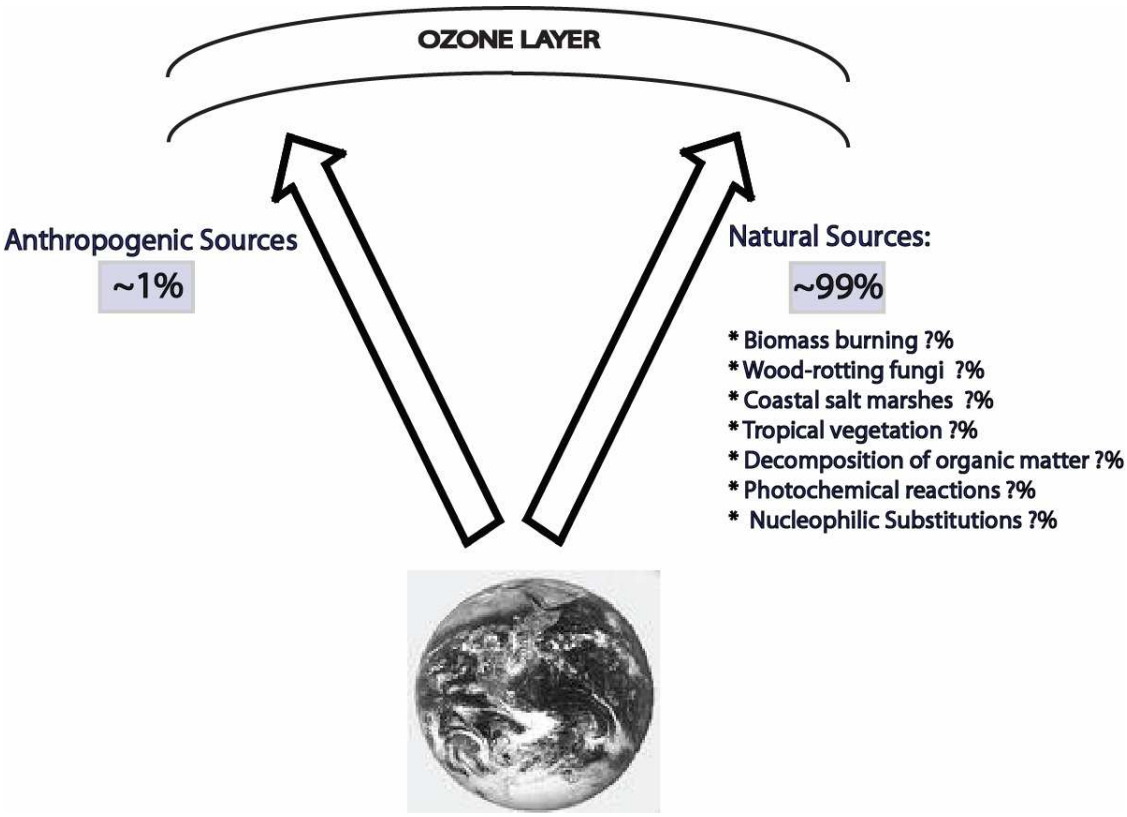

Figure 1. 1 Relative proportion of the natural and anthropogenic sources of chloromethane that cause ozone depletion.

As the destructive nature of CH_3Cl was revealed, large reductions were mandated under the Montreal Protocol[54] and as such, the amount of anthropogenic CH_3Cl reaching the atmosphere has dropped to 1 % of the total CH_3Cl flux to the ozone layer (

Figure 1. **1**). As a result, natural sources of CH_3Cl in the atmosphere now play a proportionately larger role in global stratospheric ozone depletion.[46] For this reason it is important to gain a better understanding of the natural sources and methods of formation of compounds such as CH_3Cl.

Natural sources of CH_3Cl include both biotic and abiotic contributions.[40] The most important biotic sources include biomass burning[55, 56], wood-rotting fungi[57], coastal salt marshes[58], tropical vegetation[59] and the decomposition of organic matter[60], where total ocean sources account for 9 - 11%[61]. Although a number of sources of CH_3Cl have been identified, the exact proportion of each is currently unknown. The abiotic transformation of both CH_3I and CH_3Br by nucleophilic substitution reactions with chloride ion in marine environments is responsible for additional CH_3Cl production. [40] It has been estimated that in the Pacific Ocean, CH_3I[62] and CH_3Br[63] could account for approximately 15% and 20% of the CH_3Cl flux to the atmosphere, respectively. In addition to the relatively large amounts of CH_3I and CH_3Br released from their industrial and agricultural uses, both CH_3I and CH_3Br have been shown to be produced from micro and macroalgal sources[40].

Despite a fairly thorough knowledge of where CH_3Cl occurs naturally, many of the processes for its production are poorly understood. As mentioned previously, one specific source of halomethane is from the photolysis of humic substances in natural waters.[41, 43] Due to the ubiquitous nature of humic substances, their reactivity in forming

CH_3Cl may be very important in the overall flux of this ozone depleter into the atmosphere. As a result, a thorough understanding of this process gains importance in the overall understanding of the sources of CH_3Cl.

1.3 Photochemistry of Syringic Acid and Syringyl Moieties

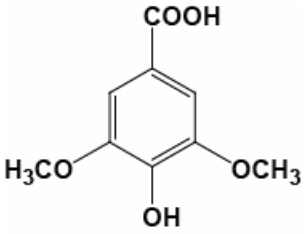

4

Syringic acid (**4**) has been identified as a component in the production of humic substances in the soil[43] and is known to be released during wood degradation by white-rot fungi.[40] It originates from syringylpropane, a component of angiosperm lignin,[64-66] with syringyl residues found in humic substances formed under deciduous hardwood vegetation.[11] Due to its structural similarity to the chemical moieties found in humic substances, **4** is a useful model for their reactivity in the environment. Previous work by Moore[43] has identified **4** as an important molecule and model humic substance for the photochemical release of halomethanes into the atmosphere and eventual input into the stratosphere. However, the mechanism for this transformation is unknown. In order to gain an understanding of the photochemistry of **4** and other compounds with the syringyl moiety (i.e. 1,3-dimethoxy-2-hydroxy-substituted benzenes), this section includes a brief overview of some of the known photochemistry of this suite of compounds. For brevity,

only those compounds deemed relevant to this work have been included in this discussion.

By using purge and trap GC/MS techniques, Moore[43] demonstrated that when **4** is photolysed at 254 nm in either seawater or water supplemented with Cl^-, CH_3Cl is formed. In addition, Moore demonstrated that the methyl group of the CH_3Cl comes from **4** by using isotope labeling studies. Specifically, when deuterated **4** (**4-d**) was photolysed, there was a detectable production of CD_3Cl by GC/MS (Equation 1.2).[43]

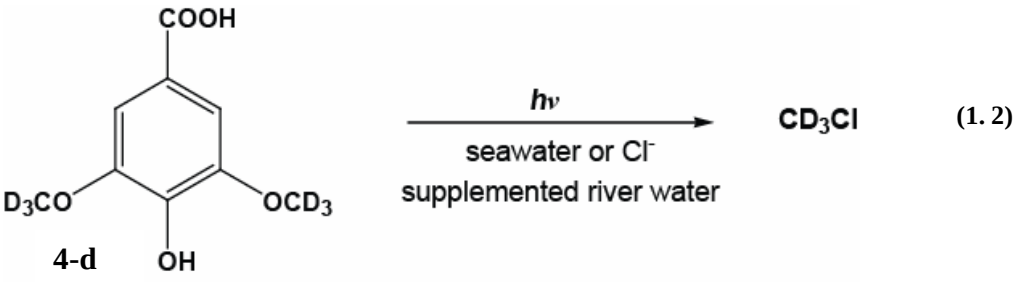

(1. 2)

Other important work on 4 was done by Stalin *et al.*,[67] where they studied the photophysics of 4 in various solvents and pHs. Using fluorometric studies to observe the shifts in the maximum absorption compared to similar compounds, the authors showed that 4 exhibits intramolecular hydrogen bonding between the phenol hydrogen and an adjacent methoxy group (Scheme 1. 3). When this effect was analyzed at different pH values, the authors were able to show that there is intramolecular hydrogen bonding present up to pH 9, at which point the phenol deprotonates (corresponding with the value of pKa_2 for 4). Shown in Table 1. 1, are the pK_a and pK_a^* (for the singlet excited state) values as determined by the authors using fluorometric titration.[67]

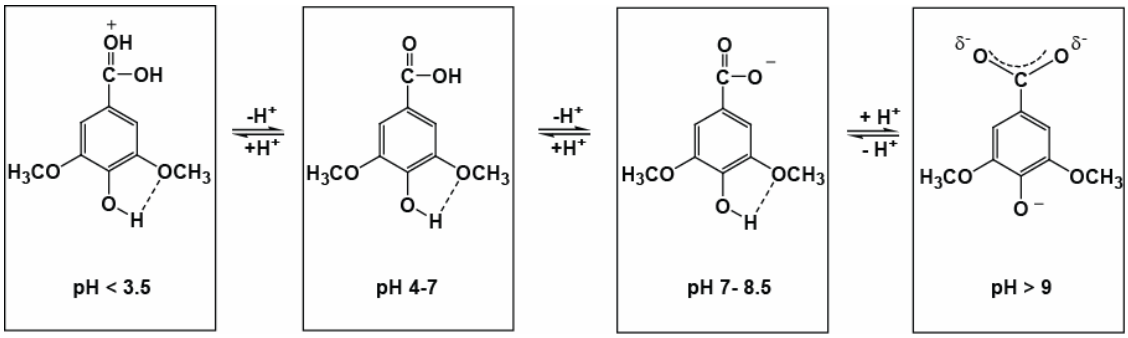

Scheme 1. 3

Table 1. 1 Acid dissociation constants for **4** in the ground and excited states. (adapted from Stalin).[67]

Equilibria	pK_a	pK_a^*
neutral ⇌ monoanion (pKa_1)	4.30	6.90
monoanion ⇌ dianion (pKa_2)	8.90	8.60

Another important paper in syringyl moiety photochemistry involves the substituted stilbene, β-*O*-4-aryl ether lignin **5**, where photochemical degradation leads to the formation of an *o*-quinone **6** (Equation 1.3).[68] The reaction is believed to involve a photoinduced redox degradation, where the aerobic production of phenoxyl radical intermediates can further react to form the *o*-quinones. The *o*-quinone product **6** is thought to be responsible for the photoyellowing that occurs in lignin-based paper products.[68]

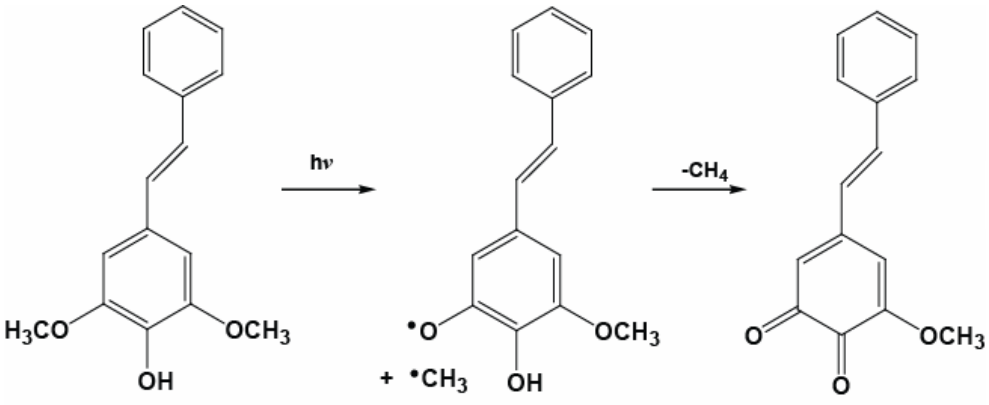

(1. 3)

5 **6**

Lanzalunga *et al.*[69] studied a suite of lignin model compounds including sinapyl alcohol **7** and *trans*-4-hydroxy-3,3',4',5-tetramethoxystilbene (**8**), both of which incorporate aspects of the syringyl moiety. The purpose of their study was to review the mechanistic aspects of the photochemistry of lignin model compounds in relation to lignin degradation and colour reversion (photoyellowing) of lignin based paper products.

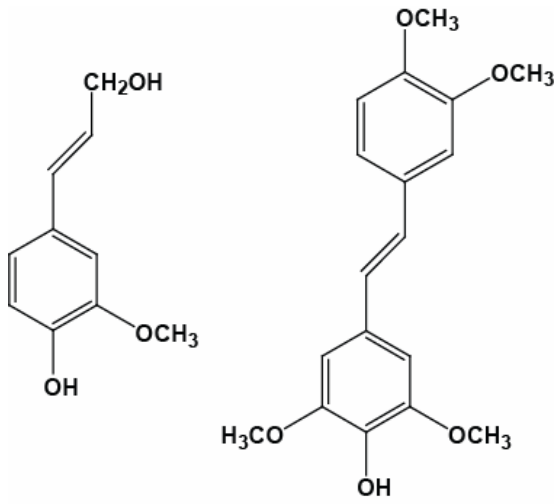

7 **8**

Photolysis of **7** in CH_2Cl_2 and *t*BuOMe solutions (300 nm) (Scheme 1.4) led to a series of products including those from the isomerization of the alkene (path **a**) and demethoxylation of **7** (path **b**). The demethoxylation pathway was attributed to the formation of a phenoxyl radical (**9**) which was able to initiate the loss of the methoxy group, leading to the catechol product **10**. The authors also believed that the phenoxyl radical is responsible for the formation of oxidized monomeric and oligomeric products.

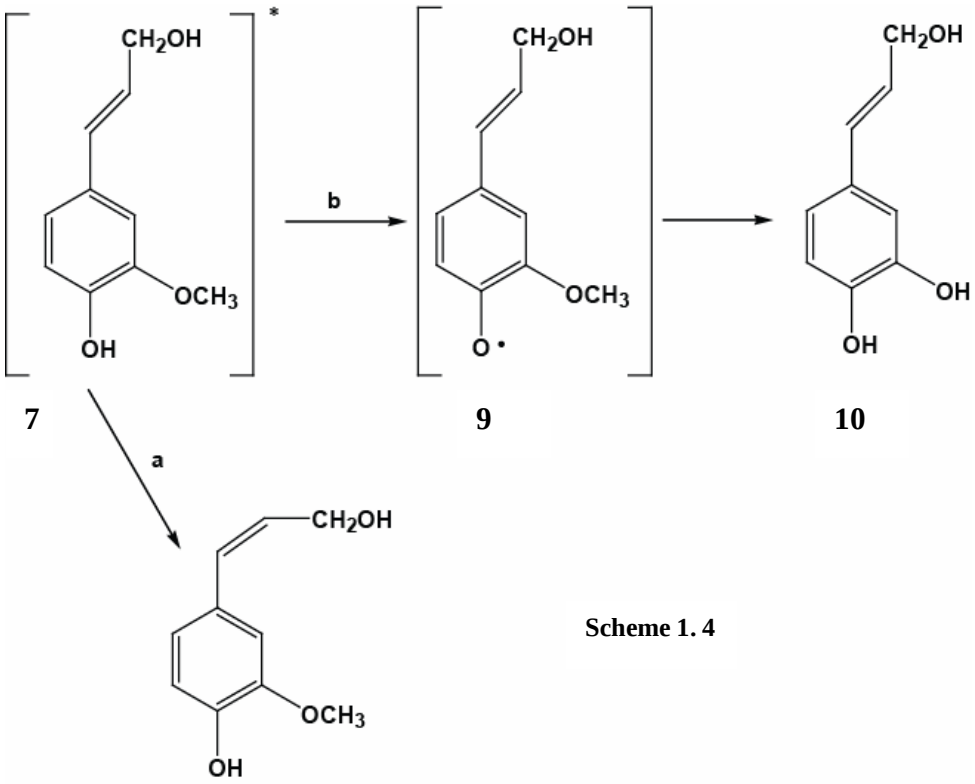

Scheme 1. 4

For **8**, the dominant photochemistry involves [2π + 2π] cycloaddition between an excited and ground state molecule to form a series of tetraphenylcyclobutanes. Other photochemistry of **8** led to the formation of a stilbene *o*-quinone **11** (Scheme 1. 5). It is

proposed that the formation of this quinone is through an electron transfer process between an excited and ground state **8** to form a radical anion **12** and radical cation **13**. It is then postulated that **13** loses a hydrogen atom from the phenol to form the phenoxyl radical cation **14**. Through resonance, this phenoxyl radical can then situate the cation on the aromatic ring, at which point water can attack nucleophilically to eventually demethoxylate and form **11**.

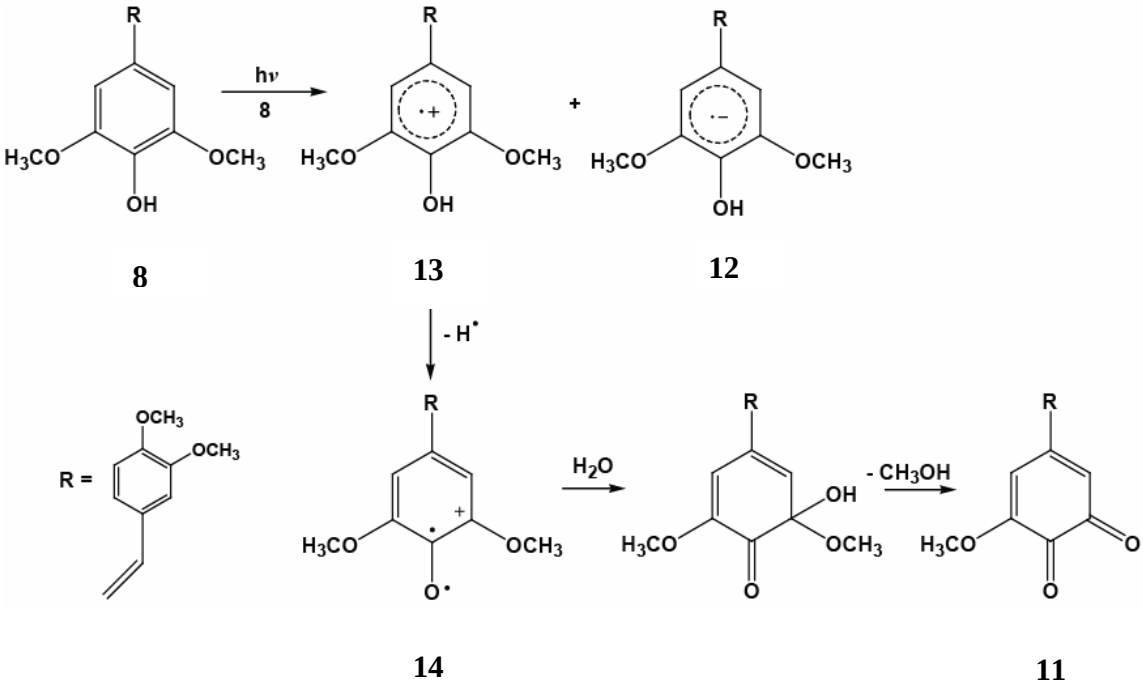

8 **13** **12**

14 **11**

Scheme 1. 5

Another compound with the syringyl moiety found in the literature was 2-hydroxy-1,3-dimethoxybenzene (**15**). Gadosy *et al.*[70] have shown that **15** rapidly loses a hydrogen atom in water to form phenoxyl radicals. This is a fairly well known photochemical reaction in which phenols will rapidly form phenoxyl radicals, often

through a radical cation intermediate resulting from an electron transfer. This topic is discussed in more depth in Section 1.5.

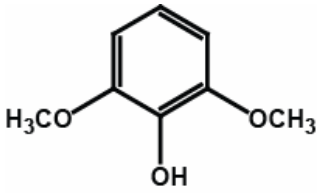

15

1.4 Photochemistry of Methoxy-Substituted Aromatic Compounds

Much of the known photochemistry of methoxy-substituted aromatics involves the excited state *ortho/meta* activating characteristics of the methoxy group in photochemical nucleophilic substitutions (Section 1.4.1).[71] Another important area of aromatic photochemistry involves photoprotonation of the aromatic ring and will be presented in Section 1.4.2.

1.4.1 Photosubstitution

Photosubstitution reactions involve substituted aromatic moieties (generally benzene) in the excited state, where a leaving group is replaced with an incoming nucleophile. This mechanism is in contrast to the type normally observed in the ground state, where electrophilic aromatic substitutions predominate.[72]

When electron donating substituents such as OCH_3 or NH_2 are present, mechanisms involving an Ortho-Meta Effect[73-75] intermediate are often observed.

Zimmerman[73-75] defined the Ortho-Meta Effect as transmission of electron density between *meta* substituents on benzenoid compounds in the singlet excited state. This is in contrast to the electron density distribution typically observed in ground state molecules. For instance, in the ground state, the methoxy group is an *ortho/para* director, but in the excited state that tendency changes so that the activation is to the *ortho* and *meta* sites.[76] In particular, Zimmerman[74] found that cationic intermediates are selectively stabilized by *meta*-methoxy groups as compared to *para*-methoxy substituents, while the corresponding *meta*-substituted radicals are at a higher energy than the comparable *para*-substituted analogs.

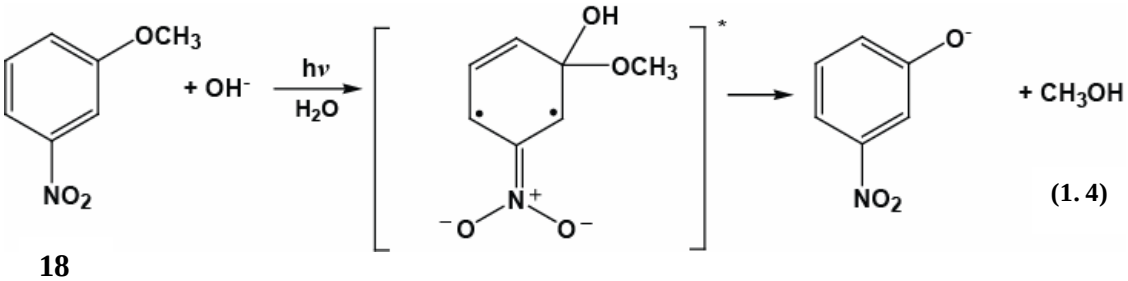

18 **(1. 4)**

An example of this is for *meta* (**18**) and *para* (**19**) nitroanisoles (Equation 1.4 and Equation 1.5). [77, 78] In Equation 1.4, the nitro group is acting as a *meta* director, thereby allowing nucleophilic substitution to occur at the *meta* methoxy group. When the nitro group is lacking a *meta* substituent, the yield of the reaction is drastically reduced since there is nothing to allow activation of the nitro site from the re-distribution of electron density. In the case of Equation 1.5, there is enough electron donation from the methoxy substituent to allow substitution of the nitro group, but in general this is not a very high yielding reaction (in comparison to its *meta* counterpart). Of particular interest in these

reactions is that the nucleophile in each is hydroxide ion, not water. In general, the neutral nucleophiles ethanol, acetic acid, acetate ion and water are unreactive towards photoexcited anisole as the nucleophilicities are not great enough to allow reaction to occur.[79]

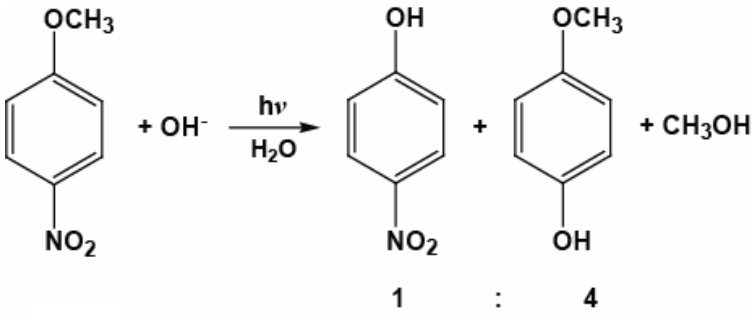

19 **(1.5)**

A good example of excited state *ortho/meta* selectivity is the conversion of 1,2-dimethoxy-4-nitrobenzene (**20**) to 2-hydroxy-4-nitroanisole (**21**) via an Ortho-Meta Effect photosubstitution with hydroxide ion. This shows that the methoxy *meta* to the nitro group is more activated towards nucleophilic substitution than the methoxy in the *para* position (Equation 1.6).

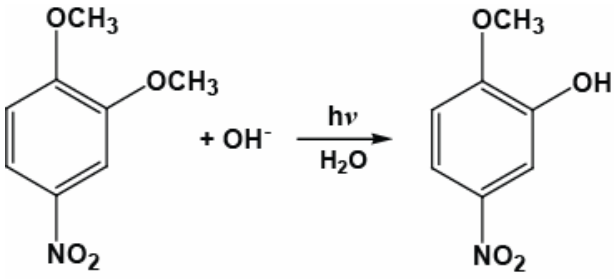

20 **21** **(1.6)**

Another type of aromatic photosubstitution mechanism is known as the $S_{R+N}1Ar^*$ reaction, where the excited state compound loses an electron to either the solution or another molecule thus producing a radical cation intermediate (e.g. **22**) (Scheme 1.6).[72] This intermediate facilitates the attack of a nucleophile onto the aromatic ring, resulting in the formation of a neutral σ–complex **23**. Loss of the leaving group produces a second radical cation **24**, which may gain an electron from a ground state substrate (ArL) to yield the substituted product. [76, 80]

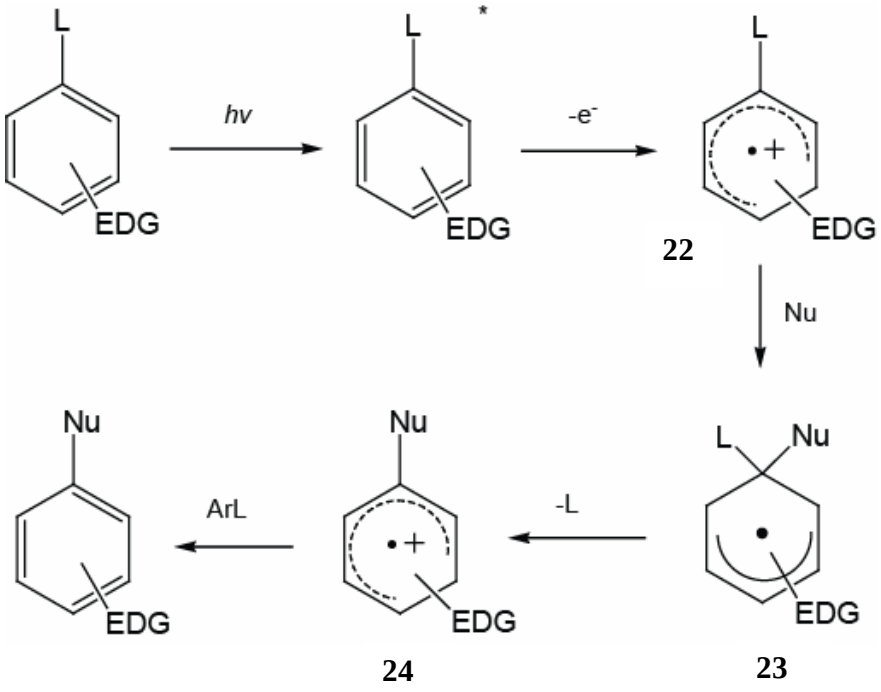

Scheme 1. 6

The photosubstitution of *p*-dimethoxybenzene (**25**) and *p*-haloanisoles **26** with CN^- are examples of reactions that have been shown to involve the $S_{R+N}1Ar^*$ mechanism as described in Scheme 1.6 (Scheme 1.7).[76] Den Heijer *et al.*[76] state that while the

formation of a radical cation is normally a two photon process, this type of photosubstitution proceeds via single photon absorption, evidenced by the lack of dependence of the quantum yield on the intensity of the incident radiation.

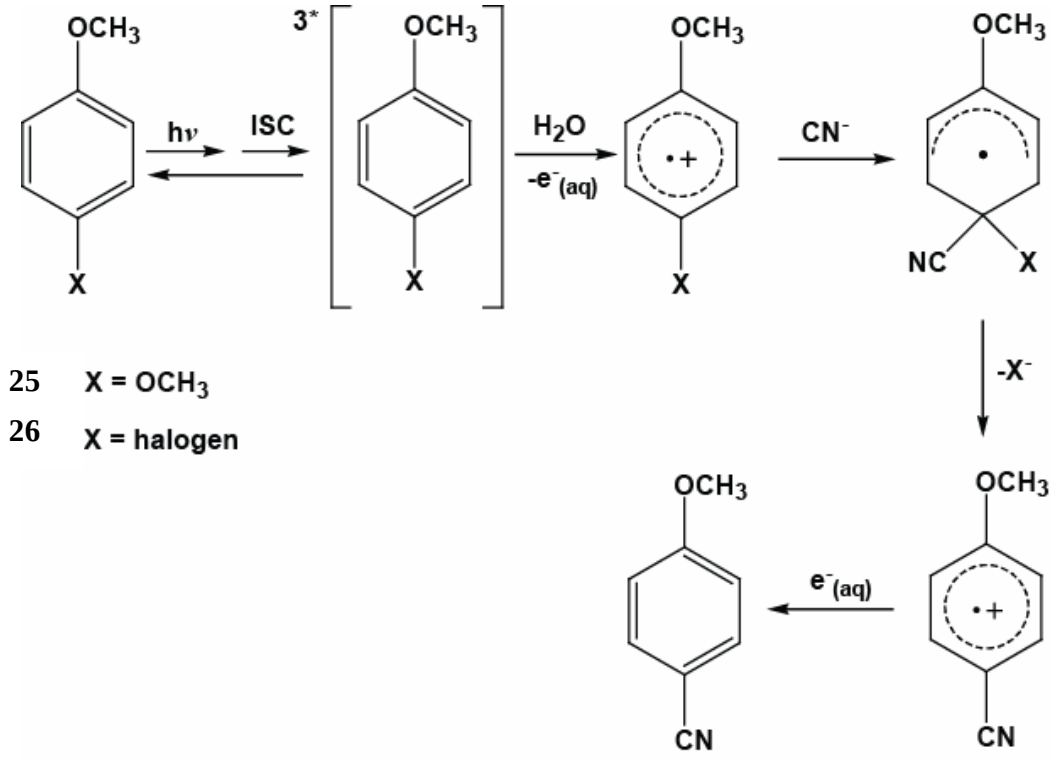

Scheme 1. 7

1.4.2 Photoprotonation

Electrophilic aromatic substitution reactions are very well known reactions. One fundamental reaction of this type is hydrogen exchange on the aromatic ring where there is electrophilic attack by a proton.[81] In general, this can be viewed as an acid-base reaction, where the aromatic ring is acting as the base. Due to the low basicity of the aromatic ring in the ground state, this reaction can be difficult to observe. In the singlet

excited state however, there is often an increase in the basicity of the ring which makes this reaction more favourable.[81]

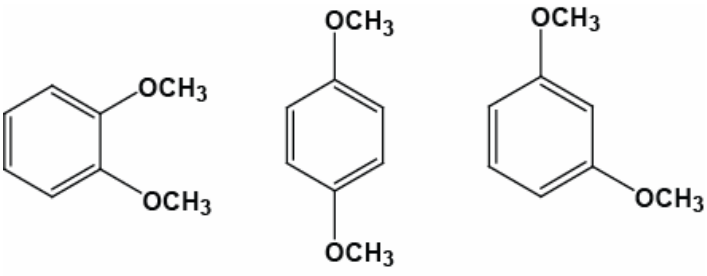

27 **28** **29**

Wan and co-workers[81] studied the photoprotonation of 1,2-dimethoxybenzene (**27**), 1,4-dimethoxybenzene (**28**) and 1,3-dimethoxybenzene (**29**). All three compounds showed photoprotonation in acid (pH < 2) as demonstrated by isotope labeling studies which revealed exchange of ring protons in the reaction product (Equation 1.7). In addition, **27** exhibited ipso substitution of the methoxy group by water (Equation 1.8) as shown by product studies and ^{18}O labeling experiments.

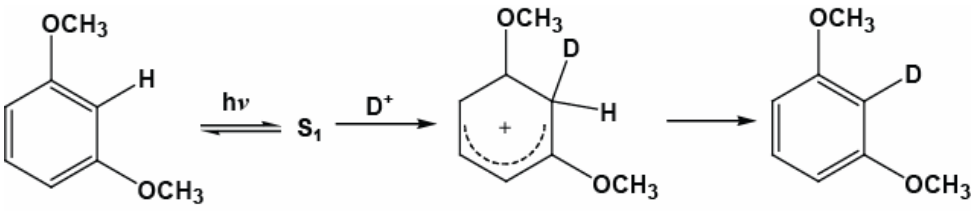

(1. 7)

29

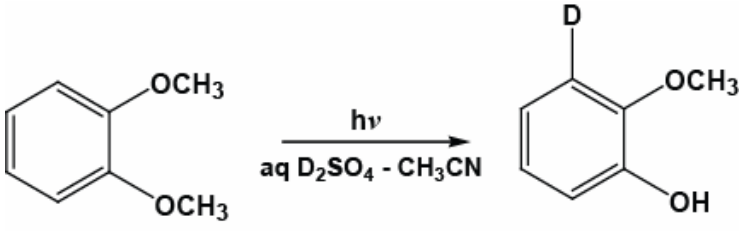

27 **31-d** **(1. 8)**

The proposed mechanism (Equation 1.9) for the methoxy exchange by water involves an initial photoprotonation step as shown by fluorescence quenching and catalysis of the reaction by acid. This initial photoprotonation led to the cyclohexadienyl cation intermediate (**30**) which facilitated ipso attack by water to yield deuterated 2-methoxyphenol (**31-d**). Neither **28** nor **29** showed any product from the ipso attack by water even though this was not suspected to occur. It was proposed that a longer reaction time was needed for those compounds to accumulate the ipso substituted product, and as such they were not observed in the time scale of the experiment. Compound **27** was found to have an order of magnitude higher reactivity for the photoprotonation which could have led to more efficient detection of **31-d**. In addition, it was proposed that the *ortho* methoxy groups had an influence on the basicity of the photoprotonation site, making it more basic and thus more highly reactive for the photoprotonation.

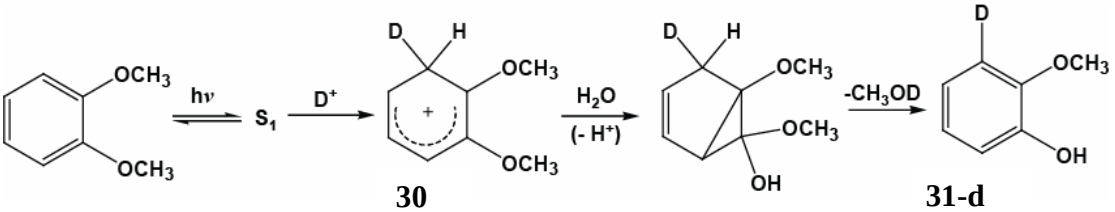

30 **31-d** **(1. 9)**

1.5 Photochemistry of Phenols: Phenoxyl Radicals

The photochemistry of phenols is varied and immense, but one topic of phenol photochemistry that is relevant to humic substances is the formation of phenoxyl radicals in aqueous media. In the presence of water, phenols can photochemically form radical cations that can easily decay via deprotonation to the phenoxyl radical.[82] The phenol radical cation is typically not observed due to its very low pK_a (< 0) in water (Equation 1.10).[83]

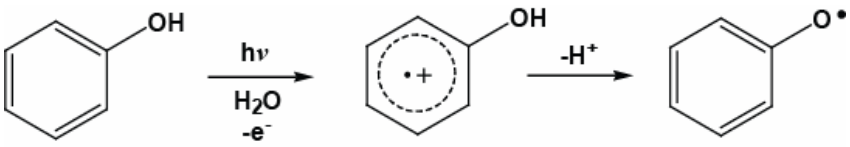

(1. 10)

Konya and Scaiano[84] have shown that *ortho*-methoxyphenols can lead to *ortho*-quinones via a two-photon process. One specific reaction involves 2-methoxyphenol (**30**) in which a phenoxyl radical is formed upon direct excitation or hydrogen abstraction. The absorption of a second photon then causes cleavage of the methoxy carbon – oxygen bond, allowing formation of the 1,2-benzoquinone (**32**) (Equation 1.11). This mechanism was elucidated using laser techniques to observe the transient species. Of note is that this reaction was only observed for *ortho* phenol – methoxy substituents.

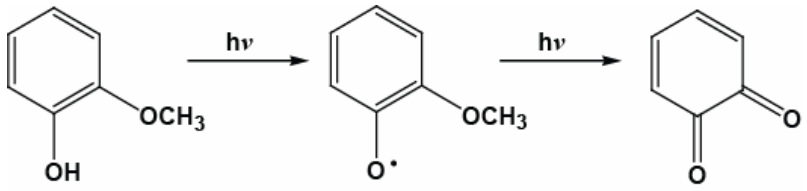

(1.11)

30 **32**

1.6 Proposed Research

As previously discussed, Moore[43] has identified CH_3Cl as a photoproduct when **4** is irradiated in aqueous media in the presence of chloride ions, however, the mechanism is unknown. Since compound **4** is a simple model for humic substances, it provides a good compound to investigate the natural production of CH_3Cl. As a known ozone depleter, it is important to understand how CH_3Cl is released via photolysis of **4**.

Chapter 2 discusses a series of product studies and other experiments designed to elucidate the aqueous photochemistry of **4**. The photochemistry of **4** was studied over a pH range of 2 – 10 to investigate the affect of pH on product distribution and probe the importance of the differing electron withdrawing capabilities of the carboxylate group in the protonated and deprotonated forms. To investigate the mechanism and probe the role of various substituents on **4**, a number of structurally similar compounds were also studied. In particular, 4-hydroxy-3,5-dimethoxyacetophenone (**33**) and methyl syringate (**34**) were investigated to determine the effect of a different withdrawing group as a replacement for the acid group in **4**. To elucidate whether the acid group in **4** was required for the observed photochemistry, 1,2,3-trimethoxybenzene (**39**) and 2-hydroxy-1,3-dimethoxybenzene (**15**) were also photolysed. These compounds were chosen since

the H in the site normally occupied by COOH in **4** was neither electron withdrawing nor donating (i.e., by definition, the Hammett substituent constant for H is 0.00).

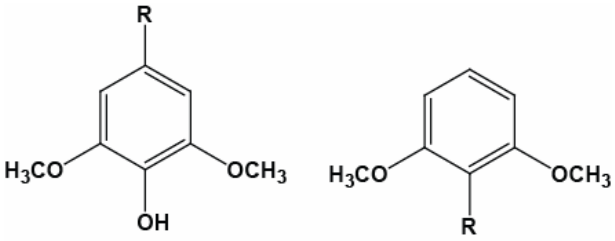

4	R = COOH	**15**	R = H
33	R = $COCH_3$	**35**	R = OCH_3
34	R = $COOCH_3$		

It was also important to determine if the combination of methoxy-hydroxy-methoxy groups was necessary for the photochemical release of CH_3OH. To investigate this, 3,4-dihydroxy-5-methoxybenzoic acid (**36**) and 3,4,5-trimethoxybenzoic acid (**37**) were photolysed under the same conditions as **4**. Finally, to determine if three donating groups on the ring were important, *m*-anisic acid (**38**) and 3,5-dimethoxybenzoic acid (**39**) were studied.

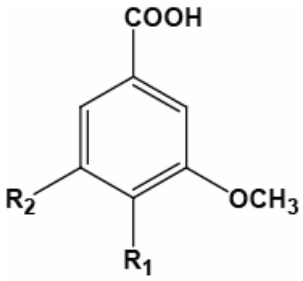

36	$R_1, R_2 = OH$
37	$R_1, R_2 = OCH_3$
38	$R_1, R_2 = H$
39	$R_1 = H$; $R_2 = OCH_3$

The identification of the aromatic photoproducts was achieved by using both ^{1}H NMR and Electrospray Ionization Mass Spectrometry (ESI-MS) in the negative ion mode. The ^{1}H NMR of isolated photoproducts and reaction mixtures were compared to authentic sample whenever possible. ESI-MS involved direct injection of the photolysis mixtures to identify specific reaction products at particular m/z ratios. In addition to the above mentioned product studies, LFP was also used to identify short-lived reaction transients to support the mechanisms for the photolysis of **4** and similar compounds.

Because CH_3Cl is a volatile product, it is rapidly lost from photolysis solutions. The production of CH_3Cl was thus continuously monitored in-situ using Membrane Introduction Mass Spectrometry (MIMS). The volatile photoproducts were circulated over a semi-permeable membrane, where they permeate the membrane and travel to an ion trap mass spectrometer. This work involved some analytical method development and is described in Section 2.3.

Chapter 2

Syringic Acid Photochemistry

2.1 Product Studies

2.1.1 Photolysis of Syringic Acid (4) in Aqueous Solution in the Presence of Cl^-, I^- and CN^-

The initial objective for this project was to deduce the mechanism of CH_3Cl formation during the photolysis of **4**, as observed by Moore, by carrying out detailed mechanistic studies using techniques developed in the Wan laboratory.[43] Preliminary experiments involved photolysing **4** in aqueous solutions in the presence of 0.5 **M** Cl^- under 300 nm irradiation (Note that the 0.5 **M** Cl^- was in all cases added as NaCl). Even though the maximum region of absorption for **4** was around 254 nm, 300 nm irradiation was chosen instead to better approximate the solar radiation that compounds like **4** would experience in the natural environment. The photolyses were performed in deuterated solvents (D_2O and CD_3CN) so that NMR spectra could be taken of the reaction mixture without workup, in an attempt to directly observe volatile photoproducts (referred to herein as "NMR scale photolysis"). The CD_3CN was used as a co-solvent to overcome the low solubility of the starting material in neat D_2O.

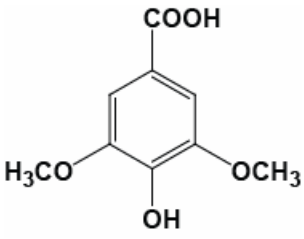

4

In an attempt to reproduce and confirm Moore's results (using NMR instead of GC/MS for analysis), **4** was photolysed in argon purged 0.5 **M** Cl^- solution using NMR scale photolysis (5:1 D_2O-CD_3CN, pD 7, 10^{-2} **M**, 300 nm lamps, argon purged before photolysis, < 15 ^oC, up to 10 hours with analysis at defined intervals). In addition, photolysis of **4** was conducted in aerated D_2O for 4.5 hours (same conditions as previously but with air purge prior to photolysis). The results of both of these experiments showed formation of a compound with a singlet at δ 3.36 ppm with very little change in the rest of the ^1H NMR spectrum. Although this was initially thought to be the methyl protons of CH_3Cl, a literature search revealed that the signal for CH_3Cl should actually be around δ 3.05 ppm. The appearance of the new singlet at δ 3.36 ppm was subsequently assigned to CH_3OH and confirmed by the addition of authentic CH_3OH added to the reaction solution. With no NMR evidence of CH_3Cl, this led to three conjectures; either CH_3Cl is not formed in sufficient quantities under the conditions employed to be detected by NMR, CH_3Cl is not formed at all or CH_3Cl is lost from solution due to its high volatility and relatively low water solubility. In this case, the CH_3Cl could have been lost from the system entirely or partitioned into the headspace of the reaction vessel.

High volatility as a possible explanation for the failure to detect CH_3Cl has validity since this compound is a gas at room temperature and is known to have very high volatility and low partitioning into the aqueous phase as measured by its vapour pressure (588 kPa at 25 ^oC)[1] and Henry's Law constant (K_H^o = 0.98 kPa m^3 mol^{-1} at 298.15K).[85] To overcome this, photolysis of **4** using the conditions described above was conducted in a closed system with a syringe used to transfer the reaction mixture directly into an NMR

tube using septa. However, this method also did not show formation of CH_3Cl upon photolysis of **4**.

If CH_3Cl was formed in the photolysis of **4**, but the technique described above suffered from material loss of CH_3Cl, then quantifying the amount of **4** reacted and the amount of CH_3OH formed could help quantify if any imbalance in the amount of reactant and product was present after photolysis. This could be accomplished by measuring the decrease in the methoxy signal integration of **4** at δ 3.89 ppm and the increase in integration of the signal for CH_3OH at δ 3.36 ppm by ^1H NMR relative to an internal standard. If the entirety of the decrease in the integration of the methoxy signal of **4** could be attributed to the formation of CH_3OH, then it would be unlikely that CH_3Cl was formed during the photolysis. Conversely, missing mass might indicate that CH_3Cl was forming, but was lost during the work-up.

To determine if there was a mass balance for the formation of CH_3OH, **4** was photolysed in 0.5 **M** Cl^- in non-aerated solution. When the ^1H NMR integrations of the methoxy signal for **4** at δ 3.89 ppm and the signal for the CH_3OH at δ 3.36 ppm from this photolysis were analysed, there was a measurable decrease in the relative amount of **4**, with an increase in the amount of CH_3OH over time. The results shown in Figure 2.1 depict a lack of mass balance for the photolysis of **4**. Besides the loss of CH_3Cl due to its high volatility, the missing mass could be from CH_3OH that evaporated out of the reaction vessel or NMR tube or other products that were not yet identified by NMR.

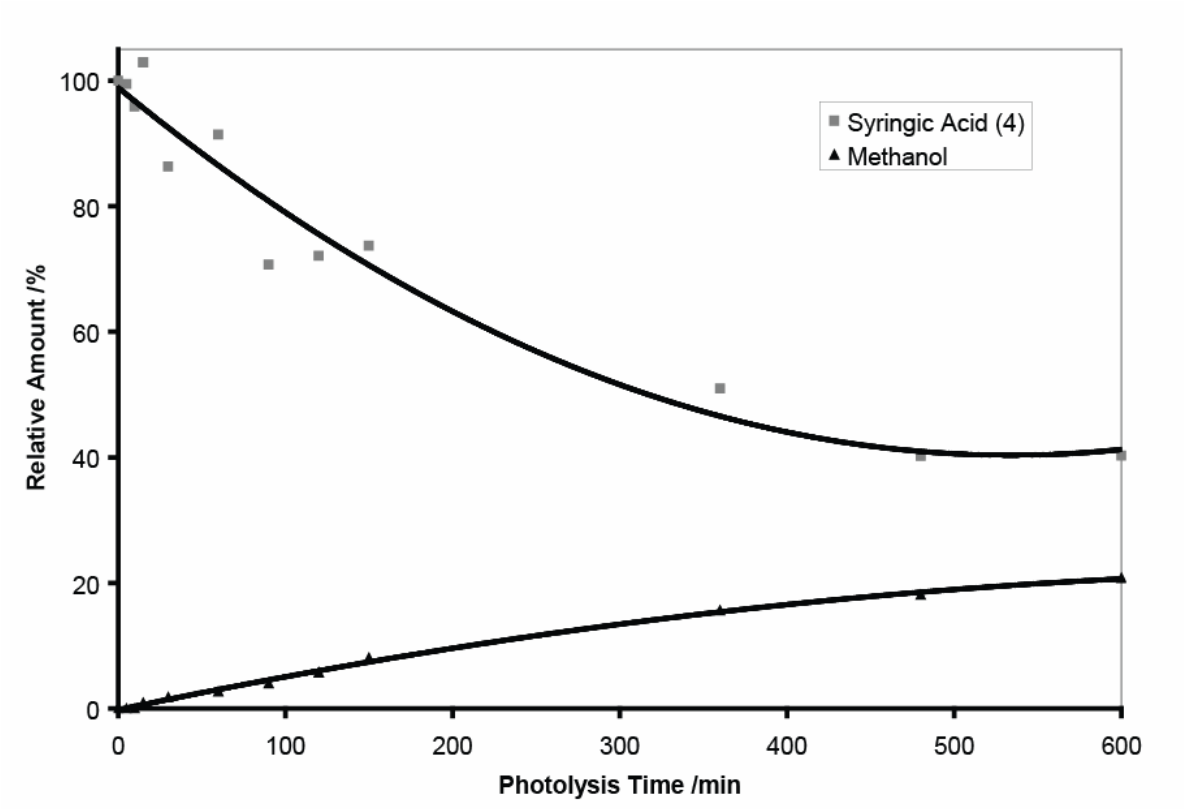

Figure 2. 1: Relative yields of syringic acid (**4**) and methanol production in the photolysis of **4** in 0.5 **M** Cl^- at pD 7 as measured by ^1H NMR integration of **4** at δ 3.89 ppm (OCH_3) and methanol at δ 3.36 ppm (relative to acetone internal standard).

Based on the results of the experiments described above, detection of CH_3Cl by NMR was not possible under the conditions used. Instead, it was postulated that if I^- was used instead of Cl^-, formation of CH_3I could be easily analyzed by ^1H NMR since CH_3I is relatively non-volatile (Table 2.1). When **4** was photolysed in 0.5 **M** I^- (added as NaI in all cases) (10:1 D_2O-CD_3CN, pD 7, 10^{-3} **M**, 300 nm lamps, argon purged before photolysis, < 15 ^oC, 3 hours) only CH_3OH was observed, with no evidence of CH_3I formation (which would be expected to appear at δ 2.2 ppm).

Table 2. 1 Selected physical constants of CH_3Cl, CH_3I, CH_3CN and CH_3OH.[86]

Compound	Vapour Pressure at 25 °C / kPa	Henry's Law Constant at 25 °C / kPa m^3 mol^{-1}
CH_3Cl	588	0.98
CH_3I	53.9	0.54
CH_3CN	11.9	-
CH_3OH	16.9	0.46

At this point we were unsure whether Cl^- and I^- were strong enough nucleophiles to allow the formation of the halomethanes under the conditions employed. Instead, CN^- was chosen as it has higher nucleophilicity than Cl^-, I^- or water (Table 2.2). In addition, the by-product of nucleophilic attack of CN^- would be CH_3CN if the reaction followed a similar pathway as for production of CH_3Cl, with the CH_3CN readily observable by ^1H NMR (at δ 2.0 ppm, miscible with water). When **4** was photolysed in 0.5 **M** CN^- (added as KCN in all cases) (9:1 D_2O-CD_3CN, pD 11, 10^{-3} **M**, 300 nm lamps, argon purged before photolysis, < 15 °C, 3 hours), only CH_3OH was observed with no detectable yield of CH_3CN.

Table 2. 2 Nucleophilicities of Cl^-, I^-, CN^-, OH^- and H_2O relative to water based on reaction with bromomethane. [1]

Compound	*n*
H_2O	0.00
Cl^-	3.0
OH^-	4.2
I^-	5.0
CN^-	5.1

Since CN^- is more nucleophilic than water, but did not form CH_3CN, the CN^- could have attacked the benzene ring instead, leading to the formation of CH_3OH. If this were the case, it should be possible to observe incorporation of CN onto the benzene ring of the photoproducts. Since the aromatic photoproducts were difficult to analyze using NMR scale photolysis (due to the small scale reaction these aromatic products were below the detection limit of the NMR), another type of experiment had to be designed. This involved photolysing a larger amount of **4** for a longer period of time, with **4** dissolved in a relatively larger volume of neat H_2O (the lower concentration of **4** meant that CH_3CN was not needed since solubility was not an issue). After photolysis, the photomixture was extracted with CH_2Cl_2 and dried with $MgSO_4$, followed by analysis using NMR or Electrospray Ionization Mass Spectrometry (ESI-MS; negative ion mode) to identify the products (this method is referred to herein as "preparatory scale photolysis").

To identify the photoproducts for the photolysis of **4** with CN^-, **4** was photolysed in 0.5 **M** CN^- in a preparative scale photolysis (H_2O, pH 11, 10^{-1} **M**, 300 nm lamps, argon purged before photolysis, < 15 ^oC, 3 hours). This revealed an assortment of photoproducts as identified by ^1H NMR and ESI-MS (negative ion mode) (Equation 2.1). The major masses identified were at 197, 183, 181, 178 and 191 g/mol corresponding to compounds **4**, **36**, **39** and CN adducts **40** and **41**, respectively, the latter being off by one mass unit, presumably due to the loss of a hydrogen atom (phenol OH) in the mass spectrometer.

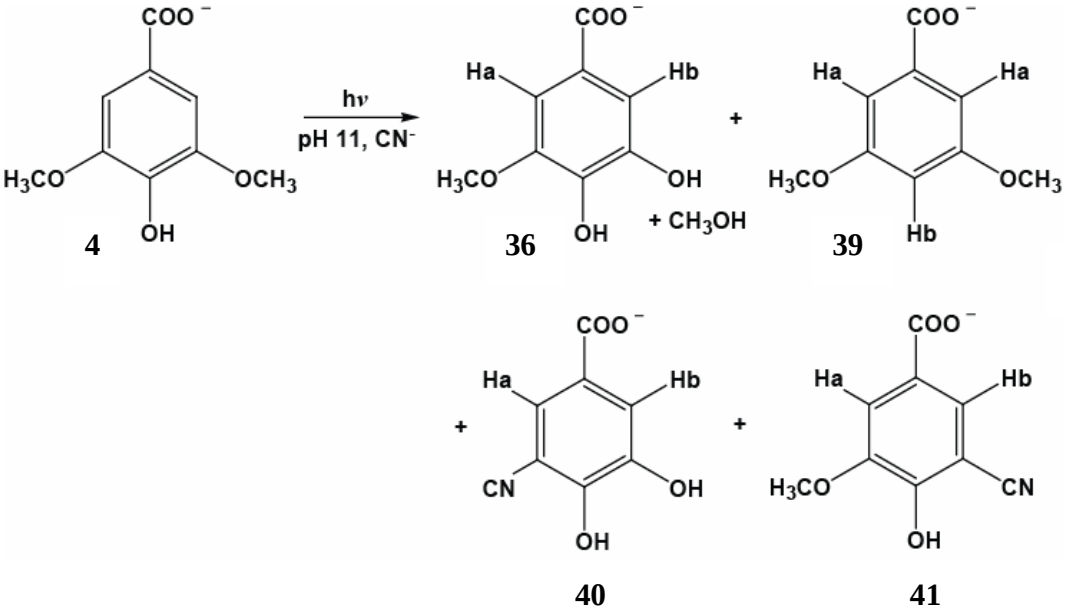

(2. 1)

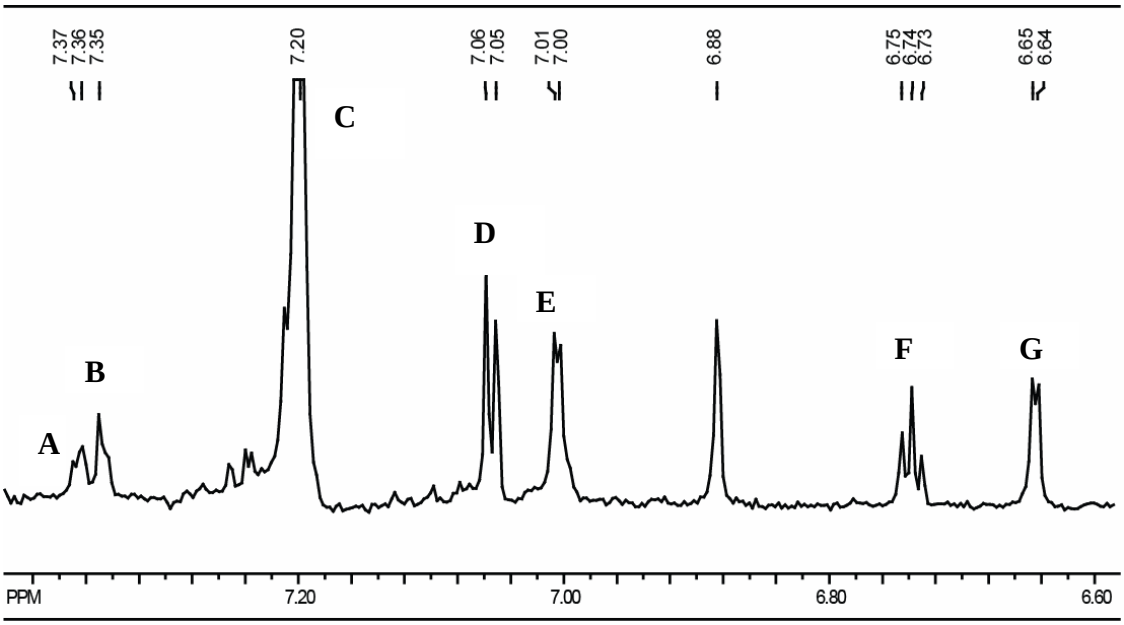

Figure 2. 2: 300 MHz ^{1}H NMR spectrum (aromatic region) in DMSO-d_6 for the 300 nm photolysis of **4** in 5:1 D_2O – CD_3CN at pD 11 in 0.5 **M** CN^-. Peaks **A** (H_a) and **B** (H_b) correspond to compound **40**; **C** to **4**; **D** (H_a) and **F** (H_b) to **39** and **E** (H_b) and **G** (H_a) to compound **41**, for the aromatic protons of each compound. Note that the aromatic signal for **36** was overlapped by the aromatic signal for **4** (peak **C**).

There was also evidence by ^{1}H NMR to suggest the formation of the CN adducts **40** and **41** by the identity of their masses by ESI-MS and postulated NMR shifts (Figure 2. 2). The signals at δ 7.37 ppm and δ 7.35 ppm can be assigned to the aromatic protons of **40** (H_a and H_b, respectively), while the signals at δ 7.01 ppm (H_b) and δ 6.65 ppm (H_a) can be assigned to the aromatic protons of **41**. The identity of the signal at δ 6.88 ppm is unknown. The relative yields are 8 %, 6 % and 7 % for compounds **39**, **40** and **41**, respectively (after 1 hour photolysis at 300 nm). Due to the overlapping of signals for **4** and **36**, it was not possible to determine the yield of **36**.

Based on the above studies, it was concluded that NMR analysis would not be useful for the detection of CH_3Cl or analogs. As will be discussed in Section 2.2, the CH_3Cl formation from the photolysis of **4** was eventually detected using Membrane Introduction Mass Spectrometry (MIMS). However, since the formation of CH_3OH from the photolysis of **4** was in itself a significant finding, the conditions necessary for its formation (and other photoproducts) was studied further using NMR (as described below).

2.1.2 Photochemical Formation of CH_3OH from Syringic Acid (4)

To further investigate the formation of CH_3OH in the photolysis of **4**, experiments were conducted in neutral aqueous conditions without added Cl^-, I^- or CN^-. NMR scale photolysis of **4** (5:1 D_2O-CD_3CN, pD 7, 10^{-3} **M**, 300 nm lamps, argon purged before photolysis, < 15 ^oC, 3 hours) gave CH_3OH (yield of ~ 12% for 1 hour photolysis) by ^{1}H NMR as measured by the signal at approximately δ 3.36 ppm (Figure 2. 3). As was the case for the photolysis of **4** in the presence of Cl^-, the CH_3OH was identified by spiking

with neat CH_3OH and showing that signals were overlapped at δ 3.36 ppm (the signal for CH_3OH varied in some reactions due to the different ratios of D_2O-CD_3CN).

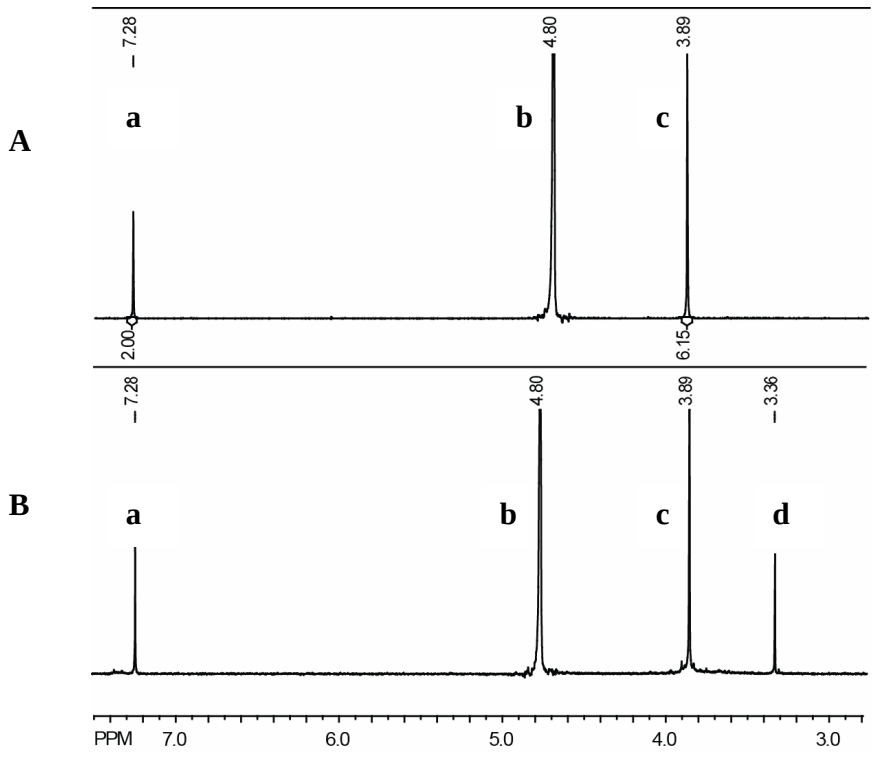

Figure 2. 3: 300 MHz ^{1}H NMR spectra in D_2O for the 300 nm aqueous photolysis of **4** at pD 7. **A**: Unirradiated **4**; **B**: **4** irradiated for 3 hours. Signal **a** (aromatic protons) corresponds to **4**, **b** is NMR solvent, **c** (methoxy protons) is from **4** and **d** corresponds to CH_3OH.

The quantum efficiency for the formation of CH_3OH was found to be dependant on water, requiring greater than 10% water for the reaction to be detectable by ^{1}H NMR (Figure 2. 4). Once the percentage of water reached approximately 40%, there was no further detectable increase in the yield of CH_3OH. This data is consistent with the requirement of water in the reaction, with the water likely acting as a nucleophile in the

formation of the CH_3OH. As such, it needs to be in sufficiently high concentration to allow reaction to occur. The data was obtained by measuring aliquots of the reaction mixture after 1 hour photolysis at 300 nm (non-aerated) for six different water concentrations ranging from 10 – 70 % D_2O. Acetone was spiked into each aliquot before analysis by ^1H NMR to act as an internal standard. The integration of the CH_3 protons of the CH_3OH (at ~ δ 3.4 ppm) was quantified relative to the integration of the acetone signal at δ 2.1 ppm. This ratio gave the relative CH_3OH production with 70 % D_2O normalized to 100% relative production for the photolysis of **4**.

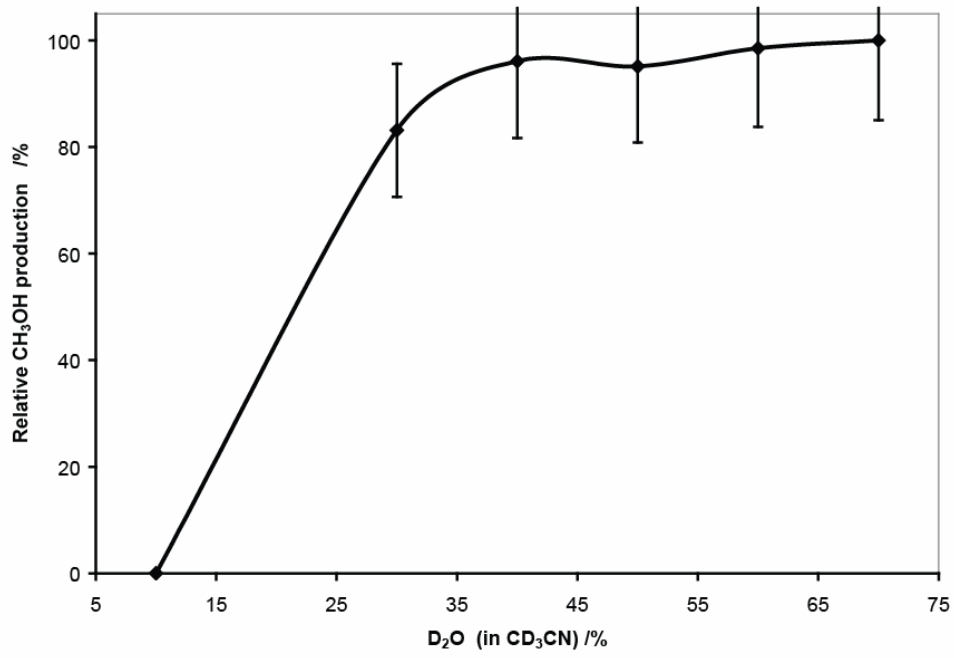

Figure 2. 4: Water dependence on the yield of CH_3OH in the photolysis of **4** in D_2O (CD_3CN co-solvent), 300 MHz ^1H NMR. Relative CH_3OH production corresponds to the integration of CH_3OH relative to acetone as an internal standard where the production of CH_3OH at 70 % D_2O was set to 100% relative production from the photolysis of **4**.

In order to determine the nature of the other products derived from **4**, a preparative scale photolysis of **4** was conducted. The products for the photolysis of **4** (H_2O, pH 7, 10^{-3} **M**, 300 nm lamps, argon purged before and during photolysis, < 15 ^oC, 2 hours; Equation 2.2) were identified by taking a ^1H NMR spectrum after extraction of the photomixture with CH_2Cl_2 and analyzing this crude mixture by ESI-MS. It was not possible to use preparative scale thin layer chromatography (TLC) with silica gel to separate the photoproducts due to the carboxylic acid moieties present on the molecules.

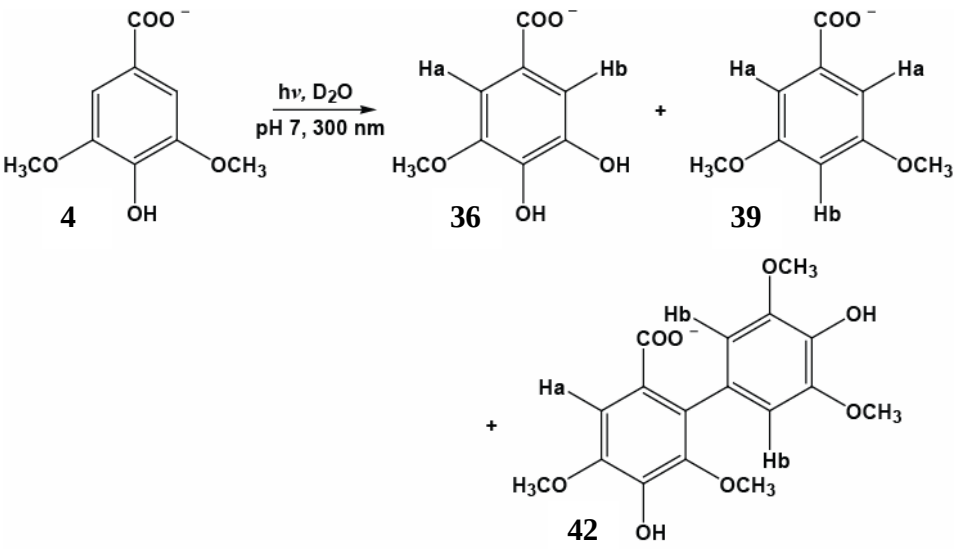

(2. 2)

The ESI-MS analysis of this reaction mixture in negative ion mode (in CH_3OH) revealed the mass for **4** at 196.9 g/mol with smaller intensity mass signals at 181.1, 182.9 and 349.3 g/mol for compounds **39**, **36** and **42**, respectively. The ^1H NMR spectrum (Figure 2. 5) complimented the ESI-MS, showing several new signals in the aromatic region, with signals at δ 7.05 and 6.73 ppm corresponding to the aromatic protons of **39**

(H_a and H_b, respectively), identified by comparison to authentic sample. The methoxy signal for **39** was also visible at δ 3.77_7 ppm.

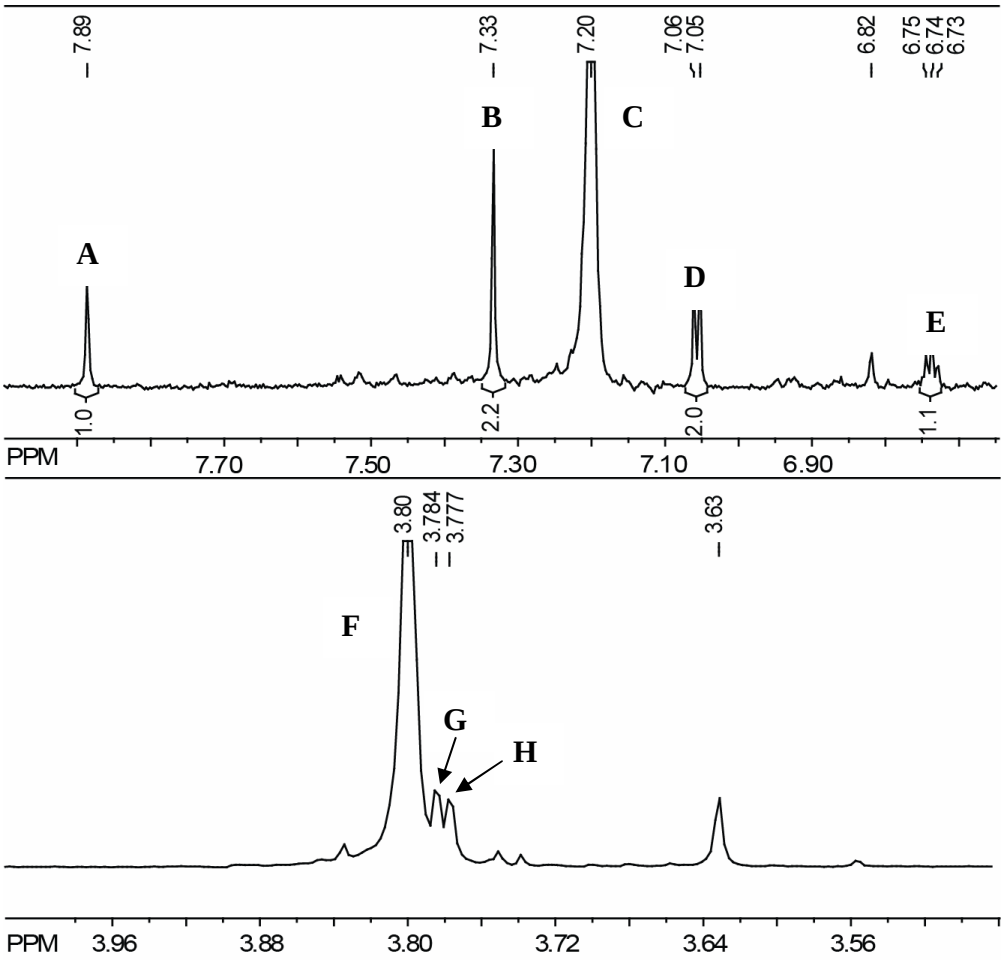

Figure 2. 5: 300 MHz ^{1}H NMR spectrum in DMSO-d_6 of the crude photolysis mixture of **4** photolysed at pH 7. Signals **A** (H_a) and **B** (H_b) correspond to biphenyl **42**; **C** (aromatic protons) and **F** (methoxy protons) of **4**; **D** (H_a) and **E** (H_b) and **H** (methoxy protons) correspond to **39**, while **G** (methoxy protons) is **36**.

The signals at δ 7.89 and 7.33 ppm correspond to the aromatic protons of the biphenyl product **42** (H_a and H_b, respectively), while the signal at δ 6.82 ppm is an unknown photoproduct (note that this appears to be the same unknown photoproduct

observed for the photolysis of **4** in CN^-). In addition, **36** was also formed, but was not visible in the aromatic region due to the overlap of the signal of the aromatic protons of **4**. Instead, **36** was identified from the corresponding mass found in ESI-MS and the ^1H NMR signal for the methoxy group which was clearly visible at δ 3.78$_4$ ppm. The yields of the reaction (as determined by NMR) were 8%, 4% and 5% for compounds **36**, **39** and **42**, respectively.

The positive identification of **36** provides the aromatic counterpart to the detection of CH_3OH from the photolysis of **4**, since **36** is identical to **4** except for one missing methoxy group (replaced with a hydroxy group). It was unknown, however if this was technically a demethylation or a demethoxylation (i.e. cleavage occurring at the Ar-OCH_3 or the ArO-CH_3 bond). In order to distinguish between these two possibilities, photolysis of **4** was conducted in ^{18}O-labeled water. If demethylation were occurring, then there would be no incorporation of the ^{18}O into product **36**. If however, the mechanism involved demethoxylation, then the mass of **36** would increase by two units (as measured by ESI-MS) from the incorporation of the ^{18}O from the nucleophilic attack by the labeled water onto the benzene ring (Equation 2.3).

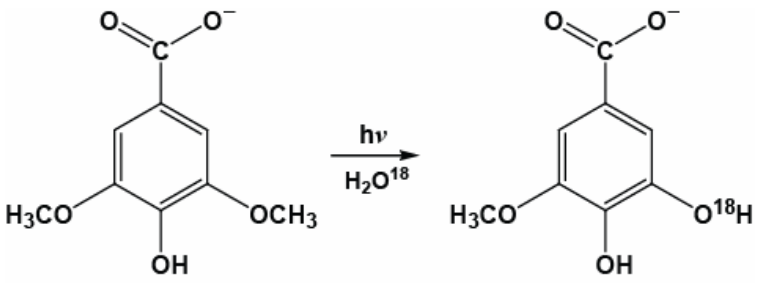

4 **36** **(2. 3)**

Photolysis of **4** in 26.4 atom % ^{18}O labeled water (pH 8, 10^{-2} **M**, 300 nm lamps, argon purged before photolysis, < 15 ^{o}C, 1 hour) led to a 10% increase in the size of the M+2 for **36** compared to a control experiment (measured by ESI-MS in CH_3OH, negative ion mode). This suggests that an Ar-OCH_3 bond in **4** was breaking and thus leading to CH_3OH as a photoproduct. Complimentary evidence for demethoxylation as opposed to demethylation was for photolysis of **4** in 1:1 D_2O-CD_3OD, where there was no observable change in the ^1H NMR after photolysis. This experiment presumes that CD_3OD would be acting as a nucleophile by attacking either the methoxy group carbon or the aromatic carbon. If demethylation were occurring, then there should have been CD_3OCH_3 observed in the NMR, but there was none. If however, the CD_3OD was attacking the aromatic carbon (as in a demethoxylation) then **4** would have been regenerated with one OCD_3 group showing up as M + 3 in ESI-MS. No **4** with an M + 3 was visible, but this may have been because of a low yield of reaction and as such does not discount the demethoxylation mechanism. As discussed previously (Section 2.1.1), the photolysis of **4** in CN^- also led to CH_3OH formation with incorporation of the CN on the aromatic ring of the photoproduct. This agrees well with the results of the ^{18}O-labeled experiment, showing that the mechanism involved demethoxylation as opposed to demethylation.

The other photoproducts for the photolysis of **4** (**39** and **42**) were clearly not related to the formation of CH_3OH, as both of the methoxy groups were still present on these photoproducts. The formation of the dehydroxylated product **39** appears to occur in any photolysis of **4** or **37** (discussed later). A preparative scale photolysis of **4** revealed some important mechanistic details in the formation of **39**, namely that the proton that

replaced the hydroxy group in **4** came from the water. This was determined by photolysing **4** in neat D_2O (D_2O, pD 9, 10^{-3} **M**, 300 nm lamps, argon purged during photolysis, < 15 ^oC, 3 hours). ^1H NMR of the photoproducts revealed a collapse of the coupling for the aromatic protons for **39**, with only a singlet at δ 7.05 ppm for the two remaining aromatic protons as opposed to the doublet at δ 7.05 ppm and triplet at δ 6.74 ppm which was observed for the photolysis of **4** in H_2O. This was indicative of replacement of the hydroxy group by a proton from H_2O (or D from D_2O) (Equation 2.4).

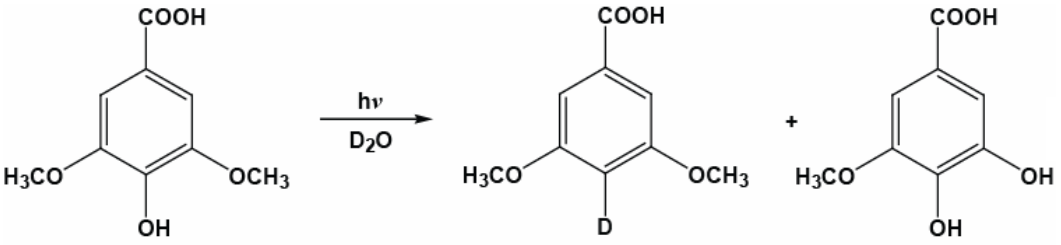

(2. 4)

4 **39** **36**

The formation of the substituted biphenyl **42** could have arisen from the decarboxylation of **4** and recombination with another molecule of **4** in the ground state (Scheme 2.1). While this mechanism was not studied in detail, there was evidence for the concurrent formation of CO_2 measured by MIMS for the photolysis of **4** (Section 2.2).

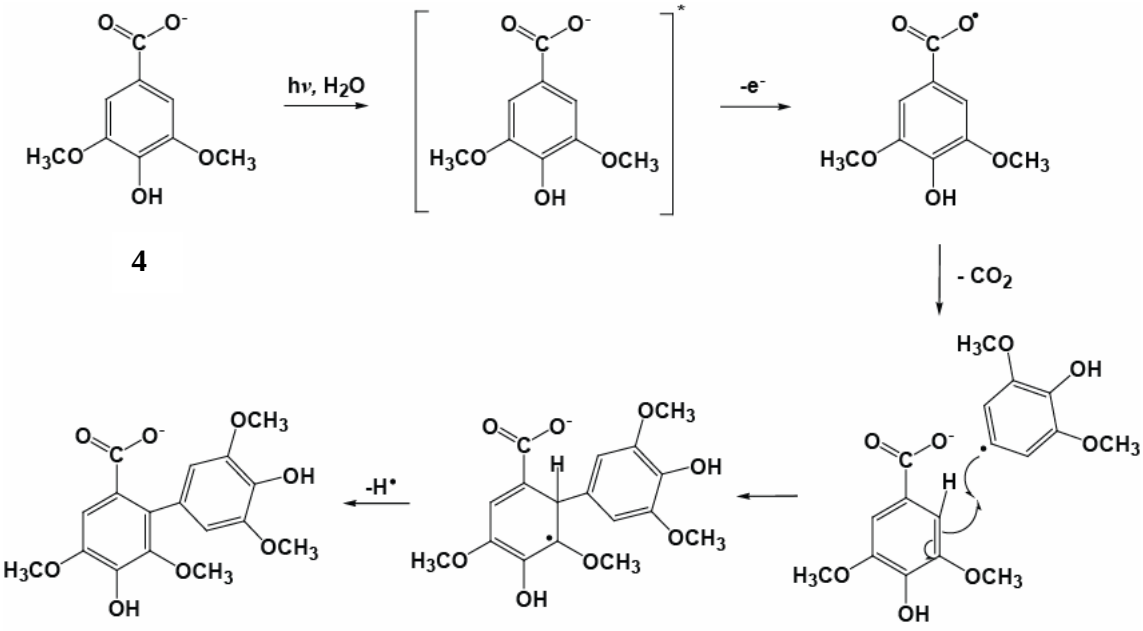

Scheme 2. 1

UV-Vis spectrophotometry was used to observe the change in the absorption characteristics of **4** upon conversion to photoproduct. The spectra were obtained in H_2O with photolysis at 300 nm for defined intervals of time at which point a spectrum was measured. H_2O was chosen as the solvent so as to model the natural process as closely as possible. Figure 2. 6 shows that after one hour of photolysis there was not a significant difference in the absorption spectra as the reaction of **4** proceeded in H_2O (purged with Ar). There was a small blue shift for the absorption at 215 nm and only slight changes to other areas of the spectrum. This was not surprising because the products for the photolysis of **4** would have very similar UV-Vis spectra since the chromophore is not changed significantly in the reaction. For this reason, UV-Vis was not deemed to be particularly diagnostic for the elucidation of the mechanisms for the photolysis of **4**.

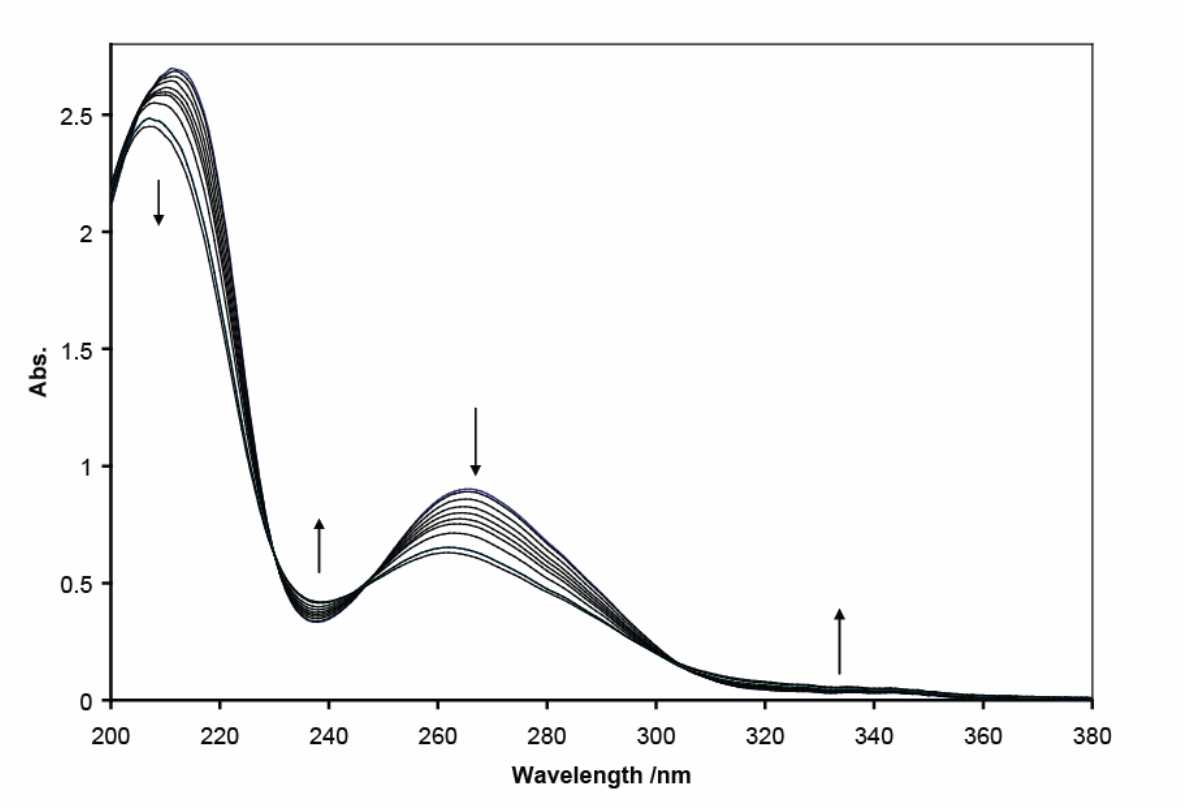

Figure 2. 6: UV-Vis absorption spectra of **4** photolysed in H_2O at pH 7 for 4 – 70 min at 300 nm.

For many kinds of photochemical reactions, important mechanistic details can be ascertained by performing the photolysis reaction in aerated solvent. For instance, if the intermediate that is responsible for the photoproducts of interest is a triplet, then often the presence of O_2 will quench the reaction. Unfortunately, O_2 can also lead to other reaction pathways (oxygenation or oxidation) that may not help in determining the mechanism. For the elucidation of the mechanism for the photoproduction of CH_3OH from **4**, it was desirable to perform the photolysis of **4** in aerated water to more closely approximate the reactions that may occur in the environment.

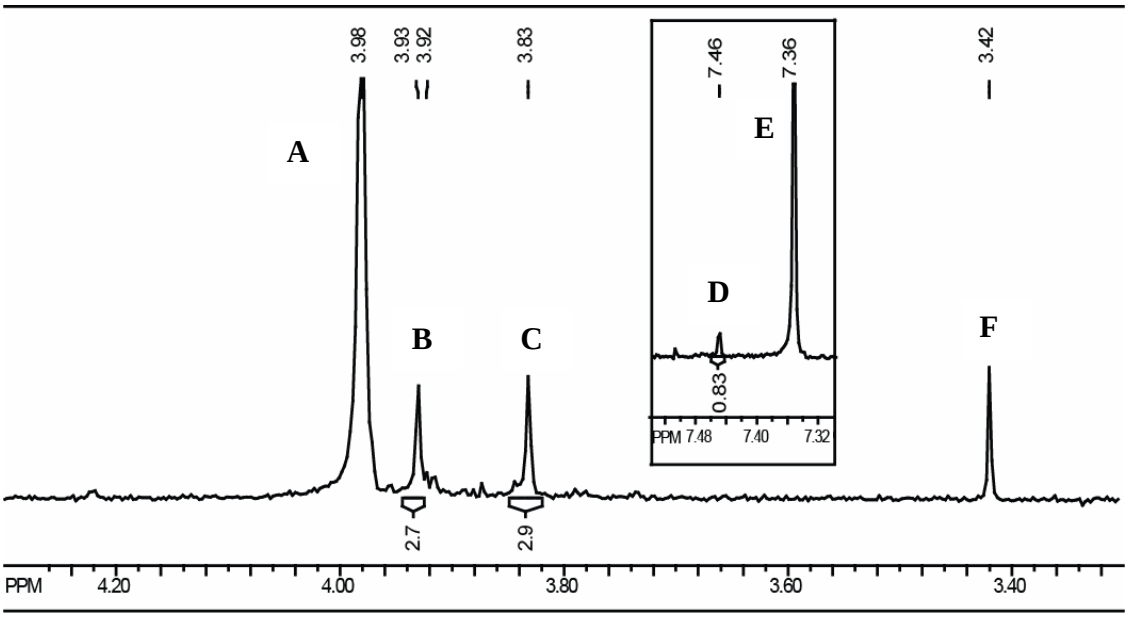

Figure 2. 7: 300 MHz ^{1}H NMR spectrum in D_2O for the photolysis of **4** at pD 7, aerated. Signal **A** (methoxy protons) and **E** (aromatic protons) corresponds to **4**; **B**, **C** and **D** are unknown photoproducts and **F** is CH_3OH. (Inset: Aromatic region of the corresponding ^{1}H NMR spectrum).

When photolysis of **4** was conducted in the presence of O_2 (10:1 D_2O-CD_3CN, pD 7, 10^{-3} **M**, 300 nm lamps, air purged before photolysis, < 15 ^oC, 4.5 hours), there was still formation of CH_3OH, but also the formation of other unidentifiable photoproducts with signals at δ 3.92, 3.83 and 7.46 ppm (Figure 2. 7). The ^{1}H NMR clearly shows formation of the CH_3OH at δ 3.42 ppm, with no indication of the other photoproducts seen previously when the reaction was conducted in the absence of O_2. It is possible that the O_2 was allowing an alternate reaction pathway that also led to the formation of CH_3OH while quenching the formation of **39** and **42**. The photolysis mixture in the aerated sample was a bright yellow colour as opposed to the darker brown colour seen in the photolysis without O_2 present, also indicating that other reaction pathways were occurring. Due to the ambiguity of the identification of the reaction mixture upon

photolysis in aerated solvent, no conclusions were made on its effect. Using Laser Flash Photolysis (LFP) did however provide some clues. This discussion can be found in Section 2.3.

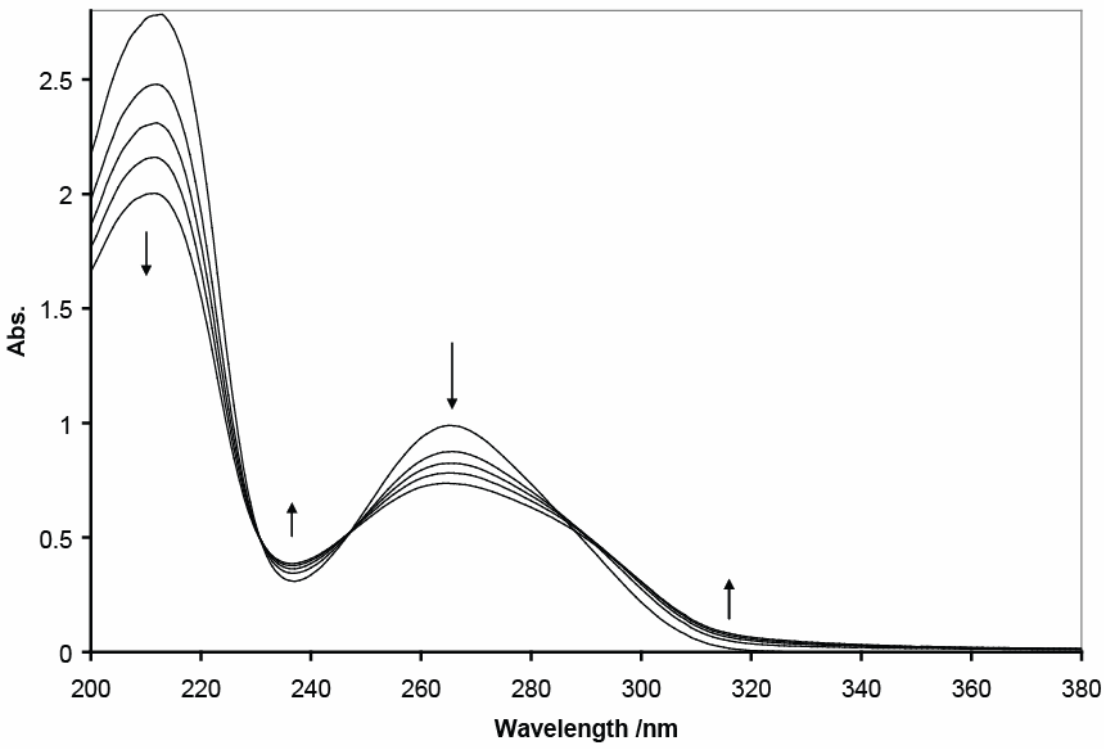

Figure 2. 8: UV-Vis absorption spectra of **4** photolysed at 300 nm in aerated H_2O at pH 7 for 1 – 5 min.

The UV-Vis spectrum (Figure 2. 8) for the photolysis of **4** in aerated water showed significant changes after 5 minutes, with conversion to the aromatic photoproducts. Of particular interest in the UV-Vis spectra (Figure 2. 8) is that the photolysis for **4** in aerated H_2O had very efficient conversion in only 5 minutes whereas the photolysis of **4** in Ar purged H_2O (Figure 2. 6) did not have nearly the degree of reaction in the 70 minutes of photolysis time (as measured by UV-Vis). Based on these

findings, and the complexity of the reaction mixture upon photolysis of **4** in aerated water, further photolysis studies in the presence of O_2 were halted even though the results would have increased the environmental relevance if the mechanism was elucidated in aerated solution. However, it should be noted that CH_3OH is still formed when O_2 is present. Due to the complexity of natural systems, it is often necessary to study environmental reactions in simpler solvent systems before elucidating mechanisms that may be taking place in the environment. This is an example of such a circumstance.

2.1.3 pH Trends

Since the presence of the carboxylic acid moiety in **4** changes the chemical characteristics of the molecule when it is protonated versus deprotonated, the pH effects for the demethoxylation reaction were investigated. When **4** was photolysed in various pHs (9:1 D_2O-CD_3CN, pD 2-10, 10^{-3} **M**, 300 nm lamps, argon purged before photolysis, < 15 ^oC, 1 hour) using NMR scale photolysis, an interesting trend revealed itself where the yield of CH_3OH is highest under basic conditions. This trend was observed by photolysing **4** and measuring the ^1H NMR integration of the CH_3OH signal at δ 3.36 ppm relative to an acetone internal standard, whereby the integration ratio was representative of the relative amount of CH_3OH present at each pH. Under acidic conditions (below pH 4) there was no detectable yield of CH_3OH, while under basic conditions (pH > 8), the yield of demethoxylation reached a maximum (Figure 2. 9).

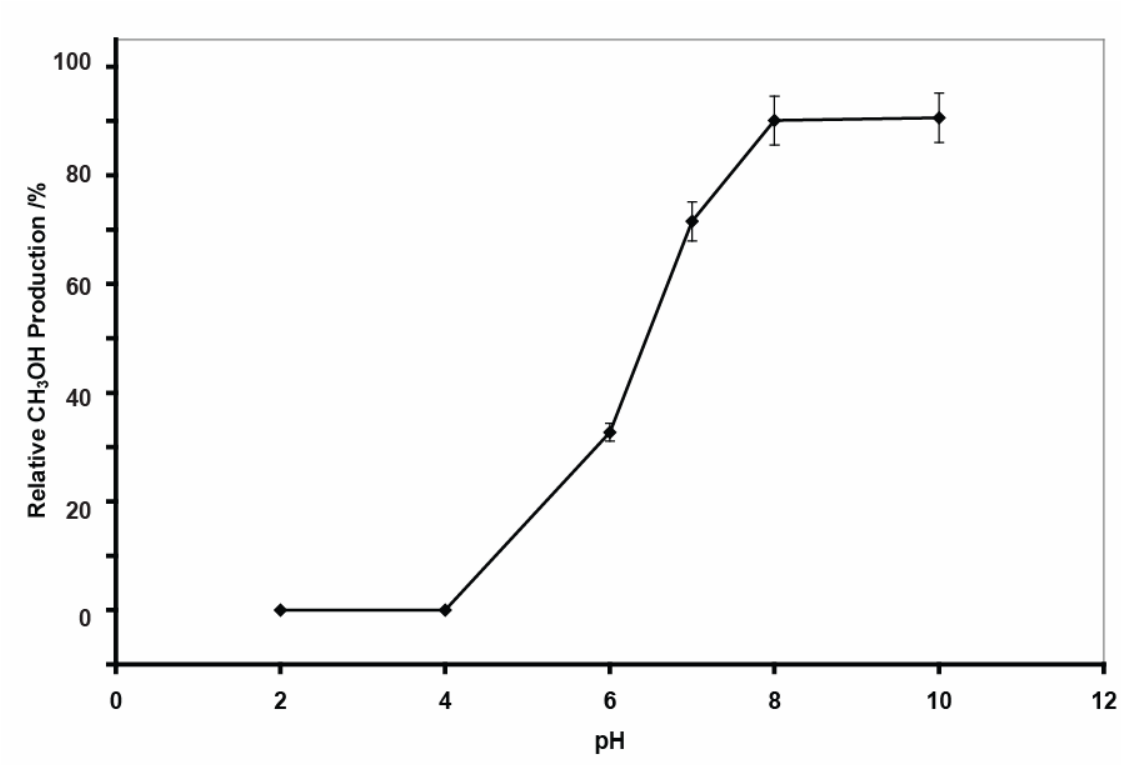

Figure 2. 9: Yield of CH_3OH on the photolysis of **4** in D_2O vs. pH (pD) (as measured by the integration of the 300 MHz ^1H NMR signal for CH_3OH at δ 3.36 ppm, relative to an acetone internal standard).

This trend, where the demethoxylation occurs at pH > 4 corresponds well to the pKa_1 of **4** at 4.34.[87] This shows that the demethoxylation reaction seems to occur only when **4** is in the carboxylate form, while the protonated form exhibits no detectable yield of CH_3OH. When the concentration of OH^- increases above pH 8, there does not seem to be a further increase in the CH_3OH production, suggesting that the form of the nucleophile (i.e. H_2O versus OH^-) was not important for the demethoxylation. In other words, the observed pH effect is not due to differences between water catalysis and specific base catalysis (e.g. $k_{H2O} << k_B$).

Using preparative scale photolysis, the identity of the products for the photolysis of **4** in basic conditions was determined (H_2O, pH 9, 10^{-3} **M**, 300 nm lamps, argon purged before and during photolysis, < 15 ^oC, 3 hours). The products observed for the photolysis of **4** in basic conditions were the same as for neutral pH (i.e. **36**, **39** and **42**). This suggests that the same mechanism is operative regardless of the pH once the pH is > 4.

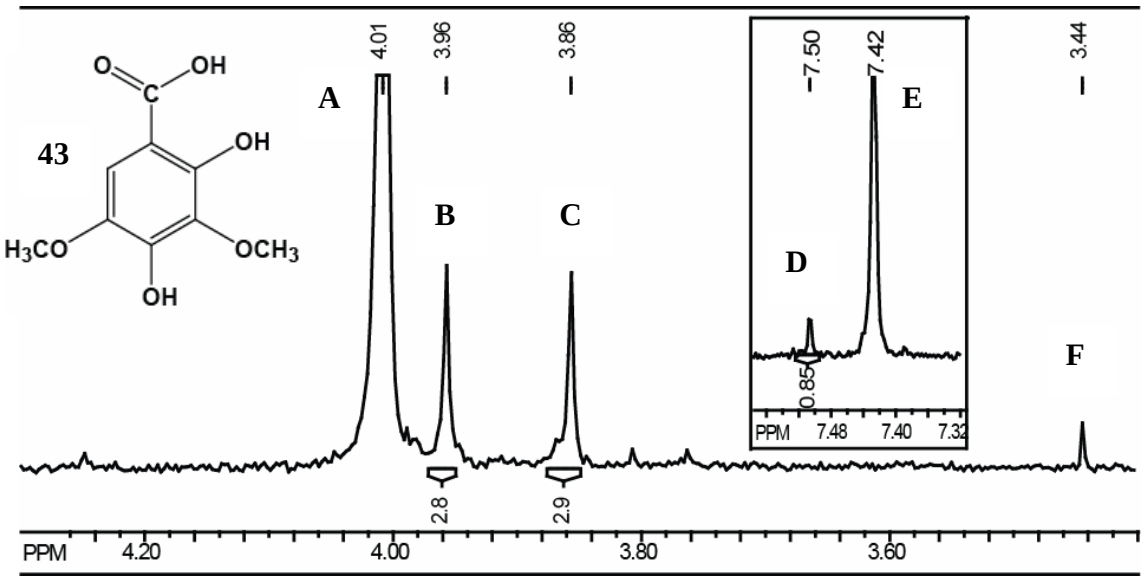

Figure 2. 10: 300 MHz ^1H NMR spectrum in D_2O for the aqueous photolysis of **4** at pD 4 and 300 nm. Signals **A** (methoxy protons) and **E** (aromatic protons) correspond to compound **4**; **B**, **C** (methoxy protons) and **D** (aromatic proton) to **43** and **F** to CH_3OH. (Inset: Aromatic region of the corresponding ^1H NMR spectrum).

The photolysis of **4** (H_2O, pH 3, 10^{-3} **M**, 300 nm lamps, argon purged before and during photolysis, < 15 ^oC, 3 hours) at pH < 4 revealed the formation of a new photoproduct. Upon closer inspection, this new compound was identified as the same photoproduct formed when **4** was photolysed in the presence of O_2 (Figure 2. 7 and Figure 2. 10). The identity of the unknown photoproduct was proposed to be 2,4-

dihydroxy-3,5-dimethoxybenzoic acid (**43**) based on the ^{1}H NMR signals at δ 3.96 and 3.86 ppm corresponding to the methoxy protons, while the signal at δ 7.50 ppm corresponds well to the aromatic proton. There was however, no confirmation of product **43** by ESI-MS. Instead, the main observable photoproduct on ESI-MS had an m/z of 185 (negative ion mode), but the identity of the compound with this mass is unknown. The mechanism of formation for **43** is also unknown.

2.1.4 Photolysis of 3,5-Dimethoxy-4-hydroxyacetophenone (33) and Methyl Syringate (34) in Aqueous Solution

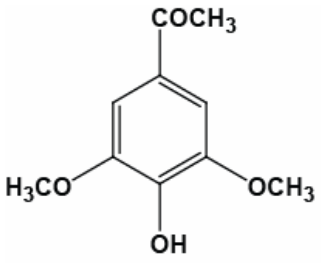

33

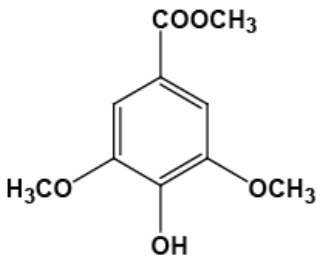

34

To further investigate the mechanism for the demethoxylation of **4**, structurally similar compounds were studied to determine what chemical moieties on **4** were important in the formation of CH_3OH. To investigate whether the acid group in **4** was important for the demethoxylation mechanism, 3,5-dimethoxy-4-hydroxyacetophenone (**33**) was photolysed (NMR scale photolysis; 7:4 D_2O-CD_3CN, pD 7, 10^{-3} **M**, 300 nm lamps, argon purged before photolysis, < 15 ^oC, up to 4 hours). A ^{1}H NMR was obtained after each hour of photolysis, illustrating the growth of the CH_3OH at δ 3.69 ppm (Figure 2. 11). The CH_3OH was identified by adding neat CH_3OH and observing the relative intensity increase of the signal at δ 3.69 ppm on ^{1}H NMR.

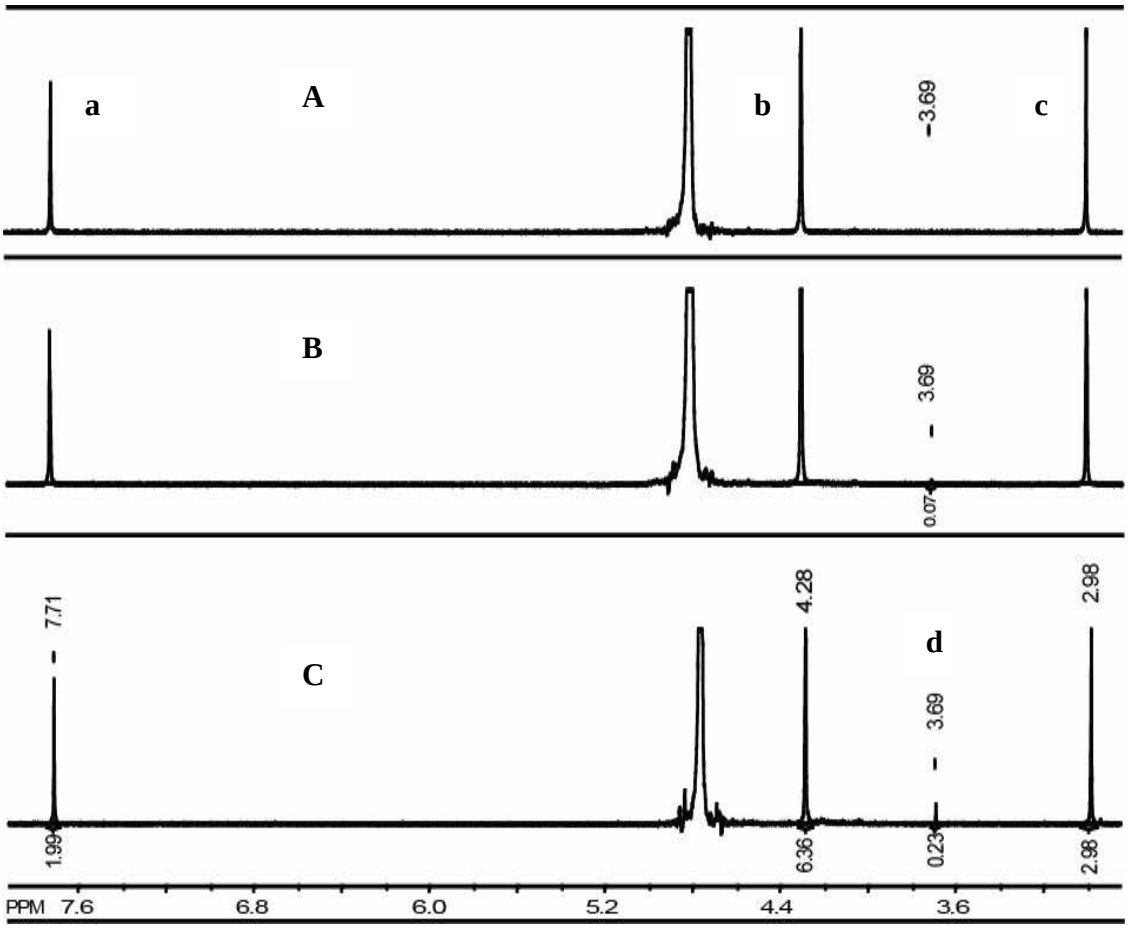

Figure 2. 11: 300 MHz ^{1}H NMR spectra in D_2O for the 300 nm aqueous photolysis of **33** at pD 7. **A**: 1 hour photolysis; **B**: irradiated for 2 hours; **C**: irradiated for 4 hours. Signal **a** (aromatic protons), **b** (methoxy protons) and **c** (acetophenone CH_3 protons) correspond to **33**, while **d** corresponds to CH_3OH.

The photolysis of ketone **33** was also used to see how changing the withdrawing or donating characteristics of the substituent in the 1-position (*para* to the hydroxy group in **4**) would affect the outcome of the demethoxylation. In the case of **33**, this change from an acid group to a ketone led to an increase in the withdrawing characteristics of the substituent in the 1-position. When the yield of CH_3OH (in terms of conversion from starting material) for the demethoxylation of **4** versus **33** was quantified, the results show that for **4** at pD 7, the conversion was 13.8% while the conversion for **33** was only 1.8%

(for 1 hour photolysis at 300 nm). Comparatively, the yield of CH_3OH for the photolysis of **4** in the protonated form (in acidic conditions) was only 0.7%. In this case, the protonated form of the carboxylic acid was more strongly donating than the deprotonated form at pD 7. This clearly shows that by changing the donating/withdrawing characteristics of that substituent, the yield of demethoxylation can be altered significantly. If we correlate these results with the Hammett substituent constants for the *meta* position (σ_m), a trend is evident (Table 2.3) where there was a greater yield of CH_3OH when the substituent in the 1-position was donating (as in **4**, carboxylate form) compared to **33** and **4** (protonated) where there was a withdrawing effect. Clearly though there is more involved since the Hammett constants for **33** and **4** in pD 4 are similar yet their conversion to CH_3OH was different.

Table 2. 3: Correlation between Hammett constants and CH_3OH conversion for **4** (in pD 7 and 4) and **33** after 1 hour photolysis at 300 nm.[88]

	CH_3OH conversion /%	**σ_m**
4 (pD 7)	13.8	-0.1
4 (pD 4)	0.7	0.37
33 (pD 7)	1.8	0.38
34 (pD 7)	0.5	0.37

Methyl syringate (**34**) was photolysed to further investigate how the substituents in the site normally occupied by the acid group in **4** affects the yield of CH_3OH production. The ester in **34** is also a withdrawing group, so it was expected that for the aqueous photolysis of **34** there would be little to no CH_3OH formed since there was little demethoxylation occurring for the photolysis of **33** (which also contains a withdrawing group). When **34** was photolysed using NMR scale photolysis (4:1 D_2O-CD_3CN, pD 7,

10^{-3} **M**, 300 nm lamps, argon purged before photolysis, < 15 ^{o}C, up to 3 hours) there was only a small yield of CH_3OH detected. In terms of conversion to CH_3OH, the amount formed was 0.5% for **34** compared to the 13.8% for **4** at pD 7. This result agrees well with the discussion for ketone **33** and **4** in acidic conditions where withdrawing groups in the 1-position drastically lower the yield of demethoxylation.

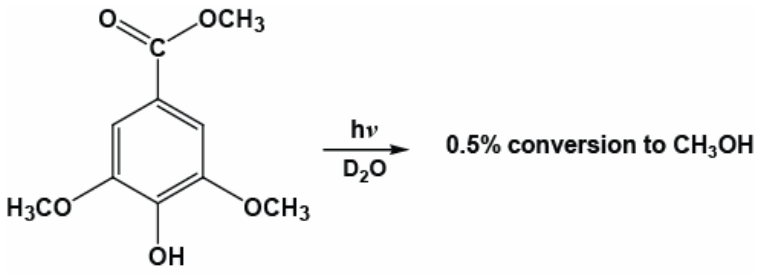

34

2.1.5 Photolysis of 2,6-Dimethoxyphenol (15) and 1,2,3-Trimethoxybenzene (35) in Aqueous Solution

Since withdrawing groups in the 1-position seemed to decrease the yield of demethoxylation, it was deemed important to investigate what the outcome would be if there was only a hydrogen in that position. To investigate this, 2,6-dimethoxyphenol (**15**) was photolysed. Since the H *para* to the hydroxy group is neither withdrawing nor donating, it was postulated that the amount of CH_3OH formed from **15** should fall between the yield of **4** (carboxylate form) and **33** (13.8% and 1.8%, respectively; for a 1 hour photolysis).

When **15** was photolysed by NMR scale photolysis (9:1 D_2O-CD_3CN, pD 7, 10^{-3} **M**, 300 nm lamps, argon purged before photolysis, < 15 ^{o}C, 3 hours) no CH_3OH was detected. This indicated that while the withdrawing or donating effects of the

substituents in the position *para* to the hydroxy group seem important (as evidenced by photolysis of **4**, **33** and **34**), there were other factors involved, otherwise there would have been a detectable yield of CH_3OH for the photolysis of **15**.

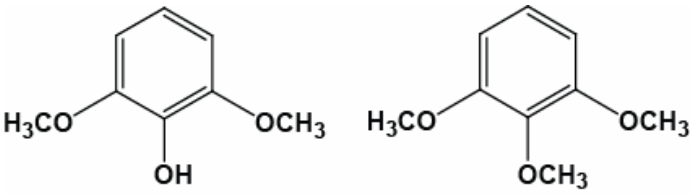

15 **35**

To further confirm this, 1,2,3-trimethoxybenzene (**35**) was also photolysed. While the three donating substituents (methoxy groups) on this compound differ from those on **4** (two methoxy and one hydroxy group), the donating abilities of these moieties are similar. Originally, it was postulated that **35** would also have a detectable yield of CH_3OH between that of **4** (carboxylate form) and **33**, but after the results of the photolysis of **15**, it was predicted that there would be no CH_3OH measured by ^1H NMR. When **35** was photolysed using an NMR scale photolysis (9:1 D_2O-CD_3CN, pD 7, 10^{-3} **M**, 300 nm lamps, argon purged before photolysis, < 15 ^oC, 3 hours), as predicted, there was no detectable yield of CH_3OH.

The results of these experiments and those discussed previously for **33** and **34** revealed that withdrawing substituents in the 1-position in **4** decrease the yield of CH_3OH. But since **15** and **35** both had no detectable CH_3OH formation despite a lack of withdrawing substituents in the 1-position, clearly more was involved in the demethoxylation mechanism. One possible explanation is that because the carboxylate

group on **4** in basic conditions is slightly donating, it could stabilize the intermediate in the reaction mechanism.

The following sections outline the next set of product studies that were undertaken to determine what other substituents on **4** were important in the formation of CH_3OH. Specifically, it was determined whether the three donating groups on the ring were important in the demethoxylation mechanism.

2.1.6 Photolysis of 3-Methoxygallic Acid (36) in Neutral Aqueous Solution

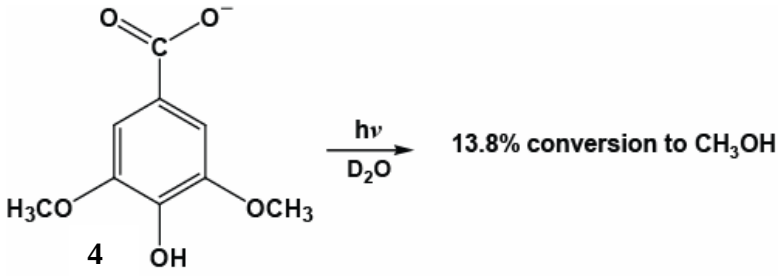

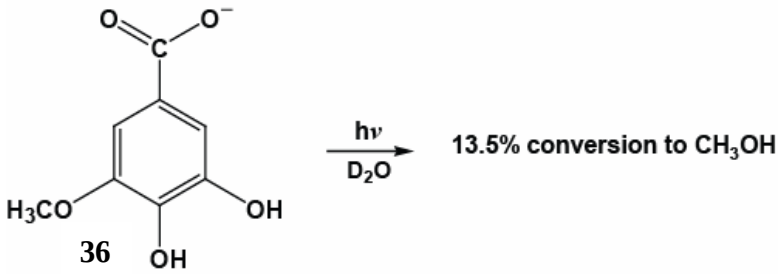

The methoxy and hydroxy substituents on **4** have similar donating abilities, so it was suspected that changing the identity of these groups would have little to no effect on the degree of demethoxylation. To test this hypothesis, 3-methoxygallic acid (**36**) was photolysed. While this compound still contains three donating groups, one of the methoxy groups on **4** has been exchanged with a hydroxy group.

When **36** was photolysed using NMR scale photolysis (4:1 D_2O-CD_3CN, pD 7, 10^{-3} **M**, 300 nm lamps, argon purged before photolysis, < 15 ^oC, up to 3 hours), the ^1H NMR signal for the CH_3OH at δ 3.6 ppm increased in size as the photolysis time increased. The % conversion to CH_3OH for a 1 hour photolysis of **36** was 13.5%, which was within experimental error of the yield of CH_3OH for **4** at 13.8%.

2.1.7 Photolysis of 3,4,5-Trimethoxybenzoic Acid (37) in Neutral Aqueous Solution

To determine if the phenol group was important in the demethoxylation mechanism, 3,4,5-trimethoxybenzoic acid (**37**) was photolysed since it is lacking the hydroxy moiety. For the NMR scale photolysis of **37** (5:1 D_2O-CD_3CN, pD 7, 10^{-3} **M**, 300 nm lamps, argon purged before photolysis, < 15 ^oC, up to 3 hours), CH_3OH was still formed, but with a conversion of only 4.0% (1 hour photolysis). This revealed that while demethoxylation was occurring without a hydroxy group, the yield was significantly smaller than that for **4** at pD 7 (13.8%) and **36** (13.5%).

To further investigate the photochemistry of **37**, a preparative scale photolysis was conducted (H_2O, pH 8, 10^{-3} **M**, 300 nm lamps, argon purged before photolysis, < 15 ^oC, 3 hours). The ^1H NMR of the extracted photoproducts revealed that **4** and **39** were formed in a 2 % and 44 % yield, respectively (Figure 2. 12). The ^1H NMR signal at δ 7.23 corresponded to the aromatic protons of **37**, while the signals at δ 3.82 and 3.73 ppm were from the methoxy protons (H_a and H_b, respectively). The signals at δ 7.05 and 6.73 ppm corresponded to the aromatic protons of **39** (H_a and H_b, respectively), with the signal at δ 3.78 ppm was from the methoxy protons. Surprisingly, the small signals at δ 7.20

and 3.80 ppm were attributed the aromatic and methoxy protons of **4**, respectively. This shows that when there are three methoxy groups on the ring, the preference is to demethoxylate the central methoxy group (4-position) as opposed to one on the sides, but with a lower yield of reaction compared to **4**. The loss of this central methoxy group was in contrast to the demethoxylation exhibited in both **4** and **36**, indicating that there was possibly a different mechanism involved. The mechanism for demethoxylation is likely the same for **37**, **4** and **36**, but **37** has a more stabilized intermediate when the central methoxy group is cleaved. This may be due steric effects within the molecule.

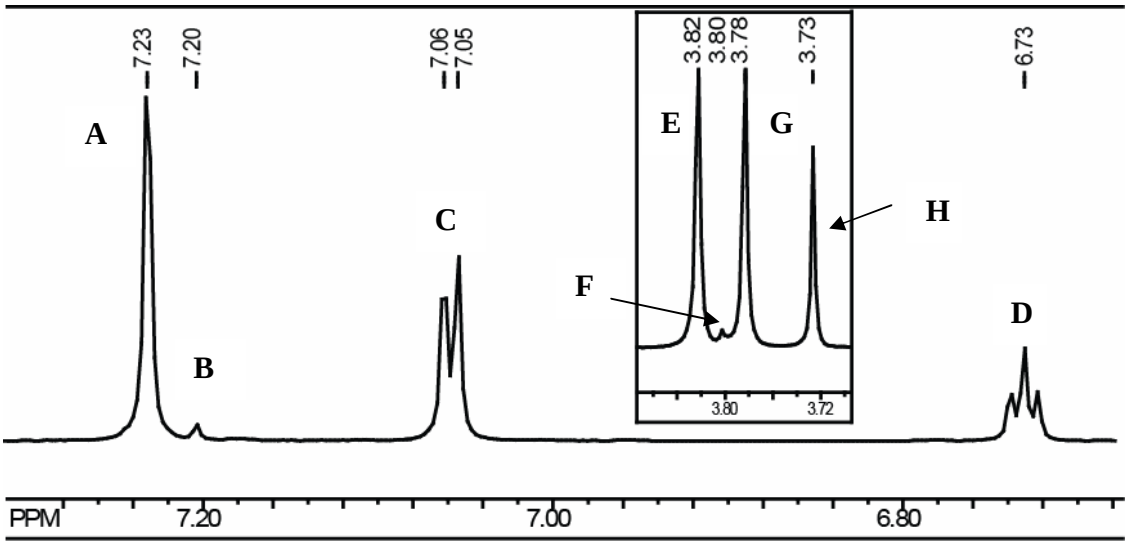

Figure 2. 12: 300 MHz ^{1}H NMR spectrum in DMSO-d_6 of the extracted photoproducts for the 300 nm aqueous photolysis of **37** at pD 8. The signals at **A** (aromatic protons), **E** (H_a) and **H** (H_b) correspond to compound **37**; **B** (aromatic protons) and **F** (methoxy protons) to **4** and **C** (H_a), **D** (H_b) and **G** (methoxy protons) to **39**. (Inset: Aromatic region for the corresponding ^{1}H NMR).

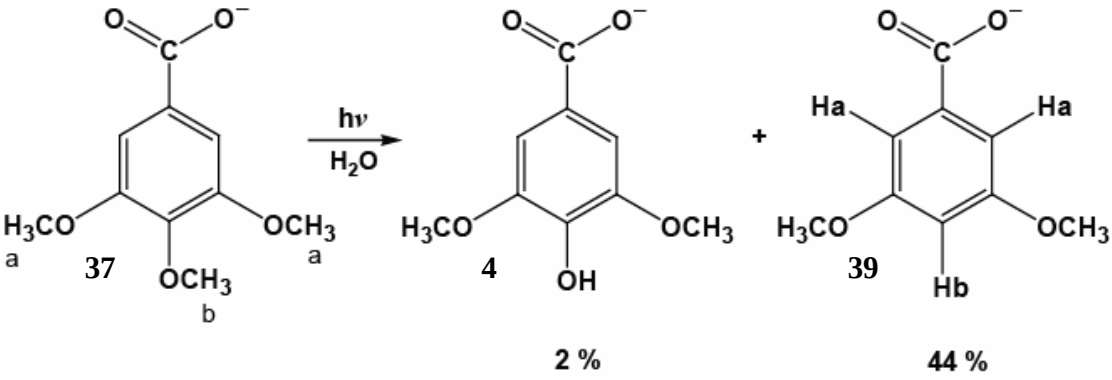

2.1.8 Photolysis of *m*-Anisic Acid (38) and 3,5-Dimethoxybenzoic Acid (39) in Neutral Aqueous Solution

To determine if three donating groups on the aromatic ring are necessary for the demethoxylation, *m*-anisic acid (**38**) was photolysed. The NMR scale photolysis (9:2 D_2O-CD_3CN, pD 7, 10^{-3} **M**, 300 nm lamps, argon purged before photolysis, < 15 ^oC, up to 3 hours) of **38** revealed no detectable yield of CH_3OH or any other product by ^1H NMR (Equation 2.5). This suggested that it is necessary to have three donating substituents on the ring in order for the demethoxylation to occur at a level that is detectable by ^1H NMR. The most plausible explanation for this is that three donating substituents are required to stabilize the intermediate in the demethoxylation. To corroborate this finding, an NMR scale photolysis of 3,5-dimethoxybenzoic acid (**39**) was conducted (7:3 D_2O-CD_3CN, pD 7, 10^{-3} **M**, 300 nm lamps, argon purged before photolysis, < 15 ^oC, up to 6 hours). The results of this experiment did not show any detectable CH_3OH formation (or any other photoproducts) as determined by the lack of a signal at δ 3.4 to 3.6 ppm on the ^1H NMR (Equation 2.6).

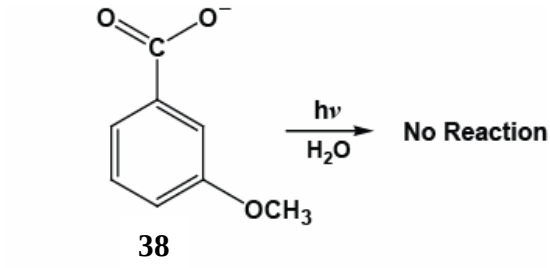

38 **(2.5)**

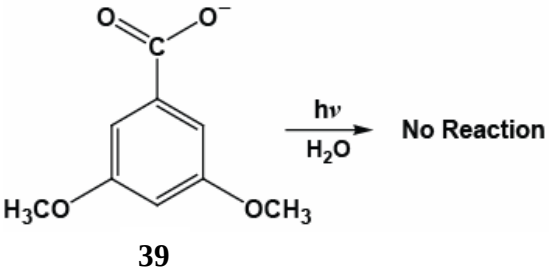

39 **(2.6)**

2.1.9 Quantum and Relative Yields of CH_3OH Formation

The quantum yield for the demethoxylation of **4** and **37** was determined using Equation 2.7 as a method of quantifying the photochemical efficiency of the reaction. This was accomplished by measuring the relative conversion to CH_3OH compared to the absolute conversion of 1,2-dimethoxybenzene (**27**) to 2-methoxyphenol under identical conditions of photon flux using ^1H NMR integration of the CH_3OH signal at δ 3.4 ppm relative to the integration of acetone as an internal standard.

$$\Phi_f = \frac{\text{moles product formed}}{\text{moles photons absorbed}} \qquad \textbf{(2.7)}$$

The quantum yield for **27** (Φ_p = 0.016 at pD 1.3, 254nm) for the photoprotonation leading to the demethoxylated product was measured by Wan and co-workers.[81] Since this reaction also formed CH_3OH, it was possible to quantify the yield using NMR scale

photolysis as conducted previously. The reaction of **27** was therefore used as a secondary actinometric standard to determine the Φ_p for the demethoxylation of **4** (Table 2.4). Specifically for **4**, the quantum yield was determined to be $\Phi_p = 0.010$, which means that 1% of the photons absorbed result in the production of methanol. While this efficiency is quite small in comparison to many photochemical reactions, this could contribute a significant load of CH_3OH to the environment, given the widespread occurrence of humic substances in marine and terrestrial surface waters. While the measured Φ_p for **4** is for a model compound in a laboratory setting, it can used to estimate the natural fluxes in the environment where compounds like **4** are present and may undergo demethoxylation with a similar yield.

Table 2. 4: Quantum yields (Φ_p) for the demethoxylation reaction of **4** and **37** in 1:1 D_2O – CD_3CN relative to the Φ_p for **27** in D_2O at 254nm.

Compound	Φ_p
27	0.016
4	0.010[a]
37	0.0058[a]

[a] Calculated using Φ_p for photoprotonation of **27** as a secondary standard by measuring for the amount of CH_3OH produced at 254 nm.[81]

The measured quantum yield for **37** agrees well with the % yield that was calculated previously for its demethoxylation. The yield of demethoxylation for **37** (4.0%) was calculated to be roughly a half to one third of that for the formation of CH_3OH from the photolysis of **4** (deprotonated, 13.8 %). As shown in Table 2.4, the quantum yield for **37** is also approximately half of the quantum yield for the demethoxylation of compound **4**.

The relative conversions to CH_3OH for the photolysis of the various compounds studied sheds some light on the structural characteristics in this suite of compounds that are important for demethoxylation to occur. Table 2.5 outlines the percent conversion (for 1 hour photolysis) to CH_3OH for the compounds of interest as measured by the ^1H NMR integration of the CH_3OH signal at δ 3.4 to 3.6 ppm relative to an acetone internal standard. The lack of reactivity exhibited by compounds **38** and **39** reveals that it was essential to have three donating groups on the aromatic ring in order for the demethoxylation reaction to occur. This was concluded since both of these compounds are missing the three electron donating groups and exhibited no detectable CH_3OH under the reaction conditions.

The order of percent conversion for **4** (pH 7), **33**, **4** (pH 4) and **34** shows the effect of the substituent in the position *para* to the hydroxy group in **4**. This reveals that it is important that this group is not withdrawing (as quantified by Hammett constants for the substituent in the 1 position for **4** (pH 7), **33**, **4** (pH 4) and **34**, σ_m = -0.1, 0.37, 0.38 and 0.37, respectively).[88] Since compounds **4** (pH 4), **33** and **34** did not form the same amount of CH_3OH despite similar σ_m values there may be other factors involved for the demethoxylation mechanism, or modified substituent constants are appropriate to reflect the electronic factors in photochemical reactions such as those being investigated here. There also does not appear to be a necessity for a hydroxyl group, since **37** was still able to form CH_3OH (albeit in a smaller yield).

Table 2. 5: Yield of CH_3OH for the aqueous photolysis of the various compounds at 300 nm in pD 7, quantified by 300 MHz ^1H NMR integration of the CH_3OH signal relative to acetone as an internal standard.

Compound	CH_3OH Conversion /%
4, pH 7	13.8
36	13.5
37	4.0
33	1.8
4, pH 4	0.7
34	0.5
35	0.0
15	0.0
38	0.0
39	0.0

2.2 MIMS and CH_3Cl Formation

2.2.1 Membrane Introduction Mass Spectrometry (MIMS) Overview

Membrane Introduction Mass Spectrometry (MIMS)[89,90,91] is an analytical technique that uses a semi-permeable membrane inlet as an online sample introduction platform to directly monitor analyte concentrations without the need for sample clean up or pre-concentration. Some benefits of this technique include the real-time analysis of the data collection and the ability to acquire the kinetics for the system. While quantum yields can be measured using a 'one point in time' analytical measurement technique such as purge-trap GC/MS, MIMS can measure this and the kinetics of complex systems that would be difficult using a standard GC/MS instrument.

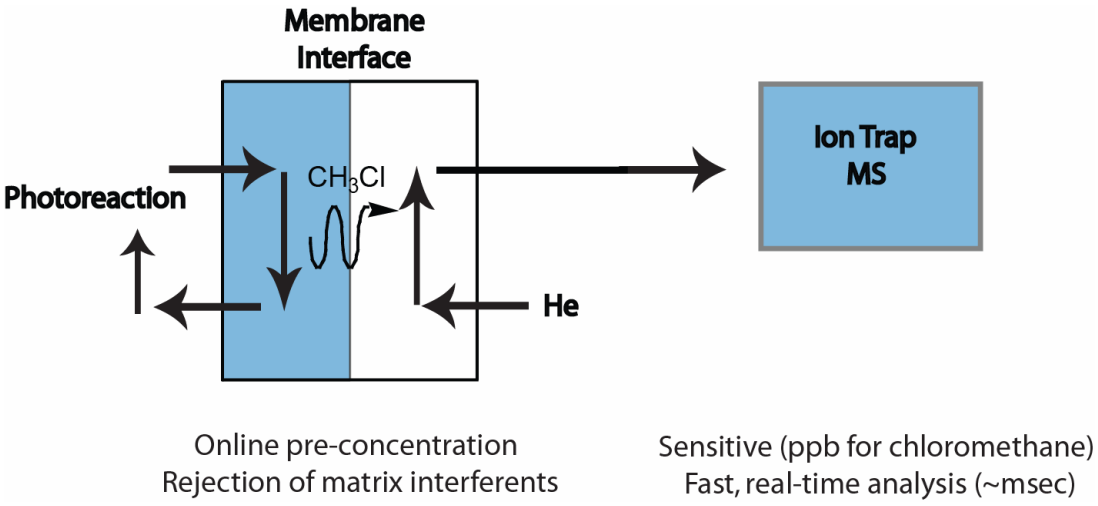

Figure 2. 13: MIMS schematic showing the circulating loop of the reaction mixture with the volatile CH_3Cl traveling through the membrane interface into the ion trap MS.[92]

Volatile and semi-volatile analytes are entrained in a helium sweep gas and continuously introduced to an ion-trap mass spectrometer for real-time quantification. The MS provides both a sensitive and selective detection system (tandem MS/MS techniques can be used to deal with isobaric interferences). This technique is well suited to the rapid trace analysis of volatile organic compounds (VOCs) and semi-volatile organic compounds (SVOCs) in complex matrices[93] and the continuous monitoring of dynamic chemical systems.[94] In the current study we employed an interface in which components of the reaction were continuously flowed over the outside of a polydimethylsiloxane (PDMS) capillary hollow fibre membrane in a closed loop configuration (Figure 2.13 and 2.14).

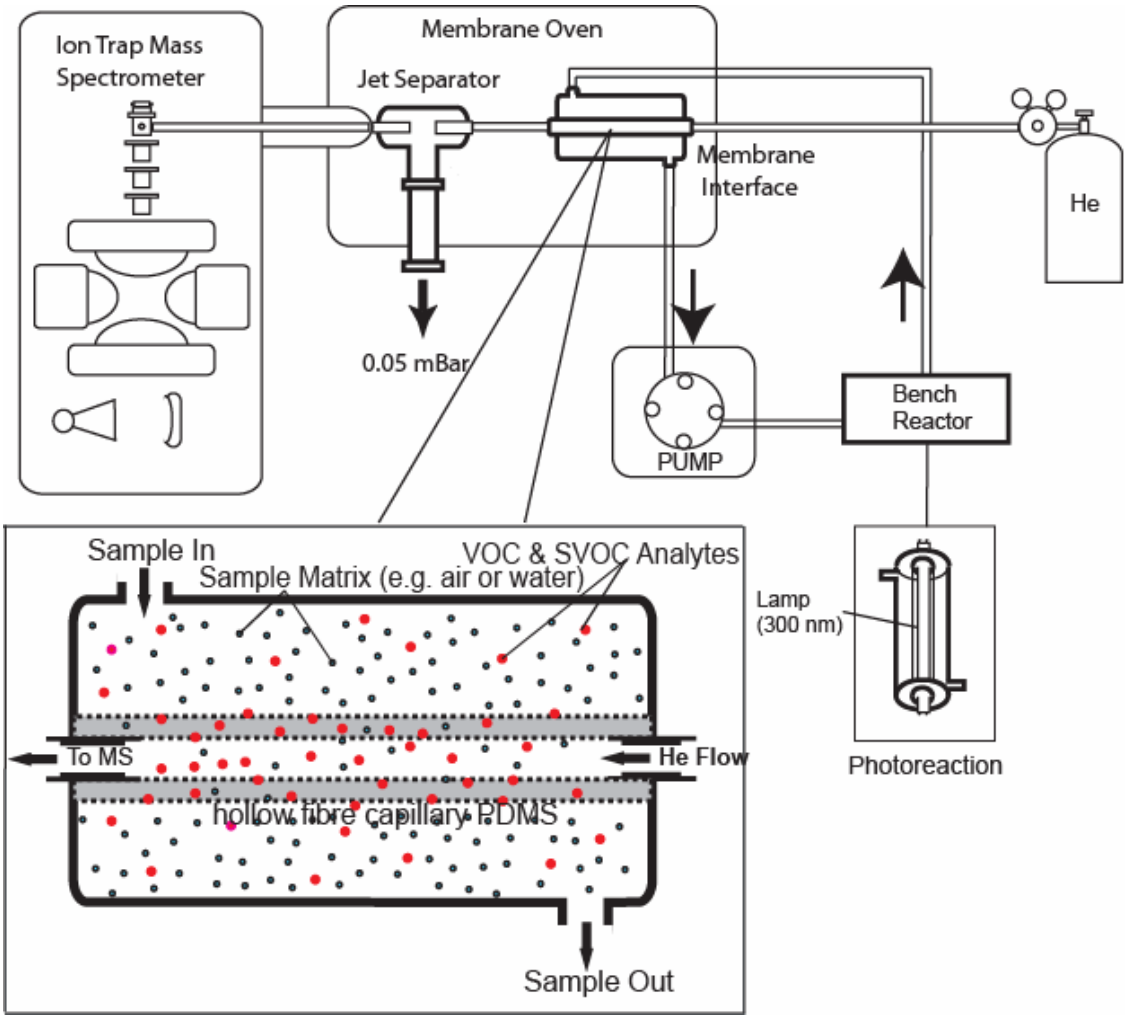

Figure 2. 14: MIMS schematic and membrane cross-section. (adapted from Nelson).[94]

2.2.2 Method Development for the Analysis of CH_3Cl using MIMS

As mentioned previously, it was necessary to abandon the search for CH_3Cl by ^1H NMR analysis due to difficulties in its detection. It was postulated that the CH_3Cl was either too volatile for analysis or was formed in such small amounts as to be below the detection limits provided by NMR. Moore has already demonstrated that CH_3Cl produced from the photoreaction of **4** is detectable by purge and trap GC/MS,[43] but in this study, MIMS was explored as an in-situ reaction monitoring technique to follow the

formation of CH_3Cl directly during the photolysis. Furthermore, MIMS techniques lend themselves to the study of CH_3Cl production in complex natural water without the need for time consuming and laborious sample work-up.

For the MIMS trials, aqueous solutions of **4** were photolysed in a closed quartz reaction vessel while being re-circulated over the membrane interface via a peristaltic pump. Selected ion monitoring (SIM) were employed to monitor target analytes, such as CH_3Cl, CH_3OH and CO_2 (recall that there was speculation that a decarboxylation reaction was responsible for the production of the biphenyl **42**). Tandem MS/MS and full scans (m/z = 40 – 250) were also explored for these analytes, but these techniques did not offer any advantages in their detection. The output for the MIMS analysis is an ion chromatogram, which displays an analytical signal (proportional to concentration) as a function of time. The total ion chromatogram (TIC) and several SIM channels are followed simultaneously, with the intensity of the SIM signals converted to concentrations using standard calibration techniques. If more than one analyte was of interest, all of the signals could be collected concurrently. In the MIMS analysis, non-volatile components such as **4** and Cl^- do not permeate the membrane interface and interfere with the MS analysis (note that H_2O vapour does permeate the membrane to a certain degree, but not enough to interfere). With the reaction attached to the MIMS in a closed loop, all volatile compounds produced could be simultaneously measured in real-time, provided that the corresponding mass spectra could be resolved.

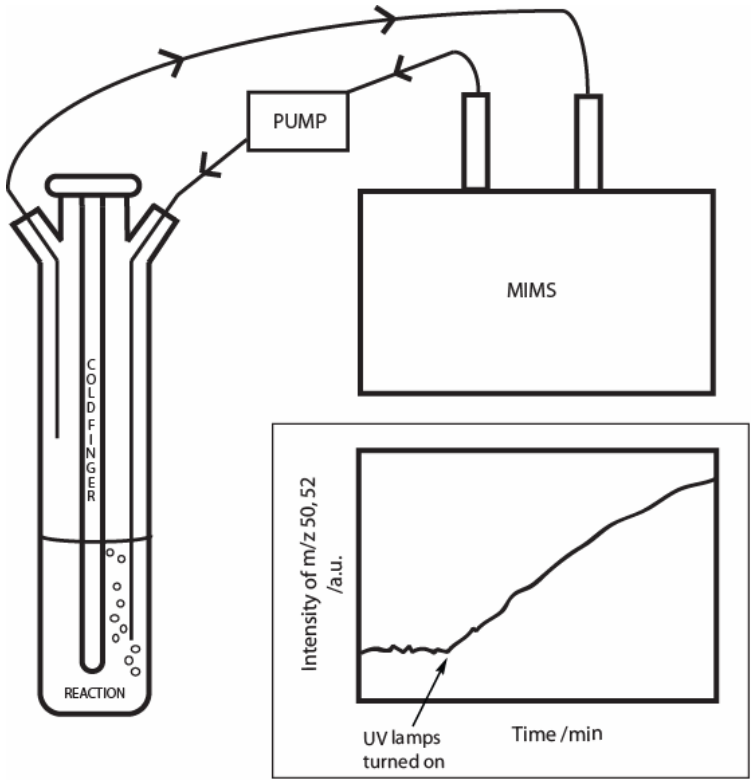

Figure 2. 15: Schematic of the MIMS set-up for the analysis of CH_3Cl in the photoreaction of **4**. (Inset: Typical MIMS output while monitoring m/z 50, 52 for CH_3Cl, indicating the time at which the UV lamps were turned on.)

Since MIMS has not been previously reported for the real-time detection of CH_3Cl, optimization of a number of system and instrument parameters was required. This included developing an on-line injection strategy for calibration spikes for analytes with a high vapour pressure, selecting appropriate solution and membrane temperatures, and MS collection parameters. Since MIMS can be operated by flowing either condensed or gas phase samples over the membrane interface, a comparison was made to assess the sensitivity of re-circulating aqueous CH_3Cl solutions as opposed to the headspace in equilibrium with CH_3Cl solutions. In addition, a series of control experiments were

preformed to assess both the thermal and photochemical stability of CH_3Cl under the reaction conditions and pH ranges investigated.

For the handling and development of the injection strategy, the high vapour pressure of CH_3Cl combined with a relatively low water solubility (resulting in a low Henry's law constant) posed challenges. To overcome these challenges, CH_3Cl solutions in CH_3OH were used for the standard solutions with a gas tight syringe used to inject the solution into the reaction vessel via Teflon backed septa.

To ensure that the signal collected for CH_3Cl was maximized, the MS collection parameters were optimized. The MS lenses were tuned on a mass of 51, which was deemed appropriate for the collection of $CH_3{}^{35}Cl^+$ (m/z = 50) and $CH_3{}^{37}Cl^+$ (m/z = 52) based on comparison to the NIST mass spectrum.[95] In selected ion mode (SIM), the width of the mass range collection window was also increased to encompass the widest mass range possible without suffering isobaric interference. This adjustment can be likened to increasing the slit width when using instruments such as atomic absorption, where the increase in slit width allows more intensity from the range measured, but decreases the resolution of the signal from the analyte. The ion collection time for the measurement was also increased in order to trap more molecular ions in the MS. Attempts to use negative ion mode and chemical ionization using CH_4, failed to improve the detection of CH_3Cl.

Due to its relatively high Henry's law constant (K_H), CH_3Cl will readily partition out of aqueous solutions into any available headspace. Therefore, a series of CH_3Cl analysis trials were carried out on standard solutions (CH_3Cl in CH_3OH) to compare re-circulating the solution phase as opposed to the gas phase in closed loop configurations.

Initially, the reservoir holding the reaction mixture and the re-circulation tubes were completely filled with water so as to minimize the headspace. Hypothetically, this meant that all of the CH_3Cl would be in the aqueous solution. When this solution was drawn through the MIMS interface, the CH_3Cl could partition out of the water and into the PDMS membrane and through to the MS, but no CH_3Cl was detected by this method. The explanation for this could be that the partitioning of the CH_3Cl from water into the PDMS membrane was not favourable or there was a location of unknown headspace in the set-up that accumulated the CH_3Cl. Conversely, when this analysis was conducted with the sample reservoir half filled with solution and plumbed so that the headspace was being re-circulated over the membrane, it was possible to measure a signal for CH_3Cl. The conclusion to these experiments was that the best method of detection for CH_3Cl was by analysis of the headspace.

Once it was ascertained that headspace analysis would provide the best results for the detection of CH_3Cl in the photoreaction of **4**, a calibration curve was obtained and method detection limits (MDL) were estimated. Calibrations were preformed by injecting methanolic standard solutions of CH_3Cl into the aqueous phase of a closed reaction vessel and allowing the equilibration of the CH_3Cl with the headspace (at a constant temperature), using the same volume fractions of headspace to reaction vessel (note that the $t_{10\text{-}90}$ rise is approximately 60 seconds). The aqueous phase concentration was plotted against the MIMS signal (SIM; m/z = 50, 52) generated from the re-circulated headspace collected over the MIMS interface. Since the proportion of CH_3Cl in the headspace and solution is constant, the amount of CH_3Cl measured in the headspace is representative of the concentration in solution. In this experiment, other

volumes of CH_3Cl were also injected to obtain a calibration curve, showing the excellent linear response for the signal of CH_3Cl by MIMS based on the R^2 of 0.999 (Figure 2.16).

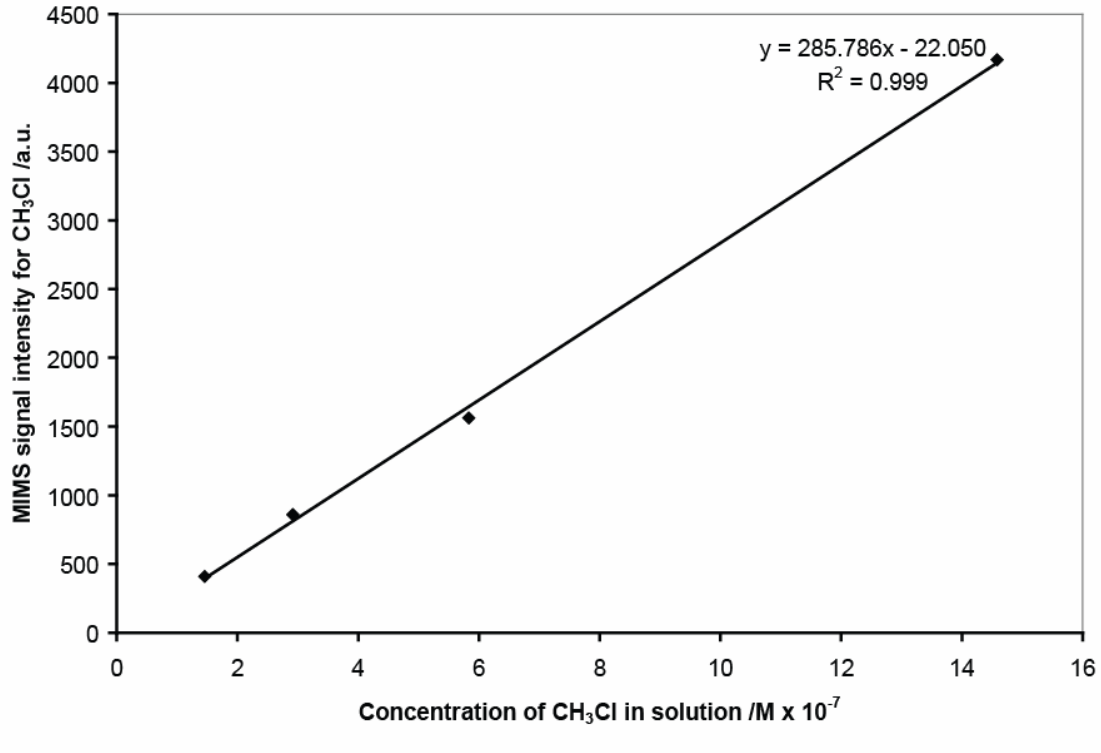

Figure 2. 16: MIMS calibration curve for CH_3Cl in solution (headspace measurement, SIM; m/z = 50, 52).

Detection limits for CH_3Cl were obtained by measuring multiple injections of the same volume of CH_3Cl standard to obtain a standard deviation of the signal response from the MIMS. The estimated detection limit for CH_3Cl under these experimental conditions is 2×10^{-8} M based on S/N = 3.

Before the actual photolysis of **4** was performed, a series of control experiments were run. These included determining whether the temperature had an effect on the intensity of the signal measured for the CH_3Cl and whether there were any thermal reactions by which **4** produced CH_3Cl. To accomplish this, a solution of 10^{-4} **M 4** and 0.5

M Cl^- was added to the quartz reaction vessel with the headspace re-circulated over the MIMS interface. A covering was put over the reaction so as to limit its exposure to ambient light, while the solution was maintained at a constant 22 ^oC. The signal for CH_3Cl was then monitored, with no formation of CH_3Cl observed over a 1.5 hour period, showing that no dark reactions were occurring. Next, CH_3Cl was injected into 400 mL of water to obtain a concentration of 2 x 10^{-6} **M** (in solution). The temperature of the solution was maintained at 22 ^oC until the signal for CH_3Cl was stabilized. The solution temperature was then ramped up to 35 ^oC over a period of 1 hour. The signal for CH_3Cl was stable over the time period of the analysis indicating that the signal intensity on the MIMS was not temperature dependant.

It was also deemed important to determine if the CH_3Cl was photochemically labile under our reaction conditions. This was accomplished by photolysing a 5 x 10^{-6} **M** solution of CH_3Cl at 300 nm for 1.5 hours and monitoring the MIMS signal in the headspace during the photolysis time. No change in the signal for CH_3Cl was observed, indicating that the CH_3Cl was not photolabile over the time frame of this experiment.

Since the analysis for the demethoxylation of **4** revealed that its mechanism was pH dependant, it was possible that the formation of CH_3Cl was pH dependant as well. To test this, the detection of CH_3Cl produced by photolysed **4** would be measured in varying pHs, necessitating a determination of the pH stability of CH_3Cl. Since specific base catalysis for the hydrolysis of CH_3Cl is known,[12] controls were run to monitor the stability of CH_3Cl in pH 7 to pH 11. To accomplish this, a 5 x 10^{-6} **M** solution of CH_3Cl at pH 7 was introduced to the reservoir, with the headspace re-circulated over the MIMS interface. Once the signal for CH_3Cl stabilized, the pH of the solution was adjusted to pH

11 using 1 **M** NaOH. No observable change was detected in the signal for CH_3Cl when the pH was adjusted to 11. Therefore, for the time scale of this experiment, the concentration of OH^- does not affect the signal measured for CH_3Cl over a range of pH 7 to 11. Similar experiments at pH < 7 were not conducted since no acid catalyzed hydrolysis is observed for CH_3Cl.

2.2.3 Photochemical Production of CH_3Cl from Syringic Acid (4) as Measured using MIMS

Preliminary MIMS reaction monitoring for the photolysis of **4** at 254 nm revealed that CH_3Cl, CH_3OH and CO_2 were readily detectable in Cl^- enriched aqueous solution.[92] Consequently, subsequent MIMS photolysis experiments were set up to monitor for CH_3Cl, CH_3OH and CO_2 concurrently using multiple SIM experiments. The photolysis of **4** (H_2O, pH 5, 10^{-4} **M**, 300 nm lamps, N_2 purged before photolysis, < 20 ^oC) shows the simultaneous production of these three VOCs in response to UV light (Figure 2.17). Note that the raw signal intensities in this figure do not represent concentrations as the response factors for each VOC can vary widely and therefore require independent calibrations. Calibration curves were only carried out for CH_3Cl, with the relative changes in the CO_2 and CH_3OH concentrations being monitored by MIMS.

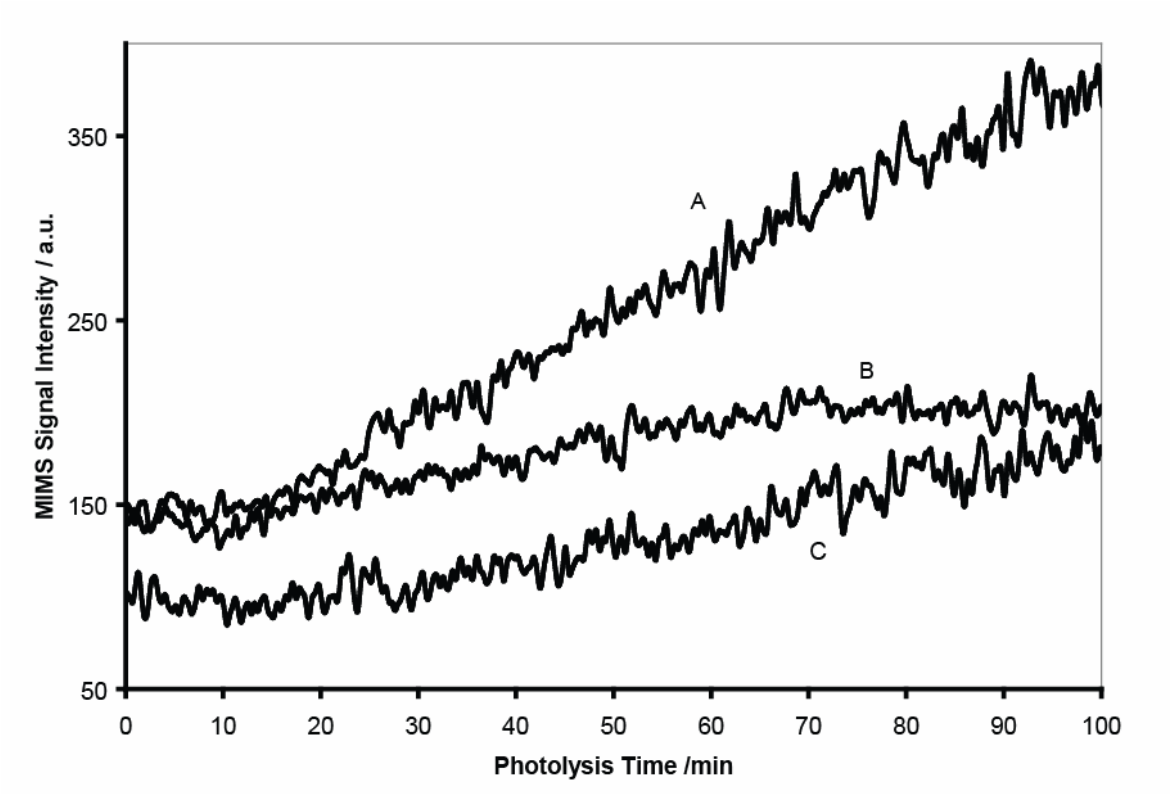

Figure 2. 17: MIMS output for the 300 nm photolysis of **4** in 0.5 **M** Cl^- (measured in the headspace) where the signal intensity has not been corrected for the concentration of the analytes. Curves **A**, **B** and **C** correspond to CO_2 (SIM; m/z = 44), CH_3Cl (SIM; m/z = 50, 52) and CH_3OH (SIM; m/z = 32), respectively.

The CH_3OH in the reaction was not quantified since MIMS headspace analysis proved inefficient due to the longer equilibration times and poor reproducibility of the CH_3OH signal. This was likely because the CH_3OH readily dissolved in the water with very little material to measure in the headspace, thus leading to very inconsistent results. In addition, the m/z for CH_3OH is isobaric with O_2^+, which was not accounted for since we were not directly interested in the CH_3OH production using this method.

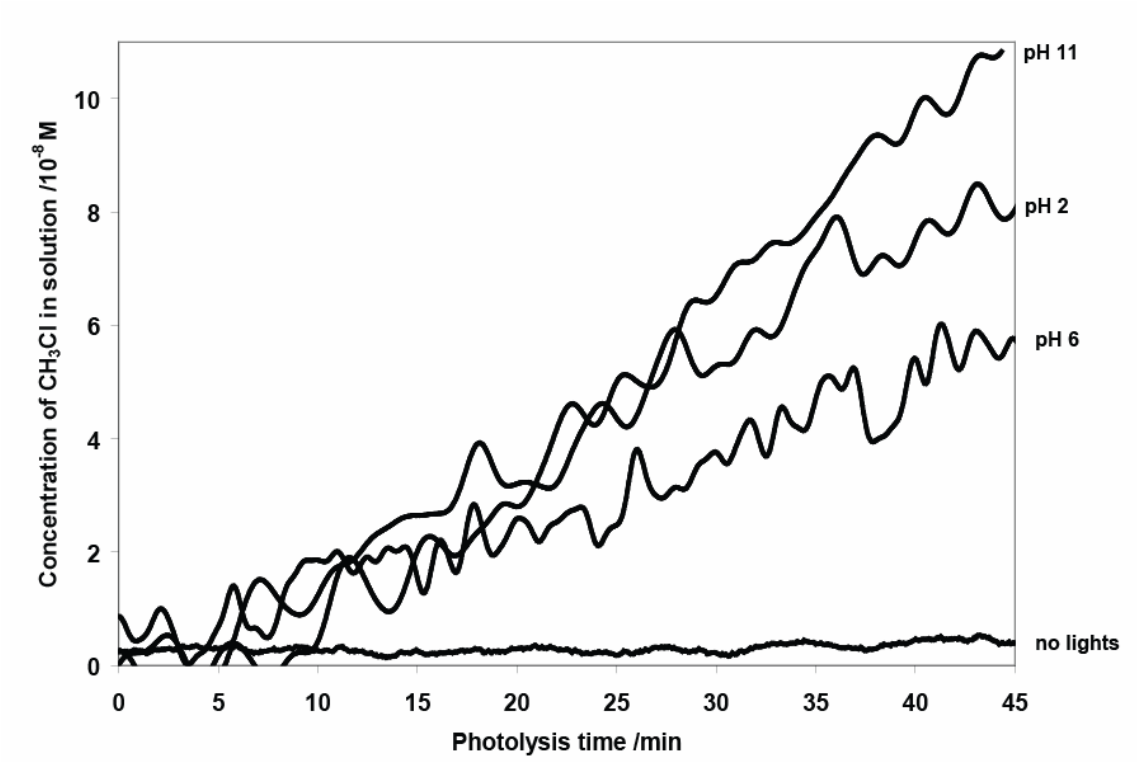

Figure 2. 18: MIMS measurement of CH_3Cl for the 300 nm photolysis of **4** in pH 2, 6 and 11 with 0.5 **M** Cl^- (compared to the dark control experiment) with results quantified in terms of molarity as calculated from the calibration curve for CH_3Cl (SIM; m/z = 50, 52).

To investigate whether the photochemical formation of CH_3Cl from **4** was pH dependant, MIMS was used to monitor VOC production at pH 2, 6 and 11 (H_2O, varied pH, 10^{-4} **M**, 300 nm lamps, N_2 purged before photolysis, < 20 ^oC). The MIMS experiments did not show there to be a significant difference in CH_3Cl formation rates over a pH range of 2 – 11, ranging from ~70 to 140 nM hr^{-1} (Figure 2.18). This observation is in contrast to preliminary work by Moore[43], but it should be noted that the concentrations of CH_3Cl being produced are in the nM range. As such, it is not possible to say with certainty whether there is a pH effect for the formation of CH_3Cl from the

photolysis of **4**. Therefore, this experiment should be repeated at higher substrate concentrations and/or higher photon fluxes to draw further conclusions.

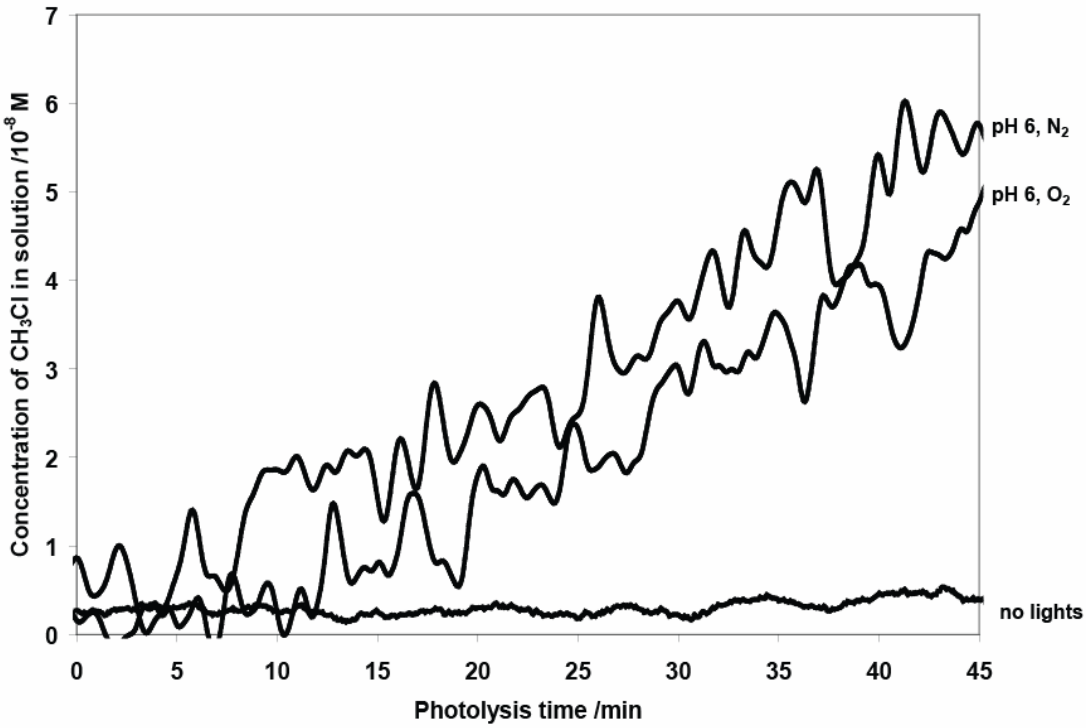

Figure 2. 19: MIMS measurement of CH_3Cl for the 300 nm photolysis of **4** in pH 6 and 0.5 **M** Cl^- purged with N_2 and air (compared to the dark control experiment) with results quantified in terms of molarity as calculated from the calibration curve for CH_3Cl (SIM; m/z = 50, 52).

As was the case for the formation of CH_3OH from **4** measured with ^1H NMR, the MIMS photolysis experiment was conducted in aerated water (Figure 2.19). This shows that there was little difference in the rate of production of CH_3Cl between N_2 saturated and air saturated solution (~70 nM hr^{-1}). Since O_2 is a known triplet quencher and electron scavenger, this result suggests that triplets and free electrons are not intermediates on the pathway to form chloromethane. There was also speculation that a methyl radical might be involved in the mechanism of formation of the CH_3Cl, since the

photochemical formation of CH_3I from molecules similar to **4** has been shown to involve these intermediates.[41] The formation of CH_3I is known to involve the addition of a methyl radical to an iodine atom, where the methyl radical is formed in the photolysis of humic substances. The presence of O_2 is known to quench these radicals though, so it seems that methyl radicals are also not involved in the formation of CH_3Cl from **4**.

Using the CH_3Cl production from the MIMS experiment as a guide, the upper limit for % conversion to CH_3Cl was estimated to be no greater than 0.002 %, which is much smaller than that of CH_3OH (13.8% at pH > 7). Because the yield of CH_3Cl was so small, it was not possible to measure an accurate quantum yield. Based on the relative conversions to CH_3Cl and CH_3OH however, the quantum yield should be on the order of 10^{-4} to 10^{-5}.

2.2.4 Photochemical Production of CH_3Cl from 3,4,5-Trimethoxybenzoic acid (37) and 1,2,3-Trimethoxybenzene (35) as Measured using MIMS

Compounds **37** and **35** were also analysed for their photochemical production of CH_3Cl using MIMS detection. The experiments were set-up the same way as the photolysis of **4**, where solutions of **37** or **35** with 0.5 **M** Cl^- were photolysed with measurement of the headspace for CH_3Cl, CH_3OH and CO_2 (H_2O, pH 7, 10^{-4} **M**, 300 nm lamps, N_2 purged before photolysis, < 20 ^oC). For both **37** and **35**, no CH_3Cl was detected. This indicates that either CH_3Cl was not formed or it was below the detection limit of the MIMS.

MIMS experiments provided direct evidence for photochemical formation of CH_3Cl from **4**. These studies suggest that pH and the presence of O_2 have little to no

affect on the rate of CH_3Cl production. It should be noted however that the concentrations of CH_3Cl observed were close to the detection limit of the MIMS and therefore further system optimization may be necessary to draw firm mechanistic conclusions. Section 2.4 includes a proposed mechanism consistent with the information obtained in these studies.

2.3 Laser Flash Photolysis

Laser Flash Photolysis (LFP) transient absorption spectra were recorded for **4** and **37** in a variety of purging gases and pHs. The intention was to possibly identify intermediates responsible for the demethoxylation and dehydroxylation mechanisms. In all cases, the absorption spectra were obtained from roughly 300 nm (or when self-absorption ended) up to 700 nm. The lifetimes of the main transient absorptions were also determined.

Shown in Figure 2. 20 are transient absorption spectra for the photolysis of **4** in H_2O at pH 10 with the solution purged with N_2 prior to laser photolysis. Besides the small absorptions at 350 and 430 nm, the main transient in the spectra exhibits a very broad absorption from roughly 480 nm to the maximum measured wavelength of 740 nm. The lifetime (single exponential decay) of this transient was measured to be 2.8 μs, while the smaller transient at 350 nm had a lifetime of 5 μs. Due to the many reaction pathways exhibited for the photolysis of **4**, it was not possible to identify the transients at 350 and 430 nm. In addition, this region of the spectrum is a prime location for many varying transients in organic photochemistry and as such makes the identification of these

difficult. The broad transient from 480 nm onward however, was much easier to identify by purging the solution of **4** in H_2O with N_2O instead of N_2 prior to photolysis (Figure 2. 21). The N_2O is a well-known and efficient electron scavenger, and was able to very effectively quench this transient, thereby allowing its identification to be made as the solvated electron ($e^-_{(aq)}$).

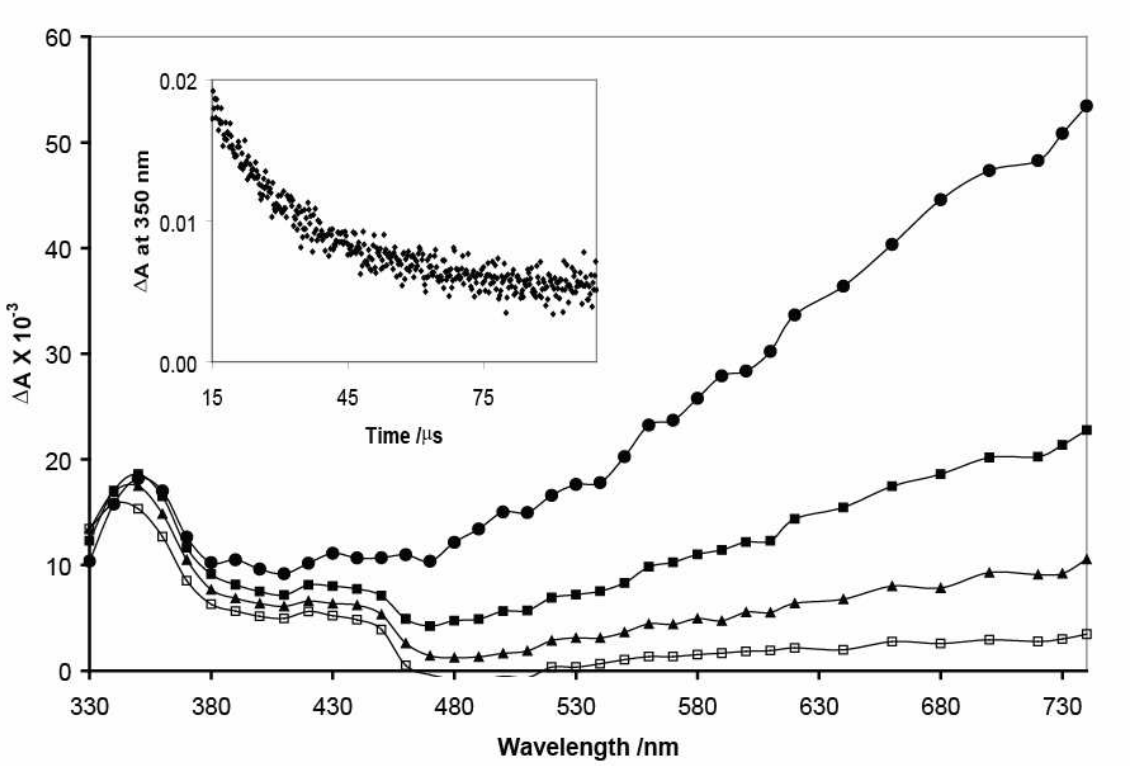

Figure 2. 20: Transient absorption spectra of **4** in pH 10 H_2O purged with N_2; time after laser pulse: (●) = 0.63 μs, (■) = 3.2 μs, (▲) = 6.3 μs, (□) = 13 μs. (Inset: transient decay taken at 2.0 x 10^{-4} ns intervals at λ = 350 nm, τ = 5 μs).

Figure 2. 21 also shows the comparison of the LFP for **4** in acid, O_2, N_2O and base. As observed, the $e^-_{(aq)}$ is only visible for the laser photolysis in base. This leads to several possibilities for the source or mechanistic details of the $e^-_{(aq)}$. Since there were no

$e^-_{(aq)}$ in the LFP for **4** in acid, it is possible that the $e^-_{(aq)}$ were important in the demethoxylation since the photolysis of **4** in acid does not yield CH_3OH. The $e^-_{(aq)}$ could also be responsible for another reaction pathway not involving the demethoxylation. For instance, the formation of the biphenyl product **42** did not occur in acid and the mechanism for its formation could possibly involve the loss of an electron from the starting material **4**. This would account for the fact that the $e^-_{(aq)}$ was visible in base and not in acid. Additionally, it is possible that the $e^-_{(aq)}$ was still formed in the acid, but was not visible in the time scale of the laser pulse.

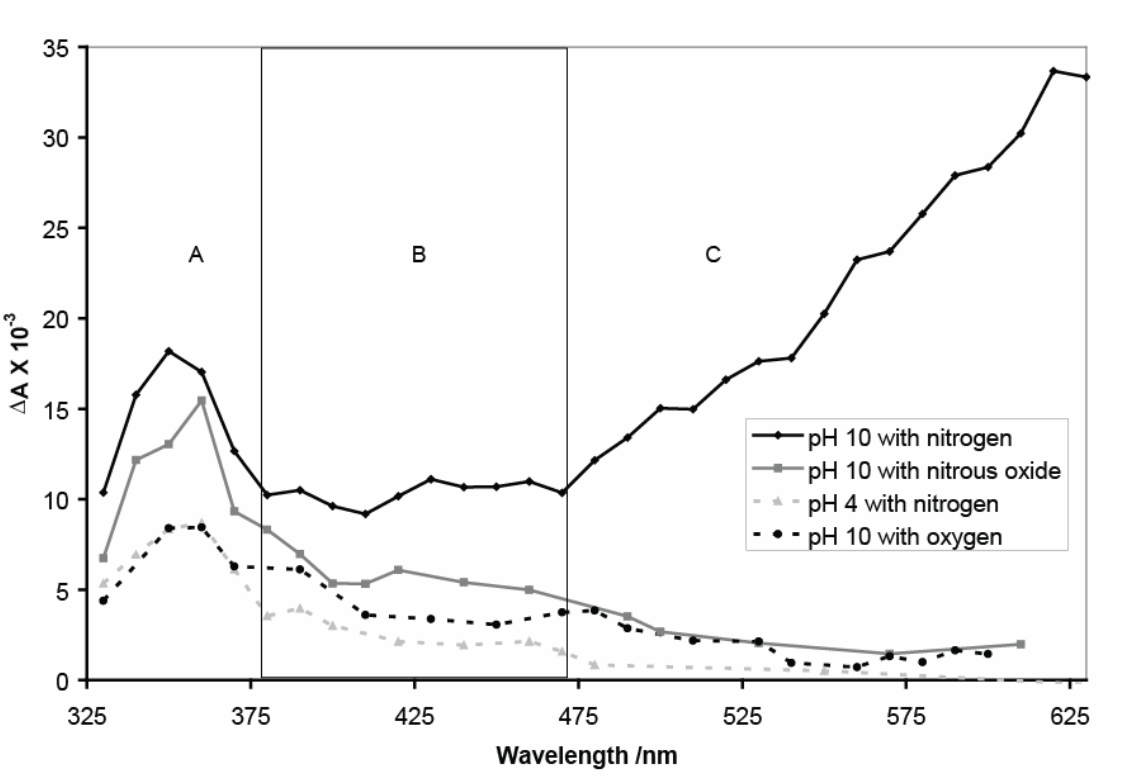

Figure 2. 21: Comparison of the transient absorption spectra for **4** in H_2O at pH 4 and 10 in various purging gases at approximately 1μs after laser pulse. (Transient lifetimes in windows A, B and C: **A** = pH 10 (N_2), pH 10 (N_2O), pH 10 (O_2) and pH 4 (N_2) at 38μs, 5μs, 0.2μs and 4μs, respectively; **B** = pH 10 (N_2) and pH 10 (N_2O) at 8.5μs and 6.2μs, respectively (no transient for pH 10 (O_2) or pH 4 (N_2); **C** = Solvated electron present in only the pH 10 (N_2) sample with a lifetime of 3.5μs).

The LFP for **4** in the presence of O_2 (Figure 2. 21) shows that the O_2 drastically affected the absorptions in comparison to the transients observed for **4** in base (purged with N_2). Specifically, the lifetime of the transient at 350 nm in base was 38 μs while the corresponding transient in the presence of O_2 was only 0.2 μs. This represents a quenching of that transient by the O_2 and may indicate that that transient was a triplet. In addition, the $e^-_{(aq)}$ was absent in the presence of O_2. This indicates that the reaction leading to the $e^-_{(aq)}$ was possibly a triplet or the $e^-_{(aq)}$ was quenched by the O_2.

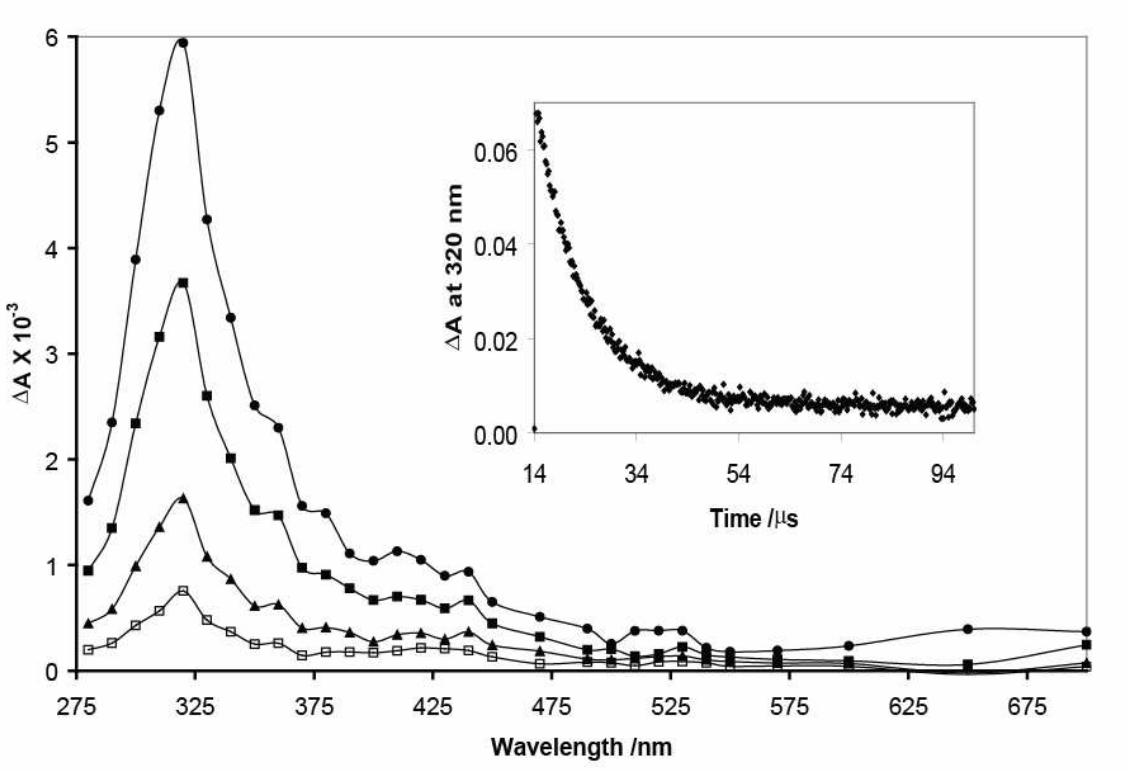

Figure 2. 22: Transient absorption spectrum of **37** in pH 8 H_2O purged with N_2; time after laser pulse: (●) = 0.9 μs, (■) = 3.6 μs, (▲) = 9.4 μs, (□) = 23 μs. (Inset: transient decay taken at 2.0 x 10^{-4} ns intervals at λ = 320 nm, τ = 4 μs).

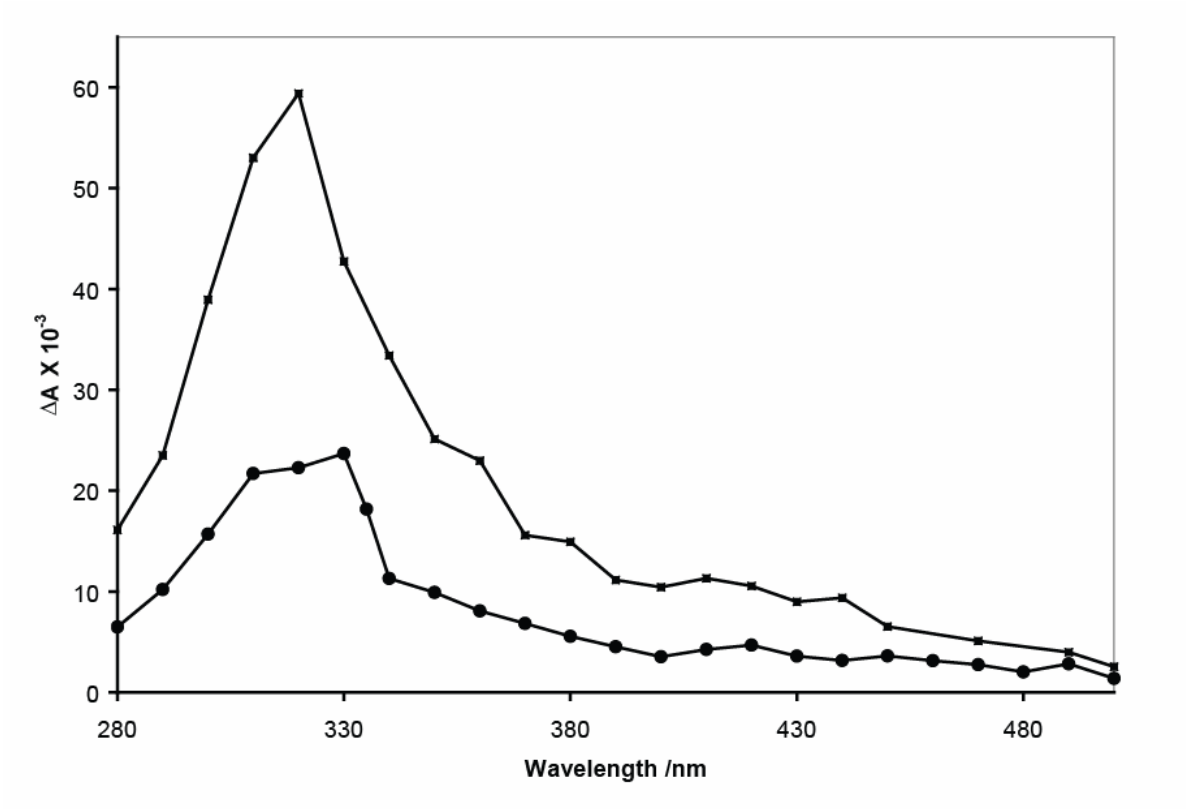

Figure 2. 23: Comparison of the transient absorption spectrum of **37** in pH 8 H_2O purged with N_2 (■) and O_2 (●) (time after laser pulse = 0.93 μs and 0.23 μs, respectively).

Since **37** undergoes similar photochemistry to **4** (i.e. both demethoxylation and dehydroxylation), the LFP for **37** was obtained. The LFP of **37** (Figure 2. 22) shows a blue shift of the main absorption compared to **4** with an absence of the $e^-_{(aq)}$. The main transient for **37** at 320 nm (4 μs) had a very similar lifetime to the transient of **4** at 350 nm (5 μs) (Figure 2.24). Also, when the LFP of **37** was conducted in O_2, a similar quenching of the transient (compared to **4**) at 320 nm was observed (Figure 2. 23). Due to the similar wavelength of absorption, quenching and lifetime, it is likely that this transient has the same identity for both molecules, but again, that specific identity is

unknown. The lack of $e^-_{(aq)}$ was however more diagnostic in the reactivity of these molecules.

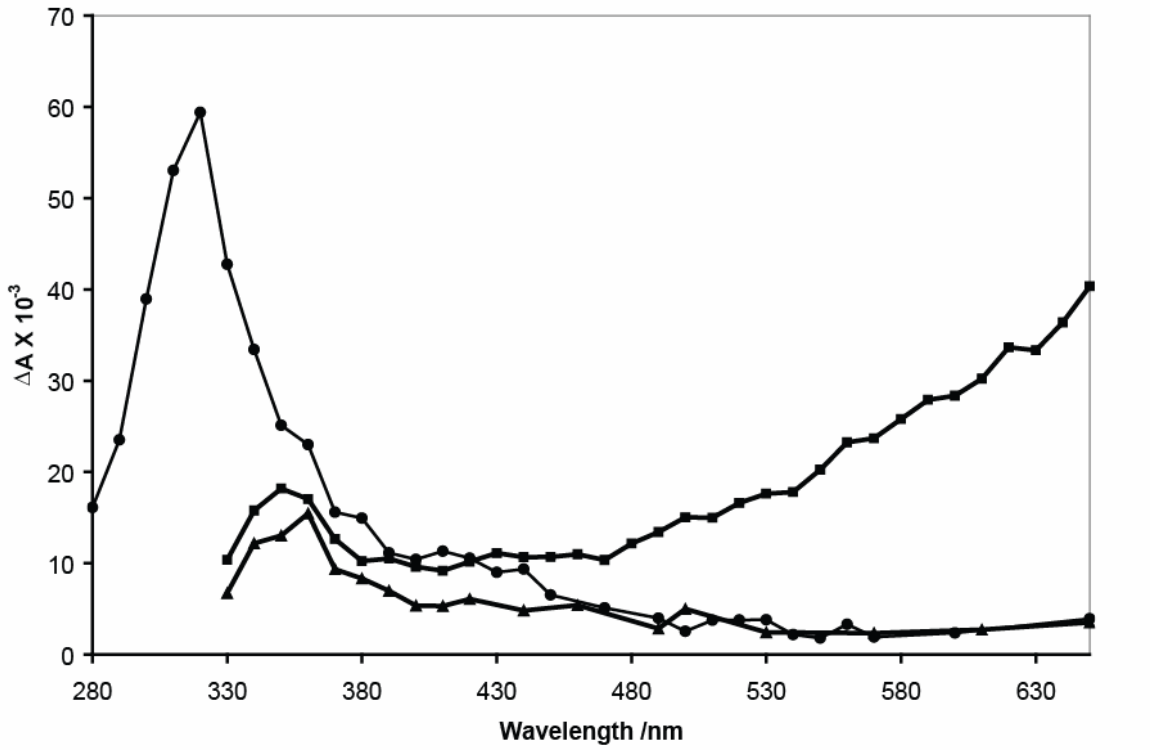

Figure 2. 24: Comparison of the transient absorption spectrum of **4** in pH 10 purged with N_2 (■) and N_2O (▲) and **37** in pH 8 H_2O purged with N_2 (●) (time after laser pulse = 0.63 μs, 1.1 μs and 0.93 μs, respectively).

The only observed reaction under the given conditions that **37** does not undergo that **4** does, is the formation of biphenyl **42**. As mentioned previously (Scheme 2.1), it was possible that the mechanism of formation of this biphenyl involves the loss of an electron from the carboxylic acid group of **4** followed by decarboxylation. Since the only structural difference between **4** and **37** is the presence of a phenol hydroxy group on **4**, it is also possible that in basic solution, **4** exists in the di-anion form at which point the

phenoxide group can lose an electron. Through resonance, the phenoxyl radical can lead to the decarboxylation observed and the formation of CO_2 and biphenyl **42** (Scheme 2.2).

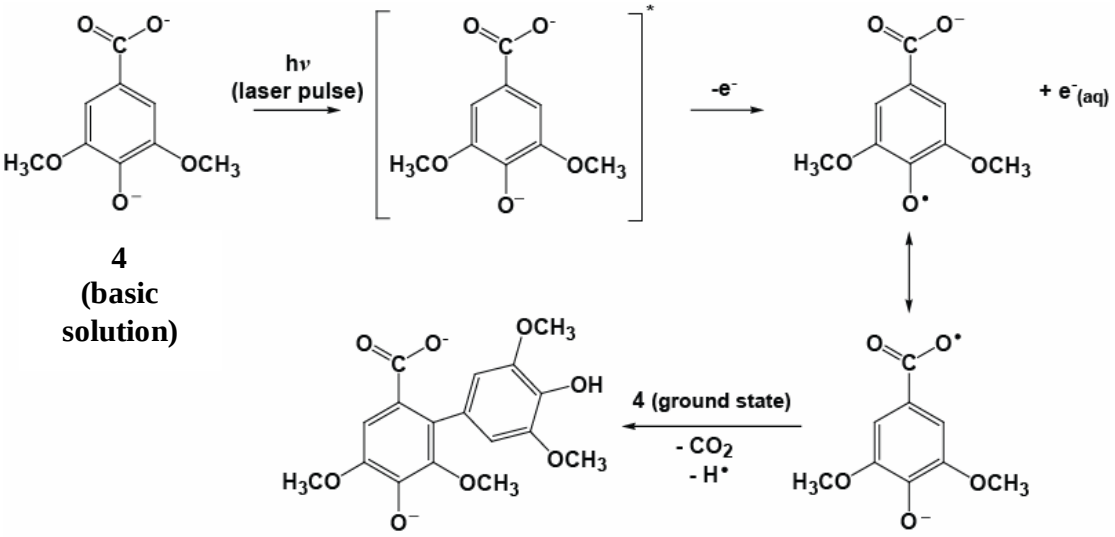

Scheme 2. 2

Since **37** is lacking the phenol hydroxy group, it would not be able to undergo this mechanism, thus accounting for the absence of the $e^-_{(aq)}$ and biphenyl **42**. Compound **37** may also be forming a $e^-_{(aq)}$, but its decay was faster than the laser pulse and therefore was not detectable in the scope of this LFP experiment. Due to the ambiguous nature of the results it was not possible to ascertain for certain where the $e^-_{(aq)}$ came from.

2.4 Mechanisms of Reaction

Using the product study data in conjunction with LFP and MIMS results, mechanisms were proposed for the formation of CH_3OH, CH_3Cl and 3,5-

dihydroxybenzoic acid (**39**) from **4** photochemically. The mechanism for the demethoxylation was initially proposed to occur via several different pathways, while only one mechanism was proposed to exist for the dehydroxylation and production of CH_3Cl. Due to the high complexity of the LFP spectra, it was not possible to identify specific transients involved in the mechanisms. Instead, the product studies and pH effect for the demethoxylation were the main sources of data for elucidating a possible mechanism. The MIMS studies provide some additional information on the extent of formation of CH_3Cl.

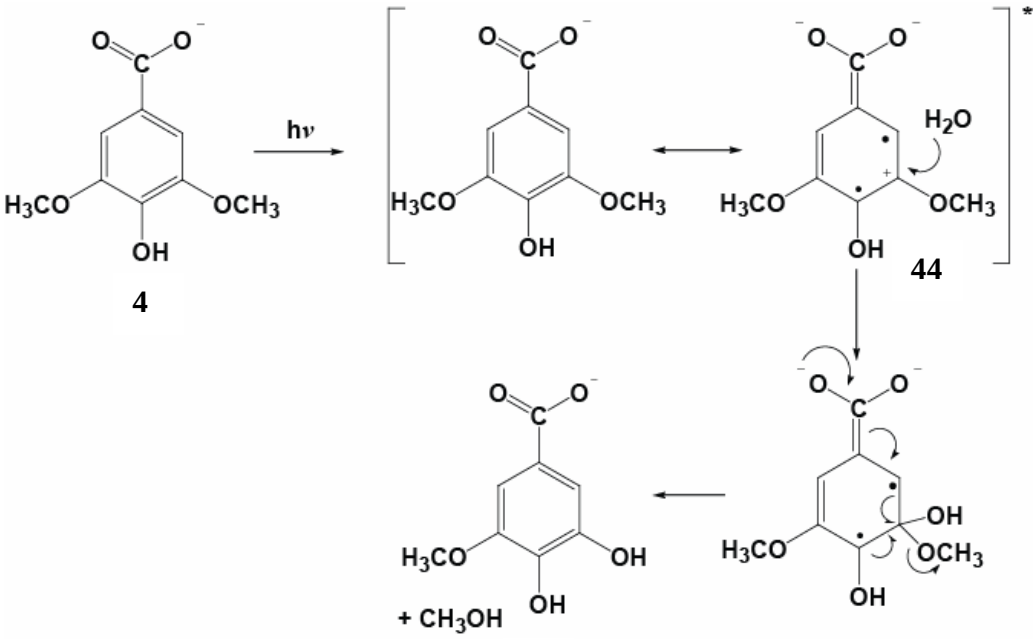

Scheme 2. 3

Since the demethoxylation can be described as a photosubstitution (methoxy group exchanged for water), two mechanisms were proposed that involve typical photosubstitution intermediates. The first proposed mechanism involves the Ortho-Meta

Effect, explained in Section 1.4.1. For this mechanism to occur, the intermediate **44** is a diradical with a cation that can allow nucleophilic attack by the water (Scheme 2.3). After the nucleophilic attack, the methoxy group acts as the leaving group, with **36** as the final product.

This mechanism agrees well with a demethoxylation (as opposed to demethylation) that is pH dependant, where the protonated acid group (pH < 4) could be withdrawing enough to destabilize the intermediate and thus quench the reaction. Additionally, this mechanism could be applied to the other compounds that demethoxylated (**37**, **36**, **33**, **34**), while the compounds that did not form CH_3OH do not have the requisite donating groups to stabilize the intermediate (**38**, **39**, **35**, **15**).

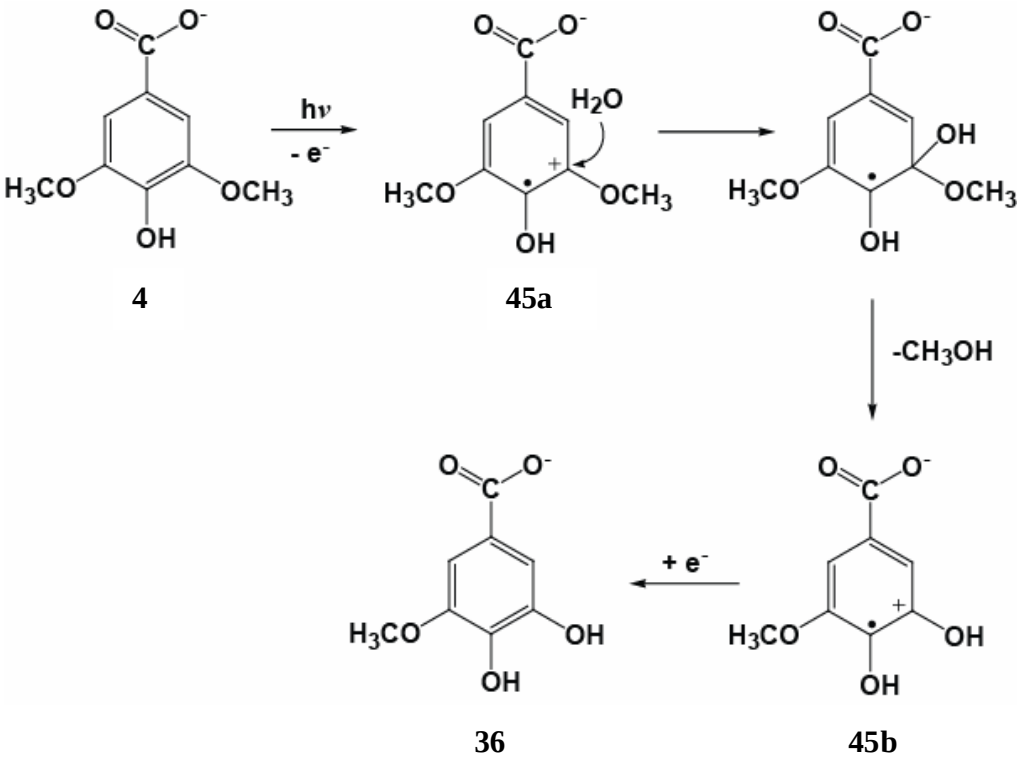

Scheme 2. 4

Another type of photosubstitution that could be involved is that which utilizes a different radical cation intermediate (Scheme 2.4). This mechanism involves the loss of an electron from **4**, producing the radical cation intermediate **45a** which can allow the nucleophilic attack by the water onto the ring. Once the methoxy group leaves, the compound returns to a radical cation intermediate (**45b**). In order to reach a neutral product however, the compound must acquire an electron, likely from water (i.e. a solvated electron ($e^-_{(aq)}$)). The fact that the LFP showed a $e^-_{(aq)}$ for the photolysis of **4** in base was a promising finding for this mechanism, but since **37**, which also demethoxylates, did not produce a $e^-_{(aq)}$, it seemed more likely that this electron was involved in a different mechanism such as the formation of biphenyl **42** from **4**.

As was the case for the Ortho-Meta Effect mechanism, the radical cation mechanism was also indicative of a demethoxylation as opposed to demethylation. This mechanism also agrees well with the observed pH effect since **4** in the protonated form would likely have a destabilized intermediate due to the withdrawing effect of the acid moiety. This mechanism also agrees well with the product studies in that all of the compounds that were found to demethoxylate have at least three donating groups on the ring (methoxy and hydroxy groups) which would be important in the stabilization of the radical cation intermediate. Comparatively, those compounds that did not have three donating groups (such as **38** and **39)** did not exhibit CH_3OH formation.

However, one confounding piece of evidence to suggest that the radical cation mechanism was not likely is that phenol radical cations very easily form phenoxyl radicals in water due to the extremely low pK_a of the hydroxy group in aqueous media.[96] Based on this, it would be virtually impossible for **4** to demethoxylate since the radical

cation would instead turn into a phenoxyl radical. In addition, it is well known that water is typically not a strong enough nucleophile to allow photosubstitution to occur on anisole derivatives. Even though this mechanism looks logical as written in Scheme 2.4, it was discounted based on the phenoxyl radical and anisole arguments. The fact that water is not typically a strong enough nucleophile for this type of compound can also help to dispute the Ortho-Meta Effect mechanism.

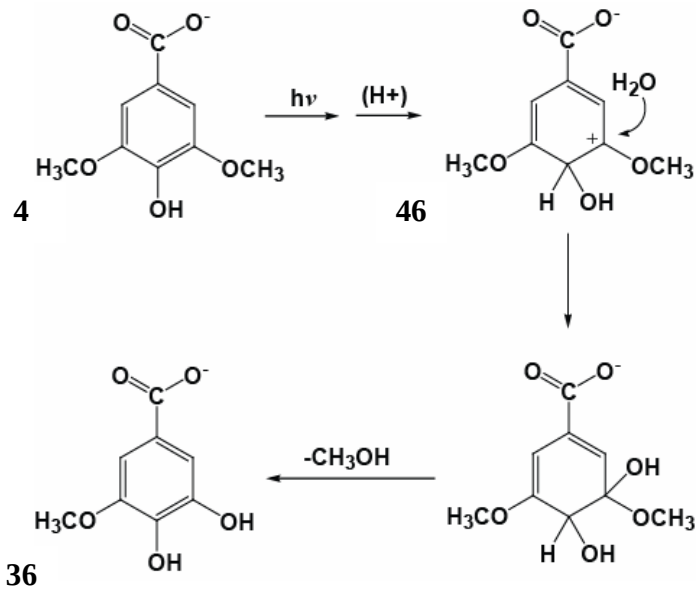

Scheme 2. 5

A third mechanistic possibility that does not involve a photosubstitution is photoprotonation. This mechanism would involve the protonation of the aromatic ring, thus forming a cation that could facilitate the nucleophilic attack by water and loss of the methoxy group (Scheme 2.5). In order for this to occur however, the aromatic ring must be basic enough to allow the protonation. In general, aromatic carbons are not considered

very basic, however photochemical reactions involving ring protonations are known and were discussed previously in Section 1.4.2.[81]

The most important piece of evidence to suggest that **4** is undergoing photoprotonation was in the formation of **39** where the hydroxy group in **4** was replaced by a proton from water. This mechanism involves the protonation of the carbon in the 4-position of **4** with a formal loss of OH^+ (Scheme 2.6). The driving force for this mechanism must be the creation of a lower energy species, likely as a result of the decreased sterics when the hydroxy group is replaced for a proton. The OH^+ would likely be consumed quite readily by the electron rich **4** (in the ground state). Another possibility is that the hydroxy group was lost via formation of hydrogen peroxide, but all attempts to identify hydrogen peroxide in the reaction mixture failed.

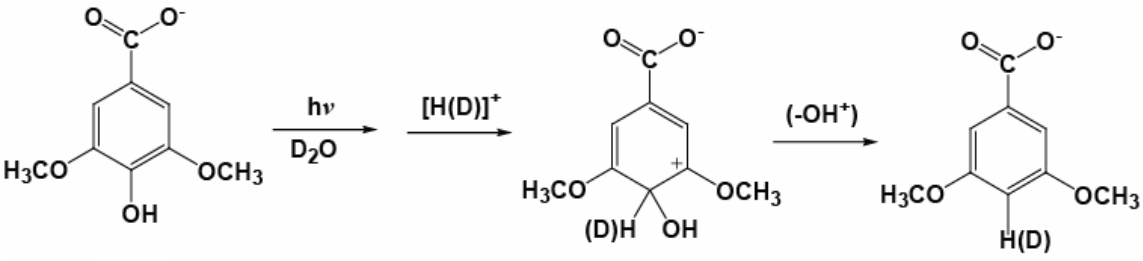

4 **39**

Scheme 2. 6

Like the other proposed mechanisms, the photoprotonation mechanism agrees well with the photolysis of the related compounds and the observed pH effect. The explanation for the pH effect again lies in the withdrawing characteristics of the acid group of **4** when it is in the protonated form. Since the photoprotonation must be a result

of increased basicity of the aromatic ring, a donating substituent would be required. It seems that the carboxylate form of the acid is donating enough to increase the basicity of the ring to allow the protonation to occur. In addition, the presence of the one hydroxy and two methoxy groups on **4** would assist in increasing the basicity since they are also donating substituents. The influence of their donating ability was evidenced by the lack of reactivity exhibited in **38** and **39**. These compounds were lacking the full assortment of donating groups, therefore resulting in insufficient basicity of the ring and no demethoxylation. The three donating groups on **4** would also be important in stabilizing the carbocation that formed after the protonation took place and since **38** and **39** were lacking all three donating groups, the intermediate may not have been effectively stabilized.

For both ketone **33** and ester **34**, the yield of CH_3OH was significantly smaller than in **4**. This indicates that even though the withdrawing groups (ketone and ester) seemed to be limiting the photoprotonation, there was another factor that was still allowing the protonation to occur. It may be that the three donating groups on these compounds have enough capacity to increase the basicity of the ring to allow the reaction to occur to some extent.

It would seem that any of the aromatic carbons (other than position 1; substituted with carboxylic acid) could be protonated during the photolysis of **4**. If either of the aromatic carbons substituted with a methoxy group were protonated however, it should have been possible to isolate starting material with a deuterated hydroxy group (if the reaction was performed in D_2O). In addition, if either of the unsubstituted ring carbons were protonated, then it still would have been possible to form CH_3OH via the loss of one

of the methoxy groups, but the protonated ring carbon would have retained a deuterium in the final product (also for reaction in D_2O). Because neither of these deuterated compounds were observed by ^1H NMR or ESI-MS, it seems that only the aromatic ring carbon substituted with the hydroxy group was protonated in the photolysis. The most likely explanation for this is that the *para* donation of the carboxylate group and *ortho* donation of the methoxy groups (in the excited state) allowed for the highest basicity on the 4-position. The other ring carbons may still have increased in basicity, but not enough to allow the protonation to occur, or they protonated in a small enough yield to be undetectable.

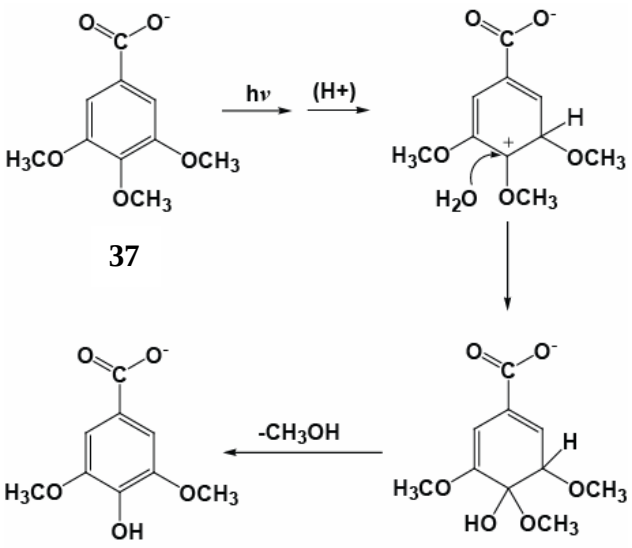

37 **4**

Scheme 2. 7

As discussed previously for the photolysis of **37**, instead of demethoxylating at the 3 or 5 position, the central methoxy group (4-carbon) on **37** was lost instead. In order for this to occur via a photoprotonation mechanism as seen for **4**, the 3 or 5 carbon would have been protonated. This is in contrast to the site of protonation seen for the

photolysis of **4** leading to demethoxylation. Therefore, the mechanism for the demethoxylation of **37** had to be slightly different than that for the photoprotonation of **4** (Scheme 2.7). The most plausible explanation for this observation was that protonation on one of the outer methoxy groups (carbon 3 or 5) was favoured sterically. This would have resulted in a lower energy intermediate, with the central methoxy acting as the leaving group.

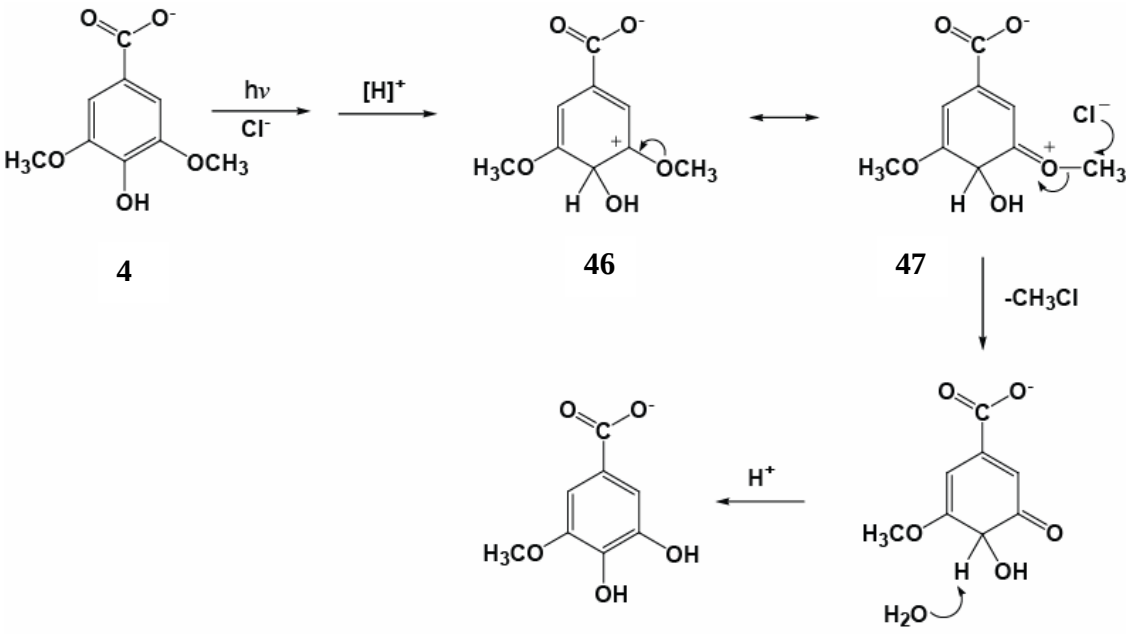

Scheme 2. 8

Conveniently, a photoprotonation mechanism can also be used to explain the formation of CH_3Cl from **4**. Some caution must be made in interpreting this mechanism though, since more work is needed on the MIMS. While, it is possible to write a mechanism for the formation of CH_3Cl using the radical cation intermediate **45**, diradical intermediate **44** or methyl radical, these were discounted as likely scenarios. For this

reason, the proposed mechanism is that which also involves photoprotonation (Scheme 2.8). This mechanism again involves the protonation of the hydroxy ring carbon (4-position), producing the carbocation **46**. Through resonance, this cation is partially situated on the oxygen of one of the methoxy groups (**47**) which would initiate the nucleophilic attack by chloride onto the methyl group of the methoxy, thus yielding the CH_3Cl.

In photochemistry it is often useful to use theoretical calculations to approximate the electronic changes on going from the ground to excited state. Since the excited state is formally formed when an electron is promoted to a higher energy orbital, HOMO-LUMO calculations are a good way of illustrating the electron migration between the ground and excited states (where the HOMO is the highest occupied molecular orbital and the LUMO is the lowest unoccupied molecular orbital). When a compound in the ground state (i.e. when the HOMO is occupied) is irradiated, an electron is promoted to the LUMO, which often results in a charge migration in the molecule. This charge migration can be viewed using the HOMO-LUMO calculations and can be useful in explaining mechanisms that have been proposed for photochemical reactions. In this study, HOMO-LUMOs were calculated using AM1 approximations in ChemDraw 3D.

Figure 2.25 shows the HOMO-LUMOs for **4** in the protonated and deprotonated states (of the carboxyl group). This shows that for **4** in acidic media, there was a migration of electrons from the benzene ring to the acid group upon excitation. In contrast, **4** in carboxylate form has most of the electron density situated on the carboxylic acid group in the HOMO, but upon excitation, all of this charge was re-positioned around the benzene ring. This difference in electron migration between protonated and

deprotonated **4** nicely explains the observed reactivity difference as a function of pH. The electron migration to the benzene ring in the LUMO for **4** deprotonated indicates an increase in basicity of the ring carbons. This increase in basicity could allow more efficient protonation and subsequent demethoxylation.

	HOMO	LUMO
4 Acidic	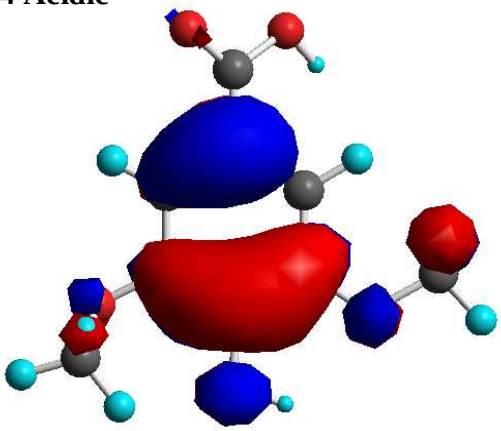	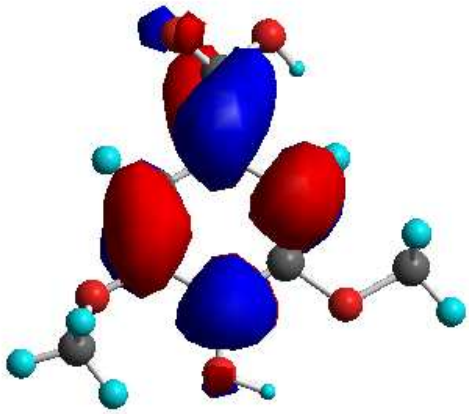
4 Basic	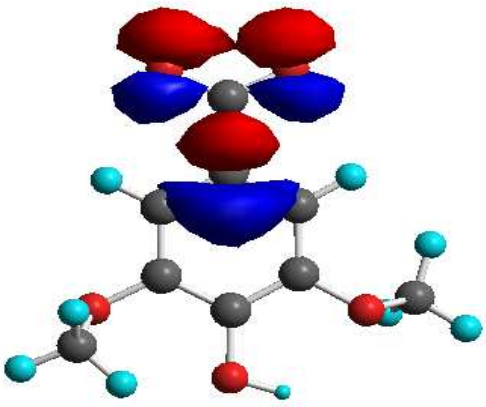	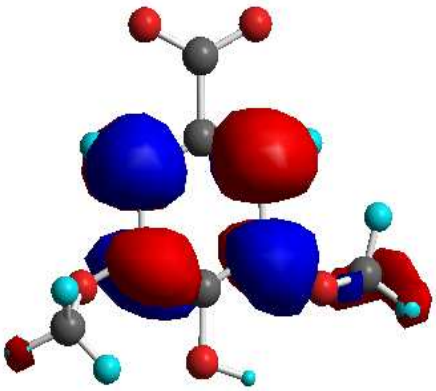

Figure 2. 25: HOMO-LUMO calculations of **4** in acid and base (AM1 approximation).

A comparison was also made between deprotonated **4** and **33** and **34**, where **4** and **34** exhibit electron migration from the HOMO to LUMO from either the acid or ester group to the benzene ring. This electron charge is re-positioned around the benzene ring so that none of the charge is left on the acid or ester moiety in the LUMO on **4** and **34**, respectively (Figure 2.25 and 2.26). Comparatively, ketone **33** also exhibits re-positioning of the electron charge to the benzene ring in the LUMO, but some of the charge remains on the ketone moiety.

	HOMO	**LUMO**
33	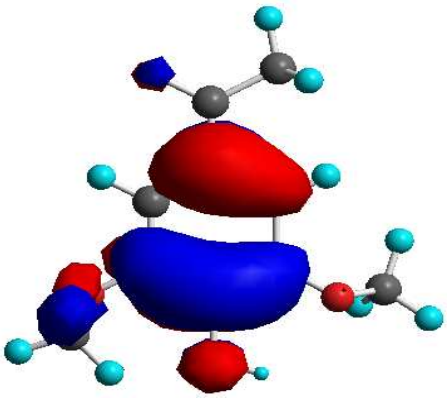	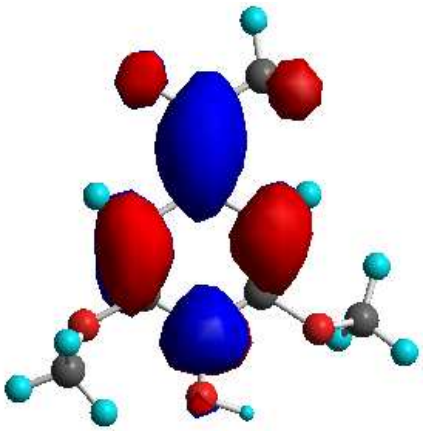
34	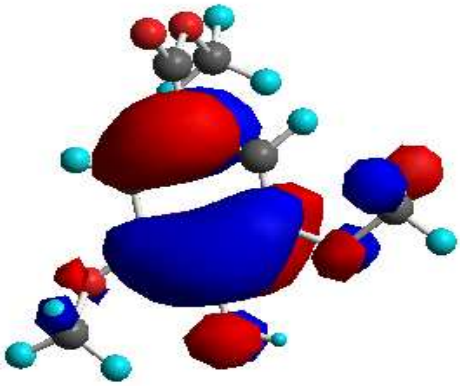	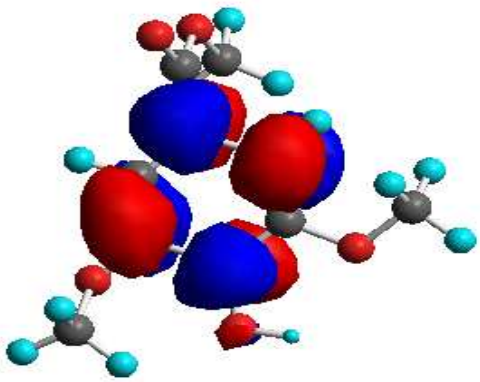

Figure 2.26: HOMO-LUMO calculations of **33** and **34** (AM1 approximation).

If a comparison were made between **33** and **34**, it would be tempting to hypothesize that ester **34** would be more reactive than ketone **33** since the HOMO-LUMO of **34** is more similar to **4** in carboxylate form, however, this was not the case. One possible explanation is that the ester may have a faster photoprotonation step due to a higher ring basicity compared to **33**, but the differing characteristics of the ester moiety may destabilize the intermediate, thus leading to a decreased yield of CH_3OH. Alternatively, the difference in the yield of CH_3OH production between **33** and **34** (1.8 % and 0.5 %, respectively) could be accounted for by the error associated with the NMR analysis used to calculate the yields. This could account for the apparent higher degree of reactivity exhibited by ketone **33** compared to ester **34**. The fact that the ketone **33** does not exhibit complete charge migration to the benzene ring represents a very large difference in the properties of the ring carbons between **4** and **33** and perhaps different reactivity since **4** produced significantly more CH_3OH than **33**.

When **37**, **38** and **39** (all in carboxylate form) were viewed using the HOMO-LUMO calculations, they look almost identical to **4** while of those three, only **37** undergoes demethoxylation (Figure 2.27). While the carboxylate form of the acid group was important for the demethoxylation, other factors had to be involved as well otherwise **38** and **39** would have formed CH_3OH under the conditions of the experiment. In this case, it is likely that the charge migration from the carboxylate group to the benzene ring was important for the creation of the intermediate via the excited state, but once there, compounds **38** and **39** did not have the requisite characteristics to stabilize the intermediate. As mentioned previously, it seems that three donating groups are necessary to stabilize the cation intermediate and since **38** and **39** do not have these three groups,

they were not able to demethoxylate. Of course these compounds may in fact demethoxylate, but reaction conditions necessary for this to occur may be different. For instance, *o*-dimethoxybenzene **27** is known to lose CH_3OH but only under acidic conditions.[81]

HOMO	LUMO
37 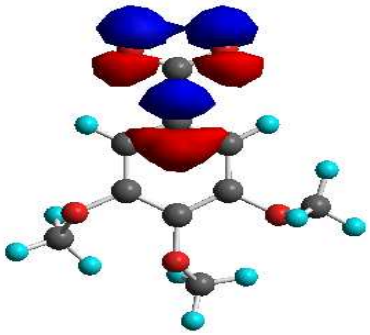	**37** 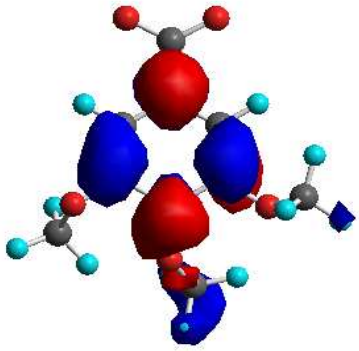
38 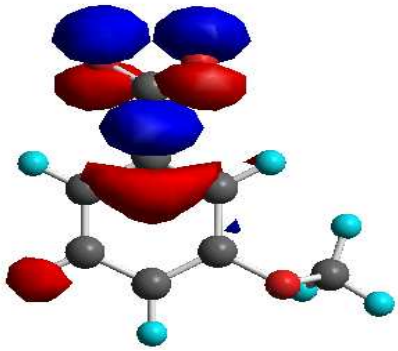	**38** 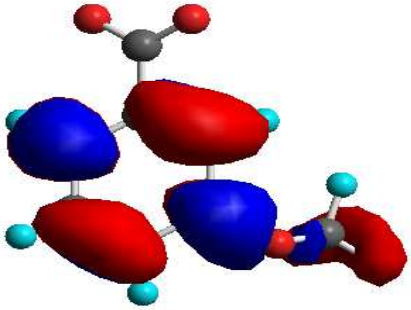
39 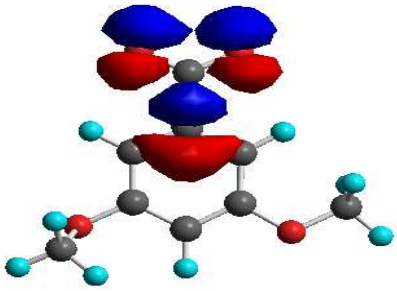	**39** 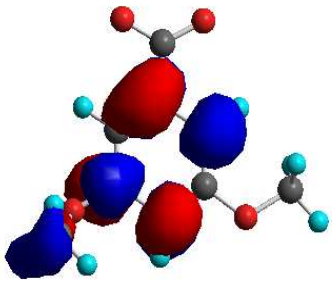

Figure 2.27: HOMO-LUMO calculations of **37, 38** and **39** (AM1 approximation).

The above mentioned calculations were useful in giving insight into the mechanisms proposed previously. Based on experimental evidence, it seems that photoprotonation was the most likely mechanism for the formation of CH_3OH, CH_3Cl and the dehydroxylated product. For the photosubstitution mechanisms, the LUMO electron density does not agree with the product studies. In particular, the mechanism for photosubstitution using an Ortho-Meta Effect intermediate, utilizes the withdrawing capabilities of the acid group to create a cation on the benzene ring at which the water can attack. For protonated **4**, the LUMO shows that there was indeed electron migration towards the acid group, but in the carboxylate form of **4** that was not case; instead the electron density was positioned around the ring. This is opposite to what would be expected if the Ortho-Meta Effect were involved for the demethoxylation of **4**.

2.5 Summary

Product studies for the photolysis of **4** and related compounds have revealed that the main photochemical reactions that **4** undergoes in water are dehydroxylation and demethoxylation, the latter to yield CH_3OH. These reactions were proposed to occur via a photoprotonation of the benzene ring when the photolysis was conducted in basic conditions. The presence of base allowed the deprotonation of the carboxylic acid group in **4** which upon radiation, led to an electron migration from the acid group in the HOMO to the benzene ring in the LUMO. This migration of electron density increased the basicity of the ring, allowing the protonation to occur. In acidic media, electron density migration into the ring is attenuated, which resulted in an insufficient increase in basicity.

Besides the presence of the acid group, the three donating groups on **4** were also found to be fundamental to the photoprotonation mechanism. Either these donating groups were responsible for stabilizing the resulting cation or they were assisting in increasing the basicity of the benzene ring to allow protonation to occur or both factors were involved. The formation of CH_3Cl was found to occur at a much lower yield (compared to CH_3OH formation) as measured by MIMS, with all three reactions rationalized as going through the same intermediate (Scheme 2.8).

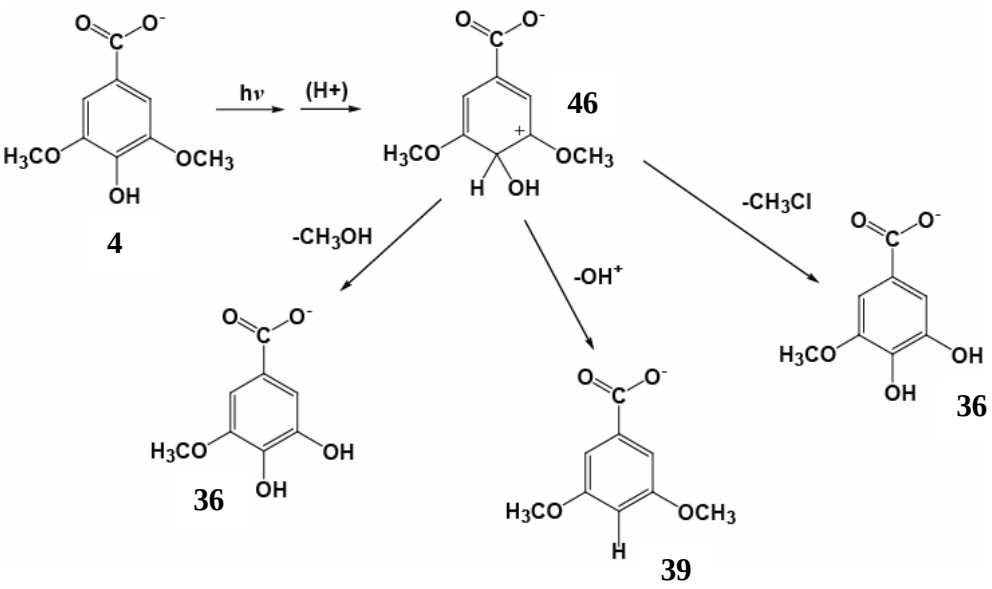

Scheme 2. 9

Chapter 3
Experimental

3.1 General

^{1}H NMR spectra were recorded on a Bruker AC 300 (300 MHz) instrument using D_2O, $CDCl_3$ or DMSO-d_6 as solvents. Chemical shifts were reported in ppm downfield from referenced TMS at 0 as determined from the residual solvent signal with the splitting patterns reported as s (singlet), d (doublet), t (triplet) or m (multiplet). Mass spectra were recorded using Electrospray Ionisation Mass Spectrometry on a Micromass Q-toff *micro* instrument in the negative ion mode with the sample in CH_3OH. UV-Vis spectra were measured on a Varian Cary 50 spectrophotometer in 1 cm diameter quartz cells. Transient UV-Vis spectra were obtained using nanosecond LFP excitation by a Spectra Physics YAG laser (Model GCR-12; 266nm excitation). pH measurements were taken using a Fisher Scientific Accumet Research Dual Channel pH / Ion meter. MIMS data were obtained using a quadrupole ion trap mass spectrometer with an external ion source (Polaris-Q™, Thermo-Electron, San-Jose, CA, USA) equipped with an in-house constructed MIMS interface.

3.2 Materials

3.2.1 Common Laboratory Reagents

All solvents (HPLC grade acetonitrile, CH_3OH, dichloromethane, diethyl ether, isopropanol) were used as received. Sodium hydroxide solutions were made by dissolving pellets in distilled water, while hydrochloric acid and sulphuric acid were used

as received after dilution. Standard solutions of CH_3Cl 2000 µg/mL in methanol were supplied in sealed ampules from Fisher Scientific and used as received.

3.2.2 Synthesis

3-Methoxygallic Acid (36)

Methyl gallate (10.1 g, 55.0 mmol) was dissolved in 800 mL of 5% aq. borax solution. A solution of dimethyl sulphate (30 mL) and NaOH (13.2 g in 50 mL water) was added dropwise over 3 hours, after which the black solution was left to stand overnight. The resulting brown solution was then acidified using approximately 25 mL of 40% H_2SO_4, resulting in a clear brown solution with white precipitate. This suspension was extracted continuously with ethyl acetate. Charcoal was used to decolourize the solution before it was concentrated under reduced pressure to leave an orange-brown oil. The resulting material was added to 100 mL of 20% NaOH (aq) and refluxed for 1 hour. The resulting brown mixture was then acidified with HCl and continuously extracted with ether to leave a red solution. The crude product was recrystallised three times in hot water (once with charcoal) to give 4.70 g of tan brown crystals. These crude crystals were then recrystallised in hot benzene and methanol (1:1) to give 1.04 g of white crystal (10% yield); ^{1}H NMR (300 MHz, DMSO-d_6) δ 3.78 ppm (s, 3 H, OCH_3), δ 7.02 ppm (d, 1 H, 2-position H), δ 7.07 ppm (d, 1 H, 3-position H), δ 9.04 and 9.28 ppm (s, 1 H each, OH), δ 12.42 ppm (s, 1 H, COOH), ESI-MS m/z 183 (negative ion mode).

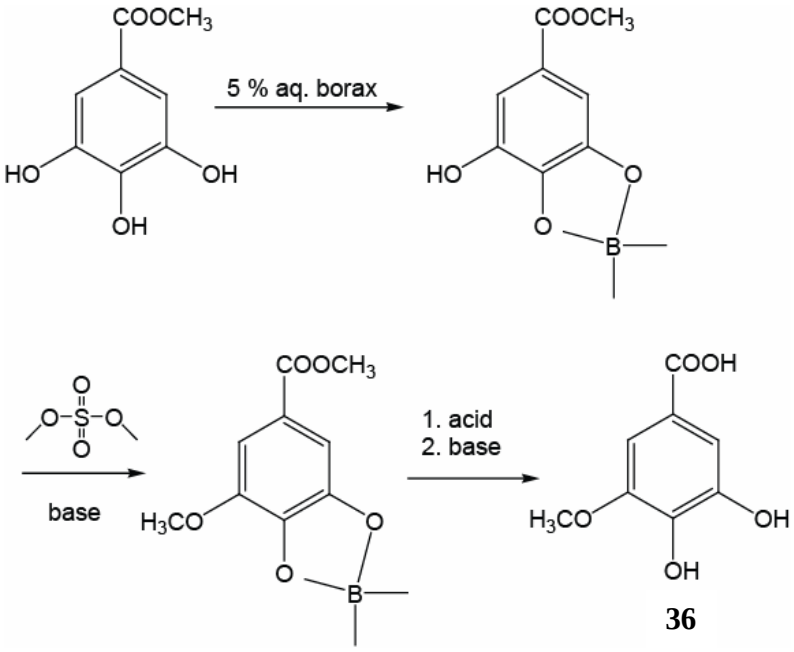

36

Methyl Syringate (34)

Compound **34** was prepared using a standard Fischer Esterification of syringic acid (**4**) (0.41 g, 2 mmol) with a catalytic amount of H_2SO_4 in 40 mL methanol. The resulting white solution was washed out of the round bottom flask with 35 mL ether and 25 mL H_2O. After draining off the H_2O layer, the ether layer was washed with 4 x 25 mL 5 % $NaHCO_3$ and 25 mL H_2O. The ether layer was dried with $MgSO_4$, with the solvent evaporated under reduced pressure. The reaction resulted in 0.40 g of white crystal (91% yield); ^{1}H NMR (300 MHz, $CDCl_3$) δ 3.87 ppm (s, 3 H, ester CH_3), δ 3.91 ppm (s, 6 H, OCH_3), δ 7.29 ppm (s, 2 H, Ar H).

3.3 Product Studies

All NMR scale and preparative scale photolyses were carried out in a Rayonet RPR 100 photochemical reactor equipped with 16-300 nm lamps. The solutions were purged with argon for inert atmosphere experiments or air using a stainless steel needle for approximately 10 minutes prior to photolysis. All photolysis experiments ranged from 30 minutes to 10 hours depending on the experiment. For all systems studied, dark reactions were monitored by measuring the ^{1}H NMR of the compounds under the specified conditions using similar gas purging and temperature in the absence of light to ensure that no reactions were taking place. No dark reactions were observed.

NMR Scale Photolysis of Syringic Acid (4) and Related Compounds

For NMR scale photolysis, the solutions were contained in a closed quartz tube (~ 25 mL) which was cooled to approximately 15 ^{o}C using an external water bath. There was no workup necessary for the NMR scale photolysis since the experiment was conducted in deuterated solvent. The solution was simply transferred to an NMR tube using a Pasteur pipette (for CH_3OH measurement) or a gas tight syringe when attempts were made to measure CH_3Cl.

For the photolysis of **4** in which the yield of CH_3OH was measured, 10 mg of **4** was dissolved (using a sonicator) in approximately 9 mL D_2O and 1 mL CD_3CN so that the concentration was 10^{-3} to 10^{-4} **M**. In some cases, the amount of CD_3CN was adjusted if there were difficulties getting **4** into solution. The pD was then adjusted as necessary using 0.1 **M** NaOD or 0.1 **M** D_2SO_4 and was measured using a Fisher Scientific Accumet

Research Dual Channel pH / Ion meter. If the photolysis required an added ion (Cl^-, I^- or CN^-), this was added as NaCl, NaI or KCN, respectively, to achieve 0.5 **M** in the reaction mixture. ^1H NMR of the reaction mixture (without workup) showed the formation of CH_3OH for pH < 4 as measured by the signal at δ 3.36 ppm (this signal varied slightly if the ratio of D_2O to CD_3CN differed). This was confirmed by spiking in neat CH_3OH and observing the overlapping of the signals. Confirmation of the CH_3OH formation was also made when the photolysis of **4** was measured using MIMS. Conversion to product was measured by the amount of CH_3OH produced by ^1H NMR (integration of the signal at δ 3.36 ppm) and by the decay of the methoxy signals of **4** at δ 3.80 ppm. During irradiation, solutions at pH < 4 had no colour change, while those at higher pH had a brown colour after photolysis that became darker as the pH increased.

Compounds **15**, **33**, **34**, **35**, **36**, **38** and **39** were photolysed as described above for the NMR scale photolysis except that different ratios of D_2O to CD_3CN were sometimes required to adequately dissolve the compound, but the final concentration remained constant.

Preparative Scale Photolysis of Syringic Acid (4)

The preparative scale photolyses were conducted in a ~ 150 mL open quartz tube that was cooled with an internal cold finger to approximately 15 ^oC. The solutions were purged with argon for inert atmosphere experiments or air using a stainless steel needle for approximately 10 minutes prior to photolysis and for the duration of the photolysis experiment using the same stainless steel needle. The general workup of the reaction mixture involved acidification using 1 **M** HCl if the pH was more than 7 followed by

extraction using 4 x 50 mL CH_2Cl_2, drying of the organic layer using $MgSO_4$, filtering to remove the drying agent and evaporation of the solvent under reduced pressure.

For the photolysis of **4** in which the photoproducts were isolated, 20 mg of **4** was dissolved in 100 mL of H_2O, with the mixture adjusted to the appropriate pH using 1 **M** NaOH or 1 **M** H_2SO_4. As for the NMR scale photolysis explained above, if the photolysis required an added ion, NaCl, NaI or KCN was added to achieve 0.5 **M**. During irradiation, the solution turned to a red/orange colour for neutral or basic pH and acquired a light yellow colour for photolysis in acidic conditions. After work-up (described above), the dried photomixture (typically a white solid) was dissolved in DMSO-d_6 for ^{1}H NMR analysis, or dissolved in CH_3OH for analysis by ESI-MS. For **4** photolysed in neutral or basic conditions, **36** was identified as a photoproduct; ^{1}H NMR (300 MHz, DMSO-d_6) δ 3.784 ppm (s, 3 H, OCH_3) and ESI-MS m/z 183 (negative ion mode) (Note that the aromatic protons were not visible since they were overlapping with the signals from **4**). Compound **39** was also identified as a photoproduct; ^{1}H NMR (300 MHz, DMSO-d_6) δ 3.777 ppm (s, 3 H, OCH_3), δ 6.74 ppm (t, 1 H, 4-position H), δ 7.05 ppm (d, 2 H, 2,5-position H) and ESI-MS m/z 181 (negative ion mode). Compound **42** was identified by ^{1}H NMR (300 MHz, DMSO-d_6) δ 7.33 ppm (s, 2 H, Ar H), δ 7.89 ppm (s, 1 H, Ar H) and ESI-MS m/z 349 (negative ion mode).

Photolysis of 3,4,5-trimethoxybenzoic acid (37)

A solution of **37** was made by dissolving 9.2 mg in 10 mL D_2O and 2 mL CD_3CN (using a sonicator). The pD was then adjusted to pD 7 using 0.1 **M** NaOD or 0.1 **M** D_2SO_4 and was measured using a Fisher Scientific Accumet Research Dual Channel pH / Ion meter. The solution was photolysed for 3 hours at 300 nm (16 lamps) after purging with Ar for 10 minutes using a stainless steel needle. ^{1}H NMR of the reaction mixture (without workup) showed the formation of CH_3OH as measured by the signal at δ 3.47 ppm. This was confirmed by spiking in neat CH_3OH and observing the overlapping of the signals. The solution was clear and colourless before and after photolysis.

Compound **37** was also photolysed using a preparative scale photolysis to determine the identity of the other photoproducts. A solution was made by dissolving 29 mg of **37** in 100 mL H_2O, adjusted to pH 8 using 1 M NaOH. The solution was photolysed 3 hours under 300 nm irradiation (16 lamps) with an Ar purge for 10 minutes before photolysis and throughout the photolysis time. During irradiation, the solution turned to a light yellow colour. After photolysis, the entire photomixure was made acidic with H_2SO_4, extracted with 4 x 50 mL CH_2C_2, dried over $MgSO_4$, filtered and evaporated under vacuum. The dried photomixture (a white solid) was then dissolved in DMSO-d_6 for ^{1}H NMR analysis. Compound **4** was identified as a photoproduct; ^{1}H NMR (300 MHz, DMSO-d_6) δ 3.80 ppm (s, 3 H, OCH_3) and δ 7.20 ppm (s, 2 H, Ar H). Compound **39** was identified by ^{1}H NMR (300 MHz, DMSO-d_6) δ 3.73 ppm (s, 3 H, OCH_3), δ 6.7 ppm (t, 1 H, 4-position H) and δ 7.05 ppm (d, 2 H, 2,5-position H).

3.3.1 Product Quantum Yield Measurements

Product quantum yields for the formation of CH_3OH from the photolysis of **4** and **37** were determined using relative methods where 1,2-dimethoxybenzene (**27**) was used as a secondary actinometric standard. This involved comparison of the CH_3OH yields from the photolysis of **27** compared to those for **4** and **37** where the quantum yield for **27** was known (Φ_p = 0.016 at pD 1.3, 254nm). Solutions of **27**, **4** and **37** were made by dissolving a known amount of compound into 1:1 D_2O-CD_3CN so that the concentrations were 5.1 x 10^{-3} **M**. The solution of **27** was adjusted to pD 1.3 using D_2SO_4 and the pD of **4** and **37** adjusted to 8 with NaOD. The solutions were Ar purged prior to photolysis for 10 minutes and then photolysed at 254 nm (14 lamps) for 1 hour in a closed quartz tube that was cooled with an external water bath to < 15 ^oC. After photolysis, 0.75 mL of the solution was syringed from the reaction mixture to an NMR tube with 1 μL of acetone spiked in as an internal standard. A ^1H NMR of this mixture was immediately taken to measure the amount of CH_3OH relative to the internal standard. All three compounds were photolysed on the same day using the same lamps, Rayonet and quartz tube. The quantum yields for **4** and **37** were determined by using Equation 4.1

$$\Phi_A = \Phi_B \, (A / B) \qquad \textbf{(4. 1)}$$

where Φ_A is the relative quantum yield of A, Φ_B is the known quantum yield of B and A/B is the relative conversion to CH_3OH as measured by the ^1H NMR integrations of the CH_3OH signals. The resulting quantum yields are the results of three trials and are tabulated in Table 2.2.

3.3.2 UV-Vis Studies

Absorption spectra for **4** were measured using UV-Vis spectrometry with the concentration of **4** at ~10^{-5} **M** in H_2O at pH 7. This concentration allowed for the main absorption at 210 nm to lie at ~2.5, with the smaller absorptions in the 240 – 300 nm region to lie at ~1.0. The absorption spectra were measured in 1 cm^2 quartz cuvettes with 3 mL of the desired solution added to the cuvette using a syringe. For those spectra that were obtained in the absence of O_2, the solution was purged with N_2 for 10 minutes prior to photolysis. After the purging was complete, the solution was photolysed at 300 nm (16 lamps) for various times, after which the absorption spectra were recorded. For the photolysis in aerated solution, the solution was purged with air for 10 minutes prior to photolysis. No significant changes to the absorption spectra were found for the photolysis of **4** with N_2 or O_2. The major difference was that decay of the absorptions occurred faster with O_2 present.

3.3.3 Laser Flash Photolysis

All LFP studies were performed using a Spectra Physics YAG laser (Model GCR-12, 266 nm excitation). The monitoring beam utilized a pulsed 150 W lamp (Oriel housing Model 66057 and PTI power supply LPS-220), angled at 90^o to the laser beam. A monochromator (CVI Digikrom 240) and a photomultiplier tube (PMT) (Hamamatsu R446, 5 dynodes) were used to measure the intensity of the light at each wavelength of analysis. A baseline compensation unit (Stanford Research Systems) was used to obtain the signal from the PMT in order to hold the value of the background intensity from the Xe lamp after the lamp pulse and before the laser fired. A digital oscilloscope (Tektronix

TDS 520) recorded the signal resulting from the laser pulse. This signal was then sent to a MacIntosh IIci computer with software (written in Labview 5.01) used to analyse the data. This software ensured that the P_o values were kept between -0.15 and 0.25 V by adjusting the PMT voltage and the monochromator slit width. The slope of the baseline was corrected for transient signals with time scales that were greater then 5 μs/div.

Due to the low quantum yield for the photolysis of **4** and **37**, a static cell (1 cm^2, quartz) was used for the LFP measurements. The desired solutions were made so that the absorption of the compound (**4** or **37**) was between 0.4 and 0.8 at 266 nm (~3 mL of solution was used). The typical concentration used was 10^{-4} M with the solution made up in H_2O with the pH adjusted using either 0.1 **M** NaOH or 0.1 **M** H_2SO_4. Prior to photolysis, the solution was purged with either N_2, O_2 or N_2O for 30 minutes.

The absorption spectra of the transients were recorded by measuring the average ΔA at intervals of 10 nm for the desired region, with four time windows measured for each wavelength. This resulted in a time resolved absorption spectrum for the desired region. Transient decays were recorded at specific time scales and wavelengths through the collection of 500 data points. A Labview program written for the University of Victoria (FitVic) was used to fit the decays.

3.3.4 MIMS

All MIMS experiments were conducted in the Applied Environmental Research Laboratories at Malaspina University-College. The data was obtained using a quadrupole ion trap mass spectrometer with an external ion source (Polaris-Q™, Thermo-Electron, San-Jose, CA, USA) equipped with an in-house constructed MIMS interface. Reactions

were monitored using full scan and selected ion monitoring (SIM) modes. The analytical signals from MS experiments are presented as full scan 40 – 250 mass units; SIM CH_3Cl m/z = 50, 52; SIM CH_3OH m/z = 32 and SIM CO_2 m/z = 44.

The MIMS interface consists of a hollow fibre PDMS membrane (10.0cm, 0.94mm OD, 0.51mm ID, 0.22mm thickness, Silastic® brand, Dow Corning, Midland, MI, USA) mounted in a flow through casing constructed of 0.25" Swagelok™ (Supelco, Bellefonte, PA, USA) connectors and stainless steel tubing. A low flow of He sweep gas (UHP grade, 99.999% pure, 2.7 mL/min) is passed through the inside of the HFM. The exit He flow is subsequently directed through a metal jet separator (model MJSC/HP5890, 15mL/min jets, SGE, Austin, TX, USA) and then to the mass spectrometer (200°C ion source, base pressure 1.0 X 10^{-5} Torr) via a heated transfer line (150°C). The jet separator was backed (5.5 x 10^{-2} Torr) using a mechanical roughing pump (Pascal 2005SD, Alcatel, Paris, France) equipped with an in-line molecular sieve trap (4 inch diameter, 13 Å sieve pore size, KJ Lesker Inc, Pittsburgh, PA, USA).[93] The MIMS interface was mounted entirely inside a programmable gas chromatograph oven (Trace GC™, Thermo-Electron, San-Jose, CA, USA). This GC was used to control overall MIMS temperature as well as regulation of the helium sweep gas flow.

A closed ~ 800 mL quartz photolysis vessel equipped with a cold finger tube and two side arm inlets was positioned inside of a Rayonet RPR 100 photochemical reactor for all MIMS photolysis experiments. All samples and reaction mixtures were re-circulated in a closed loop over the MIMS interface through 0.25 in. o.d. Teflon tubing using a peristaltic pump (model 77200-62 Easy-Load II Masterflex; Cole-Parmer, Concord, ON, Canada, with LS 25 Viton pump tubing) at a flow rate of 375 mL/min to

facilitate sample mixing and establish turbulent flow conditions at the membrane surface. Sonication using a Bransonic 220 ultrasonic cleaner was used for all samples to assist in dissolution. Solutions of **4** were made by dissolving 40 mg in 400 mL of deionized water with 0.5 **M** Cl^- and adjusted to the desired pH by using either NaOH or HCl. Prior to mixing the solutions, the water was purged with the desired gas (N_2 or O_2) for 1.5 hours. For experiments in the absence of O_2, the headspace of the photolysis tube (~ 400 mL headspace for 400 mL solution) and tubing leading to the MIMS was flushed with N_2 to ensure that no residual air remained. A cold finger inserted into the photolysis tube kept the temperature of the solution at 20 ^oC using a thermostat controlled water bath (Forma Scientific 2095 Bath and Circulator; Powers Process Controls 350 Process Controller), re-circulated using a peristaltic pump (described above). After attaching the tubing, the peristaltic pump and MIMS were set to establish a baseline for the analytes being measured. Once the signal had stabilized for a minimum of 10 minutes, the UV lamps for the photolysis chamber were turned on (300 nm, 16 lamps).

References

1. R. P. Schwarzenbach, P. M. Gschwend and D. M. Imboden, *Environmental Organic Chemistry*, John Wiley & Sons, New York, 1993.

2. N. J. Bunce, *Chemosphere*, 1987, **7**, 653.

3. N. J. Bunce, *Chemosphere*, 1982, **8**, 701.

4. N. J. Bunce, *Environmental Chemistry*, U. of Guelph, Wuerz Publishing, Winnipeg, 1991.

5. D. Dulin, H. Drossman and T. Mill, *Environ. Sci. Technol.*, 1986, **20**, 72.

6. M. Machala, L. Bláha, H. J. Lehmler, M. Plíková, Z. Májková, P. Kapplová, I. Sovadinová, J. Vondráek, T. Malmberg and L. W. Robertson, *Chem. Res. Toxicol.*, 2004, **17**, 340.

7. K. Forest, P. Wan and C. M. Preston, *Photochem. Photobiol. Sci.*, 2004, **3**, 463.

8. G. W. vanLoon and S. J. Duffy, *Environmental Chemistry: A Global Perspective*, Oxford University Press, New York, 2000.

9. G. Abbt-Braun, U. Lankes and F. H. Frimmel, *Aquat. Sci.*, 2004, **66**, 151.

10. J. P. Aguer and C. Richard, *J. Photochem. Photobiol. A: Chem*, 1996, **93**, 193.

11. N. A. Burges, H. M. Hurst and B. Walkden, *Geochim. et Cosmochim. Acta.*, 1964, **28**, 1547.

12. R. A. Larson and E. J. Weber, *Reaction Mechanisms in Environmental Organic Chemistry*, CRC, Boca Ralton, 1994.

13. J. Ralph, U.S. Dairy Forage Reseach Center, USDA Agricultural Research Service, Department of Forestry, Appita, 2005.

14. J. J. Rook, *Water Treatment Exam*, 1974, **23**, 234.

15. W. R. Haag and J. Hoigne, *Environ. Sci. Technol.*, 1986, **20**, 341.

16. J. P. Aguer and C. Richard, *Toxicol. Environ. Chem.*, 1993, **39**, 217.

17. F. Frimmel, H. Bauer, J. Hoigne and J. A. Leenheer, *Environ. Sci. Technol.*, 1987, **21**, 541.

18. R. G. Zepp, A. M. Braun, J. Holgne and J. A. Leenheer, *Environ. Sci. Technol.*, 1987, **21**, 485.

19. J. F. Power, D. K. Sharma, C. H. Cooper, R. Bonneau and J. Joussot-Dubien, *Photochem. Photobiol.*, 1986, **44**, 11.

20. J. P. Aguer and C. Richard, *J. Photochem. Photobiol. A: Chem*, 1994, **84**, 69.

21. A. Fischer, D. Kliger, J. Winterle and T. Mill, *Chemosphere*, 1985, **14**, 1299.

22. R. M. Baxter and J. H. Carey, *Nature*, 1983, **306**, 575.

23. W. J. Cooper and R. G. Zika, *Science*, 1983, **220**, 711.

24. R. M. W. Amon and R. Benner, *Geochim. et Cosmochim. Acta.*, 1996, **60**, 1783.

25. W. Graneli, M. Lindell, B. M. de Faria and F. de Assis Esteves, *Biogeochemistry*, 1998, **43**, 175.

26. I. Reche, M. L. Pace and J. J. Cole, *Biogeochemistry*, 1999, **44**, 259.

27. C. L. Osburn, D. P. Morris, K. A. Thorn and R. E. Moeller, *Biogeochemistry*, 2001, **54**, 251.

28. E. Engelhaupt, T. S. Bianchi, R. G. Wetzel and M. A. Tarr, *Biogeochemistry*, 2002, **62**, 39.

29. A. M. Fischer, J. S. Winterle and T. Mill, eds. R. G. Zika and W. J. Cooper, American Chemical Society, Washington, D.C., 1987, pp. 141-156.

30. J. F. Power, D. K. Sharma, C. H. Langford, R. Bonneau and J. Joussot-Dubien, in *ACS Symposia Series*, eds. R. G. Zika and W. J. Copper, American Chemical Society, Washington, D.C., 1987, pp. 157-173.

31. H. Joschek and L. I. Grossweiner, *J. Am. Chem. Soc*., 1966, **88**, 3261.

32. G. Grabner, G. Kohler, J. Zeehner and N. Getoff, *J. Photochem. Photobiol*., 1977, **26**, 449.

33. G. Kohler, S. Solar, N. Getoff and A. R. Holzwarth, *J. Photochem.*, 1985, **28**, 383.

34. E. Trudy, T. R. Thomas-Smith and N. V. Blough, *Environ. Sci. Technol.*, 2001, **35**, 2721.

35. M. Anbar, M. Bambenek and A. B. Ross, Natl. Stand. Ref. Data Ser., U.S. Natl. Bur. Stand., 1973.

36. B. G. Heikes, C. Wonil, M. E. Q. Pilson, E. Swift, H. B. Singh, A. Guenther, D. J. Jacob, B. D. Field, R. Fall, D. Riemer and L. Brand, *Global Biogeochem. Cycles*, 2002, **16**, 1133.

37. D. J. Jacob, B. D. Field, Q. Li, D. R. Blake, J. de Gouw, C. Warneke, A. Hansel, A. Wisthaler, H. B. Singh and A. Guenther, *J. Geophys. Res. Atmospheres*, 2005, D08303.

38. D. J. Jacob, *J. Geophys. Res*., 1986, **91**, 9807.

39. D. J. Jacob, *Atmos. Environ.*, 2000, **34**, 2131.

40. R. M. Moore, *Handbook of Environmental Chemistry*, 2003, **3P**, 85.

41. R. M. Moore and O. C. Zafiriou, *J. Geophys. Res*., 1994, **99**, 16415.

42. D. J. Kieber and N. V. Blough, *Anal. Chem*., 1990, **62**, 2275.

43. R. M. Moore, *unpublished results*, Dalhousie University (personal communication).

44. D. M. Shold and R. E. Rebbert, *J. Photochem*., 1978, **9**, 499.

45. S. E. Manahan, CRC Press, Boca Ralton, Florida, 1994, pp. 417-418.

46. F. Keppler, D. B. Harper, T. Rockmann, R. M. Moore and J. T. G. Hamilton, *Atmos. Chem. Phys. Discuss*., 2005, **5**, 3899.

47. S. A. Montzka and P. J. Fraser, World Meterological Organisation, Geneva, 2003.

48. U.S. Environmental Protection Agency, *Bromomethane Health Advisory*, Office of Drinking Water, Washington, D.C., 1989.

49. The Merck Index, *An Encylcopedia of Chemicals, Drugs and Biologicals, 11th edition*, Merck & Co. Inc., Rahway, N.J., 1989.

50. M. Sittig, *Handbook of Toxic and Hazardous Chemicals and Carcinogens, 2nd edition*, Noyes Publishing, Park Ridge, N.J., 1985.

51. *Patty's Industrial Hygiene and Toxicology, Volume IIB, 3rd revised ed.*, John Wiley & Sons, New York, 1981.

52. International Agency for Research on Cancer (IARC), *IARC Monographs on the Evaluation of the Carcinogenic Risks of Chemicals to Man. Some Fumigants, the Herbicides 2,4-D and 2,4,5-T, Chlorinated Dibenzoidioxins and Miscelleneous Industrial Chemicals. Volume 15*, World Health Organization, Lyon, 1977.

53. Agency for Toxic Substances and Disease Registry (ATSDR), *Toxicological Profile for Chloromethane (Update)*, U.S. Department of Health and Human Services, U.S. Public Health Service, Atlanta, G.A., 1998.

54. United Nations Environment Program, *The Montreal Protocol on Substances that Deplete the Ozone Layer*, Secretariat for The Vienna Convention for the Protection of the Ozone Layer & The Montreal Protocol on Substances that Deplete the Ozone Layer, London, 1990.

55. J. M. Lobert, W. C. Keene, J. A. Logan and R. Yevich, *J. Geophys. Res. A-*, 1999, **104**, 8373.

56. M. O. Andreae and P. Merlet, *Global Biogeochem. Cycles*, 2001, **15**, 955.

57. R. Watling and D. B. Harper, *Mycol. Res.*, 1998, **102**, 769.

58. R. C. Rhew, B. R. Miller and R. F. Weiss, *Nature*, 2000, **403**, 292.

59. Y. Yokouchi, M. Ikeda, Y. Inuzuka and T. Yukawa, *Nature*, 2002, **416**, 163.

60. F. Keppler, R. Eiden, V. Nieden, J. Pracht and H. F. Scholer, *Nature*, 2000, **403**, 298.

61. R. M. Moore, *Chemosphere - Global Change Science*, 2000, **2**, 95.

62. L. A. Barrie, J. W. Bottenheim, R. C. Schnell, P. J. Crutzen and R. A. Rasmussen, *Nature*, 1988, **334**, 138.

63. J. H. Butler and J. M. Rodriguez, in *The Methyl Bromide Issue*, eds. C. H. Bell, N. Price and B. Chakrabarti, Wiley & Sons, 1996, p. 27.

64. E. Adler, *Wood Sci. Technol.*, 1977, **11**, 169.

65. T. Higuchi, *Wood Research*, 1981, **67**, 47.

66. G. Weissenbock, *Biologie in Unserer Zeit*, 1976, **6**, 140.

67. T. Stalin, G. Sivakumar, B.Shanthi, A. Sekar and N. Rajendiran, *J. Photochem. Photobiol. A: Chem*, 2006, **177**, 144.

68. B. Durbeej and L. A. Eriksson, *J. Phys. Chem. A.*, 2005, **109**, 5677.

69. O. Lanzalunga and M. Bietti, *J. Photochem. Photobiol. B: Biol.*, 2000, **56**, 85.

70. T. A. Gadosy, D. Shukla and L. J. Johnston, *J. Phys. Chem. A.*, 1999, **103**, 8834.

71. J. Den Heijer, O. B. Shadid, J. Cornelisse and E. Havinga, *Tetrahedron*, 1977, **22**, 779.

72. J. Cornelisse, in *CRC Handbook of Organic Photochemistry and Photobiology*, eds. W. M. Horspool and S. Pill-Song, CRC Press, 1995, p. 250.

73. H. E. Zimmerman, *J. Am. Chem. Soc.*, 1995, **117**, 8988.

74. H. E. Zimmerman, *J. Phys. Chem. A.* , 1998, **102**, 5616.

75. H. E. Zimmerman and V. R. Sandel, *J. Am. Chem. Soc*., 1963, **85**, 915.

76. J. Den Heijer, O. B. Shadid, J. Cornelisse and E. Havinga, *Tetrahedron*, 1977, **33**, 779.

77. R. O. De Jongh and E. Havinga, *Recl. Trav. Chim. Pays-Bas*, 1966, **85**, 275.

78. R. L. Letsinger, O. B. Ramsay and J. H. McCain, *J. Am. Chem. Soc*., 1965, **87**, 2945.

79. J. Cornelisse and E. Havinga, *Chem. Rev*., 1975, **75**, 353.

80. S. Nilsson, *Acta. Chem. Scand*., 1973, **27**, 329.

81. R. Pollard, S. Wu, G. Zhang and P. Wan, *J. Org. Chem.*, 1993, **58**, 2605.

82. R. Hermann, S. Naumov and G. R. Mahalaxmi, *Chem. Phys. Lett.*, 2000, **324**, 265.

83. F. G. Bordwell and J. P. Cheng, *J. Am. Chem. Soc*., 1991, **113**, 1736.

84. K. Konya and J. C. Scaiano, *J. Photochem. Photobiol. A: Chem*, 1996, **100**, 119.

85. R. M. Moore, C. E. Geen and V. K. Tait, *Chemosphere*, 1995, **30**, 1183.

86. D.R. Lide ed., *CRC Handbook of Chemistry and Physics (87th edition)*, internet version, 2007.

87. T. Stalin and N. Rajendiran, *Spectrochim. Acta Part A*, 2005, **61**, 3087.

88. S. L. Murov, I. Carmichael and G. L. Hung, *Handbook of Photochemistry 2nd edition*, Marcel Dekker, Inc., New York, 1993.

89. M. A. LaPack, J. C. Tou and C. G. Enke, *Anal. Chem.*, 1990, **62**, 1265.

90. R. C. Johnson, R. G. Cooks, T. M. Allen, M. E. Cisper and P. H. Hemberger, *Mass Spectrom. Rev.*, 2000, **19**, 1.

91. R. A. Ketola, T. Kotiaho, M. E. Cisper and T. M. Allen, *J. Mass Spectrom.*, 2002, **37**, 457.

92. E. Krogh and C. Gill, Applied Environmental Research Laboratories, personal communications, 2007.

93. A. J. Thompson, A. S. Creba, R. M. Ferguson, E. T. Krogh and C. G. Gill, *Rapid Communications in Mass Spectrometry*, 2006, **20**, 2000.

94. J. H. L. Nelson, E. T. Krogh, C. G. Gill and D. A. Friesen, *J. Environ. Sci. and Health, Part A*, 2004, **39**, 2307.

95. NIST Mass Spectral Library, 2005.

96. M. R. Ganapathi, S. Naumov, R. Hermann and O. Brede, *Chem. Phys. Lett.*, 2001, **337**, 335.